Mechanosensing of Substrate Dimension and Migration State in Adherent Cells

Submitted in partial fulfillment of the requirements for
the degree of

Doctor of Philosophy
in
Biomedical Engineering

Stephanie S. Chang

B.S., Chemical Engineering, California Institute of Technology

Carnegie Mellon University
Pittsburgh, PA

September, 2015

Acknowledgements

To my advisor, Professor Yu-li Wang: Thank you for pushing me when I hesitated, for inspiring me when I was stuck, and for reassuring me when I thought I could not continue. I would also like to acknowledge funding from the Department of Biomedical Engineering and from NIH grant GM-32476 to YLW.

To my thesis committee, Professor Adam Feinberg, Professor Philip LeDuc, and Professor Brooke McCartney: Thank you for your encouragement and your valuable time. I appreciate your help in making my research complete.

To members of the Wang Lab: Thank you for creating such a collaborative environment for sharing ideas, proofreading manuscripts, and generally making the lab run so smoothly. In particular, Dr. Wei-hui Guo and Dr. Andy Rape walked me through my first years and taught me all the tricks for running experiments.

Most of all, to my family: Thank you for your unconditional love and unwavering support. I am always thinking of you.

Abstract

The behavior of adherent cells is known to be affected by both chemical signals and physical cues in the extracellular environment, including substrate topography and rigidity. The process of sensing physical features and converting them to intracellular signals is believed to rely on the formation of adhesion structures and the generation of actomyosin-based traction forces. Equally important is signaling in the reverse direction, as internal cellular activities regulate mechanical output to the extracellular environment. This thesis explores how substrate dimension and migration state are monitored by adherent cells and how they affect cell behavior. By micropatterning soft hydrogels, I am able to simultaneously control cell size, shape, and migration as well as measure mechanical output. I find that migrating NIH 3T3 fibroblasts use traction forces to differentiate between one-dimensional lines and two-dimensional surfaces. Furthermore, oncogene-transformed fibroblasts, which generate disorganized traction forces, are unable to sense a change in substrate dimension. Additionally, I show that stationary cells confined to micropatterned islands exhibit significantly increased traction forces, less dynamic focal adhesions, and altered protein phosphorylation patterns compared to cells migrating freely. These results suggest that migration state itself can act as an input to control both mechanical and signaling behavior in adherent cells. Microtubules are involved in this migration-dependent regulation of traction forces, as migrating and stationary cells

respond differently to microtubule depolymerization. The mechanism of migration-dependent regulation of mechanical output likely involves altered interactions between microtubules and focal adhesions. Understanding how cells sense and respond to mechanical signals provides insight for diseases where mechanical properties are altered, including cancer. These insights may lead to new strategies for disease diagnosis and treatment.

Contents

List of Tables

List of Figures

Chapter 1

Introduction

1.1 Physical cues guide cell behavior

1.1.1 Cell behavior is regulated by external, environmental mechanics

In addition to chemical signals, cells are able to respond to mechanical signals in their environment. External mechanical signals include topographic features and substrate dimension which have been shown to affect many important cellular processes. Some of the earliest studies have focused on cell behavior in response to substrate topography. In a phenomenon termed contact guidance, multiple types of cells including epithelial cells, neurons, and fibroblasts have been shown to elongate and align parallel to substrates with micron- or nano-scale grooves (Curtis & Wilkinson, 1997; Rajnicek *et al.*, 1997; Teixeira *et al.*, 2003; Kim *et al.*, 2009). In addition to cell orientation, grooved surfaces have been shown to induce faster neurite growth and to change migration speed depending on the groove spacing and depth (Rajnicek *et al.*, 1997; Kim *et al.*, 2009). Mode of migration can also vary, as cells that encounter a transition from a smooth surface to a pillar topography develop elongated protrusions instead of a broad lamellipodia (Ghibaudo *et al.*, 2009). Of particular interest to biomedical engineers is the ability of substrate topography to influence stem cell behavior. Poly(ε-caprolactone) fibers electrospun in an aligned manner were able to enhance neural differentiation of embryonic stem cells more than fibers spun in a random pattern (Xie *et al.*, 2009). Stem cell differentiation was also enhanced when cells were seeded on substrates with deep nanopits (Zouani *et al.*, 2012) or on titanium nanotubes with a 70-100 nm diameter (Oh *et al.*, 2009). Interestingly, 30 nm diameter nanotubes did not promote differentiation, which indicates that the response to topography is highly sensitive.

Conventional cell culture relies on two-dimensional surfaces which are sometimes coated with extracellular matrix proteins. However, cells in vivo experience a more complex, often three-dimensional environment. Recently, researchers are becoming more aware that substrate dimension can drastically alter cell behavior (Figure 1.1) (Baker & Chen, 2012). Fibroblasts adopt a dendritic structure in collagen matrices but not on collagen-coated surfaces (Grinnell *et al.*, 2003). Elongation and loss of large, stable focal adhesions was also observed when integrins on the dorsal side of cells were activated in a sandwich-type culture (Beningo *et al.*, 2004). Additionally, multiple modes of migration exist in three-dimensional cultures (Doyle *et al.*, 2009; Fraley *et al.*, 2012) which are not well characterized by parameters commonly used to describe two-dimensional cell migration. Such dramatic changes in morphology and basic behaviors like migration suggest that research done on two-dimensional substrates may not translate fully to cells in more complex environments.

Along with readily observed features such as topography and dimension, substrate stiffness is also becoming an important parameter in cell mechanics (Discher *et al.*, 2005). Hydrogels made with varying amounts of crosslinkers are now routinely used to control substrate compliance (Beningo & Wang, 2002). Early studies found that substrate rigidity regulates rates of proliferation and apoptosis (Wang *et al.*, 2000), migration direction and speed (Lo *et al.*, 2000; Pathak & Kumar, 2012), tissue formation (Guo *et al.*, 2006), and traction force generation (Lo *et al.*, 2000; Trichet *et al.*, 2012). Like other mechanical inputs, substrate rigidity is also known to affect stem cell differentiation. Differentiation of stem cells into particular lineages has been shown to be enhanced on substrates of optimal stiffness. That is, soft (<1 kPa) substrates favor neurogenic differentiation, moderately stiff (11 kPa) substrates favor myogenic differentiation, and stiff (34 kPa) substrates favor osteogenic differentiation

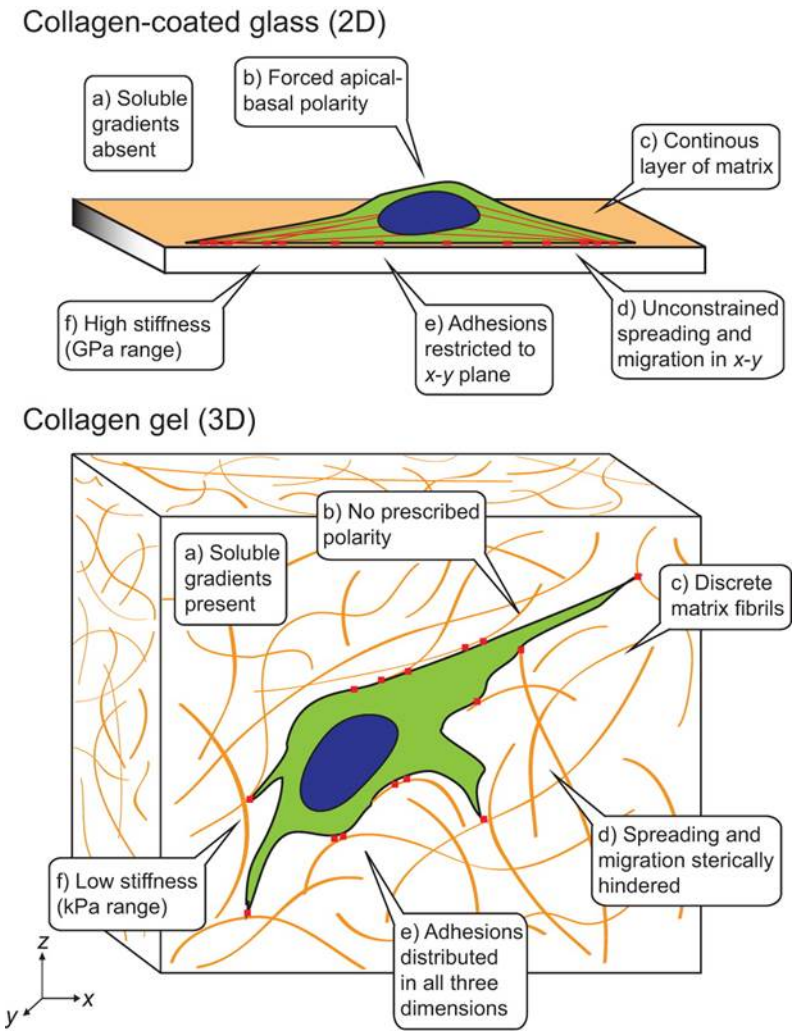

FIGURE 1.1. Three-dimensional substrates differ from two-dimensional cell culture substrates. Adhesive, topographical, mechanical, and soluble cues differ in 2D and 3D, which affects cell polarity, migration, and focal adhesion distribution and maturation. Adapted with permission from *Journal of Cell Science* (Baker & Chen, 2012).

(Engler *et al.*, 2004, 2006). Thus physical features of the extracellular environment alter intracellular signaling to change cell behavior in a form of outside-in signaling.

1.1.2 Cell behavior is also regulated by internal, cellular mechanics

Adherent cells are also able to monitor their own mechanics and change behavior in response. Distinct from the external features described above, such internal features include cell spreading, cell shape, and elongation or aspect ratio. In normal cells, spread area has been shown to affect growth and apoptosis rates (Chen *et al.*, 1997), traction force generation (Rape *et al.*, 2011), and terminal differentiation of human epidermal keratinocytes (Watt *et al.*, 1988). Increasing aspect ratio has also been linked to increasing traction force generation (Rape *et al.*, 2011), increasing collagen I expression in human tendon fibroblasts (Li *et al.*, 2008), and decreasing proliferation rates in vascular smooth muscle cells (Thakar *et al.*, 2009). In macrophages, imposing cell elongation was shown to enhance the expression of the pro-healing M2 phenotype over the pro-inflammatory M1 phenotype (McWhorter *et al.*, 2013).

Beyond normal conditions, cells in extraordinary conditions, such as stem cell differentiation or cancerous epithelial-to-mesenchymal transition (EMT) can also be manipulated by mechanical features of the cell. Confinement of stem cells to small spread area enhanced maintenance of stemness without affecting the ability to differentiate later (Zhang & Kilian, 2013). When exposed to mixed media, human mesenchymal stem cells confined to small areas became adipocytes, but became osteocytes when allowed to spread to a large area (McBeath *et al.*, 2004). Elongation promoted more robust myocardial differentiation (Tijore *et al.*, 2014). Shape has

also been shown to direct differentiation to an adipogenic lineage or an osteogenic lineage (Kilian *et al.*, 2010). Limiting cell area prevented MMP3-induced epithelial-to-mesenchymal transition in mouse mammary epithelial cells (Nelson *et al.*, 2008). Regions of high mechanical stress in cells or groups of cells correlated with areas of high traction force generation (Li *et al.*, 2010) and were shown to regulate spatial patterning of EMT (Gomez *et al.*, 2010). It is believed that RhoA activity plays a role in many of these shape-based phenomena (McBeath *et al.*, 2004), suggesting that cells are able to regulate intracellular signals based on size and shape.

1.2 Cytoskeletal structures mediate mechanosensing

1.2.1 Focal adhesions link the cytoskeleton and the extracellular matrix

Focal adhesions are composed of hundreds of proteins, including integrin, paxillin, focal adhesion kinase (FAK), and vinculin. Super-resolution imaging of adhesion proteins revealed that focal adhesions are organized into functional layers that mediate integrin signaling, force transduction, and actin regulation (Figure 1.2) (Kanchanawong *et al.*, 2010). Integrin engagement to the extracellular matrix (ECM) initiates signaling cascades that recruit more adhesion proteins and drive mechanotransduction. Phosphorylation of paxillin is involved in assembly of focal adhesions (Zaidel-Bar *et al.*, 2007), likely by regulating recruitment of vinculin (Pasapera *et al.*, 2010), FAK (Choi *et al.*, 2011), and talin (Kwak *et al.*, 2012). FAK phosphorylates paxillin (Pasapera *et al.*, 2010) and recruits talin (Lawson *et al.*, 2012). Vinculin was believed to mostly function as a scaffolding protein, known for its interactions with talin and actin (Humphries *et al.*, 2007). More recent studies have suggested that vinculin is able to regulate adhesion protein recruitment and release (Carisey *et al.*, 2013), and its functions are activated by talin (Case *et al.*, 2015).

Focal adhesion signaling is capable of activating multiple pathways associated with force generation. Integrin signaling has also been associated with activation of both RhoA (Ren *et al.*, 1999) and Rac (Wehrle-Haller, 2012). Paxillin signaling is able to activate Rac (Vicente-Manzanares *et al.*, 2009). FAK activity has been shown to suppress Rho activity (Ren *et al.*, 2000) to regulate focal adhesion turnover (Hamadi

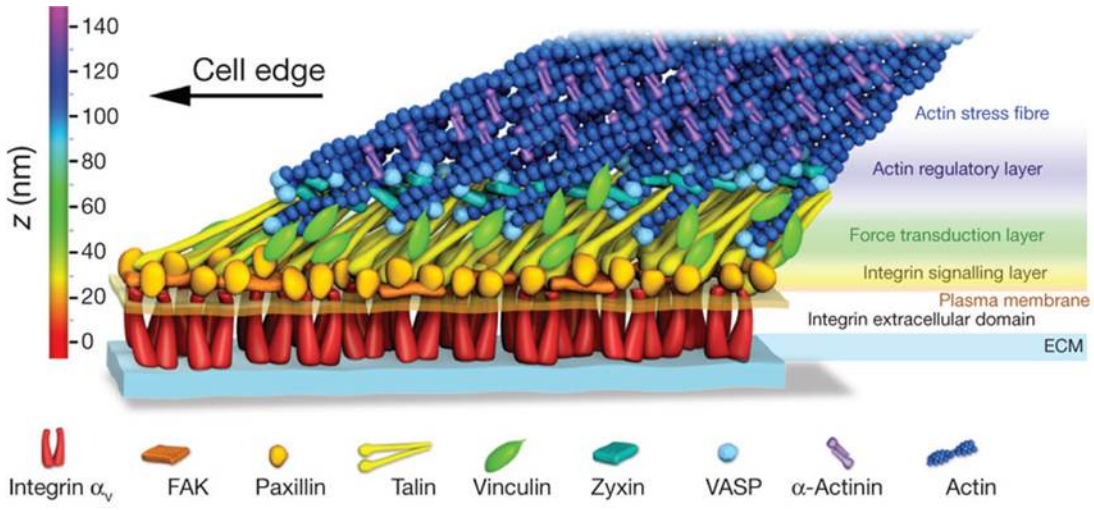

FIGURE 1.2. Focal adhesions are composed of many proteins that interact physically and chemically. Schematic model of focal adhesion molecular architecture. Focal adhesions mediate interaction between the cytoskeleton and the extracellular matrix with direct binding to the ECM via integrins and to actin. Proteins in the adhesion plaque undergo phosphorylation and conformation changes during mechanotransduction. Adapted by permission from Macmillan Publishers Ltd: *Nature* **468**: 580-584, copyright 2010 (Kanchanawong *et al.*, 2010).

et al., 2005), and it is a key player in many mechanosensing behaviors (Wang *et al.*, 2001a). Signaling in the reverse direction, referred to as inside-out signaling, tension was shown to regulate the binding strength between integrins and ECM (Friedland *et al.*, 2009).

Early work correlated adhesion assembly with force (Balaban *et al.*, 2001; Galbraith *et al.*, 2002). However, other work suggests that the relationship between traction force and focal adhesion size is more complex (Beningo *et al.*, 2001; Stricker *et al.*, 2011). More recent work observed force fluctuations within individual focal adhesions (Plotnikov *et al.*, 2012), suggesting that focal adhesions may function as force sensors themselves. Individual proteins in the focal adhesion may also act as force sensors. Fluorescence resonance energy transfer experiments revealed that vinculin can exist in a closed, inactive state as well as an open, active state (Chen *et al.*, 2005), and the conformational change is dependent on tension (Carisey *et al.*, 2013). Talin, too, is capable of stretch-activated unfolding to promote binding to vinculin (del Rio *et al.*, 2009). Focal adhesion proteins further function as a molecular clutch, with some reports suggesting a critical role for vinculin (Thievessen *et al.*, 2013). During cell migration the actin polymerization rate is increased compared to retrograde flow because the linkage between actin and focal adhesions shifts some of the forces driving retrograde flow to the substrate (Alexandrova *et al.*, 2008; Vicente-Manzanares *et al.*, 2009).

1.2.2 The actin network facilitates migration and mechanotransduction

Migration on a two-dimensional substrate has been extensively studied and distilled into a multistep process. In general, migration involves cell polarization, extension of protrusions, formation of adhesions, cell contraction, and release of the rear (Lauffenburger & Horwitz, 1996; Ridley *et al.*, 2003). Of all the molecules involved in migration, actin plays the most prominent role. Initial protrusions at the leading edge, including lamellipodia and filopodia, are driven by actin polymerization (Pollard & Cooper, 2009). As mentioned above, adhesion stabilization is force-dependent. Stress fibers are anchored to focal adhesions (Hotulainen, 2006), and myosin II incorporated along the stress fibers generate contractile force that may enhance adhesion maturation. Actomyosin contractility funneled through focal adhesions also provides the traction force for forward translocation (Beningo *et al.*, 2001; Ridley *et al.*, 2003). Even though current understanding of adherent cell migration depends on heavily on actomyosin contractility, stress fibers may not be necessary for migration, as cells in three-dimensional environments rarely have stress fibers (Cukierman *et al.*, 2002; Beningo *et al.*, 2004). Furthermore, it has been observed that non-migrating cells often have thicker stress fibers while migrating cells have fewer, thinner stress fibers (Pellegrin & Mellor, 2007). These observations point to an important role for regulation of actin dynamics in normal cell behavior.

A complex relationship exists among focal adhesions, actin, and traction forces (Discher *et al.*, 2005). The downstream effect of these interactions means that actin stress fibers are force-sensitive. It has been shown that substrate stiffness affects stress fiber alignment (Prager-Khoutorsky *et al.*, 2011). Stress fibers are also dependent

on myosin II-mediated contractility (Chrzanowska-Wodnicka & Burridge, 1996), as inhibition of contractility with blebbistatin abolishes stress fibers. GTPase activity mediates both outside-in and inside-out signaling through its ability to regulate actin dynamics. Rho directly promotes stress fiber formation, Rac promotes lamellipodia and membrane ruffle formation, and Cdc42 promotes filopodia formation (Burridge & Wennerberg, 2004; Tojkander *et al.*, 2012). Rho-kinase (ROCK) enhances the formation of stress fibers and focal adhesions by activation of myosin light chain and by inactivation of myosin phosphatase (Totsukawa *et al.*, 2000). Precise spatiotemporal control of GTPase activities at the leading edge is essential for efficient cell migration (Machacek *et al.*, 2009).

1.2.3 Microtubules interact with focal adhesions and enhance cell polarity

Microtubules, another major component of the cell cytoskeleton, are portrayed as a structural counterpart to actin. Microtubules have a longer persistence length compared to actin (Gittes *et al.*, 1993) and are considered incompressible. For this reason, mechanical models of the cell liken microtubules to struts that resist actomyosin contractility (Wang *et al.*, 2001b). However, other studies indicate that actin and microtubules work in concert to promote cell migration (Waterman-Storer & Salmon, 1999) through both physical interactions and chemical signaling.

Microtubule kinetics are characterized by dynamic instability (Brouhard, 2015) with periods of fast polymerization capped by rapid depolymerization. Interestingly, a subpopulation of microtubules may become protected from this tendency for catastrophe. Though the mechanism of microtubule stabilization is still unknown,

others have observed that microtubules become stabilized after interaction with focal adhesions (Kaverina *et al.*, 1998) and that FAK and Rho signaling facilitates stabilization (Palazzo *et al.*, 2004).

Besides microtubule stabilization, interaction between microtubules and focal adhesions is known to promote focal adhesion disassembly (Kaverina *et al.*, 1999), a process which requires FAK and dynamin (Ezratty *et al.*, 2005). A number of microtubule associated proteins mediate the interaction between microtubules and focal adhesions (Figure 1.3). Cytoplasmic linker associated protein (CLASP) (Mimori-Kiyosue *et al.*, 2005), adenomatous polyposis coli (APC) (Näthke *et al.*, 1996), and MACF1/ACF7 (Karakesisoglou *et al.*, 2000) mediate the interaction between microtubule plus tips and the cell cortex. Further studies showed that CLASPs cluster at focal adhesions, possibly facilitating the exocytosis of matrix metalloprotease (MMP)-containing vesicles to promote focal adhesion disassembly (Stehbens *et al.*, 2014). Alternative microtubule-based mechanisms of focal adhesion disassembly focus on the role of microtubules in intracellular transport. Focal adhesions were shown to enlarge after inhibition of the molecular motor kinesin-1 (Krylyshkina *et al.*, 2002), suggesting that microtubules transport a focal adhesion modulation signal. Focal adhesion disassembly was also dependent on dynamin, hinting at a possible role for microtubules in the integrin endocytosis and recycling process (Ezratty *et al.*, 2005). Others have also speculated that membrane type 1 matrix metalloprotease is transported to adhesion sites via microtubules (Stehbens & Wittmann, 2012).

Microtubules also play a role in Rho GTPase signaling. Early studies noted that microtubule disruption increased cell contractility (Danowski, 1989), an observation later attributed to an increase in RhoA activity (Ren *et al.*, 1999).

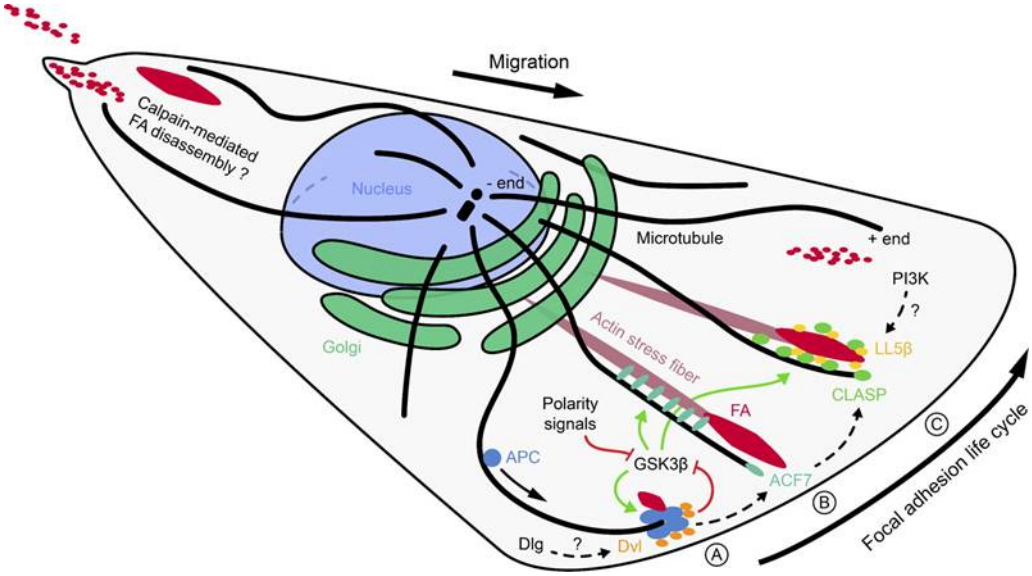

FIGURE 1.3. Microtubule interactions with focal adhesions are mediated by microtubule associated proteins. Polarity signals result in local inactivation of GSK3β which then stimulates activity of various microtubule-associated proteins. APC is delivered by microtubules to the cell edge and stabilizes nascent adhesions (A). MACF1/ACF7 mediates microtubule interactions with actin and guides microtubules to focal adhesions (B). CLASPs stabilize microtubules at mature focal adhesions (C). Copyright Stehbens and Wittmann, 2012. Originally published in *The Journal of Cell Biology* **198**: 481-489.

The favored mechanism to explain how microtubules regulate RhoA activity involves guanine nucleotide exchange factors (GEFs), in particular GEF-H1 which binds both to microtubules and to the active form of RhoA. Accordingly, microtubule polymerization sequesters GEF-H1 and active RhoA, while microtubule depolymerization releases RhoA to induce cell contractility (Krendel *et al.*, 2002; Chang *et al.*, 2008).

While not required for migration, microtubules are important in establishing cell polarity and persistent migration (Etienne-Manneville, 2013). Structurally, polarization can be seen in the distribution and orientation of microtubules in migrating cells (Etienne-Manneville, 2013) and the increase in stable microtubules pointing to the leading edge (Gundersen & Bulinski, 1988). Cell polarity is reinforced through precise spatiotemporal control of Rac1, RhoA, and Cdc42 activity that occurs at the leading edge of migrating cells (Machacek *et al.*, 2009). Part of this regulation has been attributed to the organization of RhoA activity at the leading edge by GEF-H1 and microtubule polymerization (Nalbant *et al.*, 2009). These studies are focused on the effect of microtubules at the leading edge of migrating cells, but recent studies suggest that microtubules also play a role in defining the tail by redistributing inhibitory signals (Zhang *et al.*, 2014a).

1.3 Experimental techniques in cell mechanics

1.3.1 Control of mechanical forces experienced by adherent cells

The discovery that substrate stiffness affects almost all aspects of cell behavior was enabled by the use of hydrogels with tunable rigidity, usually polyacrylamide. By varying the ratio of acrylamide and bis-acrylamide crosslinker, the compliance of polyacrylamide hydrogels can be readily adjusted to match the compliance of soft tissues (Pelham & Wang, 1997; Tse & Engler, 2010). While conventional hydrogels have a Young's modulus that remains constant in space and time, a number of strategies have been explored to create hydrogel substrates with dynamic properties. Efforts to create stiffness gradients have included casting thin polyacrylamide gels over a stiff topography (Kuo *et al.*, 2012) and layering polyacrylamide with different degrees of crosslinking over each other (Choi *et al.*, 2012). Inclusion of a UV-sensitive crosslinker into polyacrylamide gels allowed spatiotemporal control over substrate softening. This technique was used to observe cell behavior in response to localized softening at the front or at the tail of polarized NIH 3T3 cells, and results indicated that rigidity sensing occurs at the cell anterior (Frey & Wang, 2009). Dynamic control of a three-dimensional cell culture system was developed with UV-degradable polyethylene glycol (PEG) hydrogels (Kloxin *et al.*, 2009). Others have explored ways to create stiffening substrates by modifying hyaluronic acid so that it gradually stiffens over time to match the mechanical properties of a developing chicken embryo heart. In that study, the authors found that cardiomyocyte maturation was enhanced on the time-stiffening substrate compared to a static susbtrate (Young & Engler, 2011). Alternative approaches for manipulating substrate rigidity include changes induced

by pH, temperature, enzymes (Vats & Benoit, 2013).

Micropatterning in biological applications makes it easy to isolate and study single cells or small defined groups of cells with high reproducibility and at high throughput. Early biological applications employed microcontact printing of alkanethiols on gold surfaces; extracellular matrix protein was then adsorbed to the alkanethiol ink, and the remaining surface backfilled with non-adhesive polymers (Whitesides *et al.*, 2001). Others soon improvised methods to circumvent the need for gold deposition, fabrication of stamps, and the limited resolution of initial microcontact printing protocols. Deep-UV illumination through a chrome mask was used to pattern poly-L-lysine-grafted-polyethylene glycol on glass (Azioune *et al.*, 2009). A two-photon confocal microscope was used to ablate patterns into a polyvinyl alcohol monolayer coated on glass (Doyle *et al.*, 2009). ECM protein could then be adsorbed to uncovered glass surfaces. Micropatterning on soft hydrogels proved more difficult, and typically required an extra chemical activation step. Our lab developed a new protocol that allowed oxidized protein to be covalently linked directly into the hydrogel surface during the initial polymerization step (Figure 1.4) (Rape *et al.*, 2011). Dynamic micropatterning has been demonstrated with self-assembled monolayers that release patterned, confined cells upon stimulation. Electrochemical desorption was used to study polarization induced by cell shape (Jiang *et al.*, 2005), and UV-induced release of polyethylene glycol was used to study collective cell migration (Rolli *et al.*, 2012). Spatiotemporal patterning using lasers to ablate portions of a nonadhesive monolayer have been used to change cell shape in real time (Vignaud *et al.*, 2012).

Besides micropatterning and tuning substrate rigidity, other techniques to mechanically probe adherent cells have been developed. Microneedle manipulation of soft substrates has been used to observe reorientation of migration (Wang *et al.*,

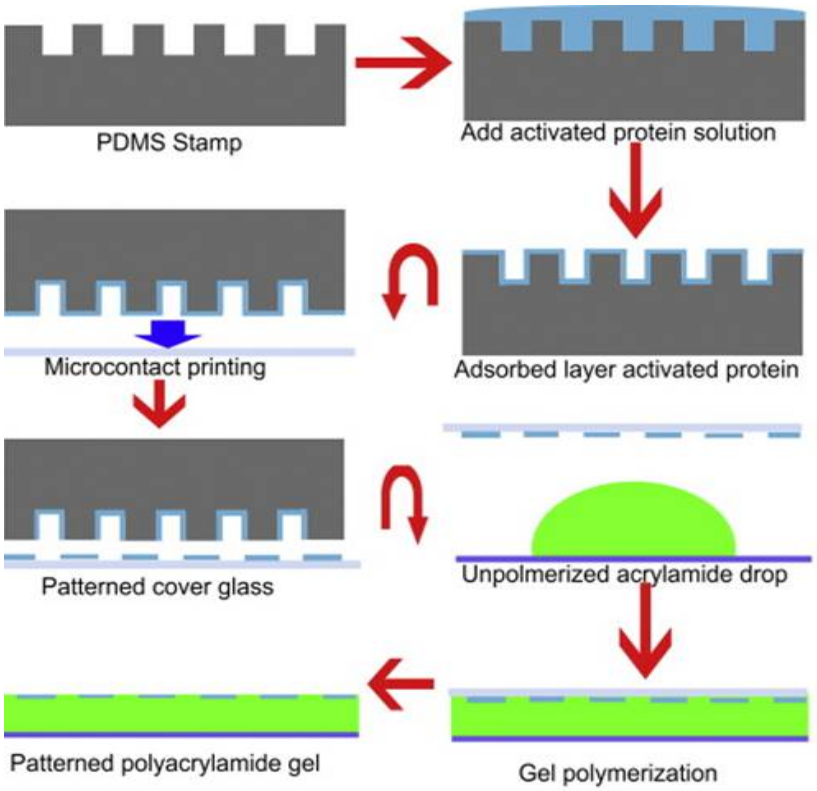

FIGURE 1.4. Micropatterning polyacrylamide gels with oxidized protein. Schematic describing our protocol for micropatterning soft hydrogels. The desired pattern is microcontact printed onto a small coverglass using a PDMS stamp coated with oxidized ECM protein. A drop of acrylamide solution is placed on a large coverslip that has been activated with Bind-Silane. The small coverglass containing the protein pattern is inverted on top of the acrylamide drop during polymerization. After polymerization is complete, the small coverglass is carefully removed to reveal a polyacrylamide hydrogel with ECM protein covalently linked directly into its surface. Adapted with permission from Elsevier: *Biomaterials* **32**: 2043-2051, copyright 2011 (Rape *et al.*, 2011).

2001a; Plotnikov *et al.*, 2012) and to study filopodia stability during cell spreading (Wong *et al.*, 2014). Laser ablation of actin stress fibers has been used to release isometric tension (Kumar *et al.*, 2006) and to initiate new leader cells in a migrating cell sheet (Reffay *et al.*, 2014). Application of shear flow and cyclic cell stretching has also been shown to affect cell organization and function, especially in endothelial cells (McCue *et al.*, 2004; Califano & Reinhart-King, 2010).

1.3.2 Measuring the mechanical output of the cell

Efforts to detect the mechanical output of adherent cells started with scientists plating cells on very thin silicone substrates and measuring the length of the resulting wrinkles (Harris & Wild, 1980). Traction force microscopy as we know it began with the development of polyacrylamide hydrogels embedded with fluorescent beads to act as fiduciary markers (Beningo & Wang, 2002). Bead position is imaged before and after removal of an adherent cell, bead displacement is calculated, and traction stress is numerically computed from the displacement field (Dembo & Wang, 1999). Efforts to improve the spatial resolution and the reconstruction of the traction field have since been introduced, including Fourier transform traction cytometry (Butler *et al.*, 2002), traction reconstruction with point forces (Schwarz *et al.*, 2002), use of two bead colors (Sabass *et al.*, 2008), and introduction of sparsity regularization (Han *et al.*, 2015).

Polydimethylsiloxane (PDMS) micropillars are a common alternative to flat polyacrylamide gels for measuring traction force. The micropillars are deflected when cells are plated on top, and force is easily calculated using beam bending equations (Tan *et al.*, 2003). The effective rigidity of the micropillars can be tuned without changing the geometry presented to the cell by changing the pillar length (Fu *et al.*,

2010). Using micropillars to measure traction force has the advantage of being less computationally intensive, and it facilitates measurement of traction force generated by collective cell migration (du Roure *et al.*, 2005). However, the micropillars are challenging to fabricate, the spatial resolution of traction is limited by the number of pillars, and the topography presented to cells is unnatural with likely effects on focal adhesion distribution.

Recently, two groups published separate methods to measure cell-generated forces using DNA tension probes (Blakely *et al.*, 2014; Zhang *et al.*, 2014b). The tension probes consist of DNA hairpins, a fluorophore-quencher pair, and an adhesive peptide. The DNA hairpins were designed to unravel in response to different levels of force such that the fluorophore is separated from its quencher to produce a high fluorescence signal. The number of force-transducing integrin receptors can be measured since each tension probe can only bind to a single receptor. This type of probe is able to report forces at a sub-focal adhesion resolution and is not restrained to hydrogels or pillars. However, the probes can only function as a switch, and are unable to report direction of traction and limited in range.

The development of three-dimensional traction force microscopy had been hampered by difficulties associated with imaging and tracking fiduciary markers in three-dimensions and with calculating forces from those deflections. A method to calculate traction forces generated by green fluorescent protein (GFP)-tagged fibroblasts encapsulated in PEG hydrogels was recently published (Legant *et al.*, 2010). Matrix deformations were visualized by tracking the displacement of 60,000-80,000 fluorescent beads near the cell. The cell was lysed with detergent to obtain a reference state, a discretized Greens function was applied to a finite element mesh generated around the cell boundary, and traction stress was obtained by numerical calculation. The

authors reported that the largest strains occur near long thin protrusions, suggesting that the lack of large focal adhesions does not hamper force generation. Tools tailored for cells in a three-dimensional environment are needed since cell migration in a three-dimensional matrix is known to differ from migration on a two-dimensional surface.

1.4 Mechanobiology offers insight into disease

Increased crosslinking following injury creates scar tissue that is significantly stiffer and may interfere with normal tissue function. This type of pathology is especially prevalent in cardiovascular and liver disease (Janmey & Miller, 2011). Cancer, too, is characterized by tumor formation caused by unregulated cell growth which results in a cell mass with different mechanical properties than the surrounding matrix (Paszek *et al.*, 2005). While cancerous tissue becomes more rigid, an increasing degree of fibroblast transformation corresponds with decreasing Young's modulus of the cell (Efremov *et al.*, 2014). Fibroblasts transformed with the *ras* oncogene also have unorganized traction forces which may underlie the irregular motility observed in these cells (Munevar *et al.*, 2001). A more recent study using cell lines derived from breast, prostate, and lung cancers found a positive correlation between traction stress and metastatic potential (Kraning-Rush *et al.*, 2012). Thus, disease progression changes the mechanics of the in vivo extracellular environment as well as the mechanical output of individual cells.

Changes in cell and tissue mechanics may also play a role in disease advancement. Increased actin-binding by a mutated form of α-actinin was shown to change force generation and to promote renal disease (Ehrlicher *et al.*, 2015). High mechanical stress promotes EMT in mouse mammary epithelial cells treated with transforming growth factor β (TGFβ) (Gomez *et al.*, 2010). Cancer cells were more invasive when mechanical stimulation was applied using a magnet to deform paramagnetic beads embedded within a substrate (Menon & Beningo, 2011). Increased matrix crosslinking has been shown to enhance integrin signaling to promote cancer malignancy (Levental *et al.*, 2009). Increasing matrix rigidity has also been linked to changes in signaling

pathways during disease progression. Stiff substrates lower the threshold of epidermal growth factor necessary to override contact inhibition of proliferation (Kim & Asthagiri, 2011). Stiff substrates also causes epithelial cells to undergo EMT instead of apoptosis after treatment with TGFβ (Leight *et al.*, 2012). These observations suggest that matrix stiffening is not just a byproduct but may play a role in cancer progression.

Recent efforts to test drug efficacy are starting to take into account how the mechanical environment affects cancer cell behavior. Results show that cancer cells respond differently to drug treatment depending on substrate dimension (Weigelt *et al.*, 2010) and matrix stiffness (Tokuda *et al.*, 2014). These results show that breast cancer cells readily adapt to different environments which may contribute to drug resistance. Signaling pathways that alter mechanical forces may also be targeted. The destabilizing effect on tissue architecture, which resulted from an increase in matrix stiffness and the corresponding increase in Rho activity, was reversed when extracellular signal-regulated kinase (ERK) activation or contractility was inhibited (Paszek *et al.*, 2005). Inhibition of lysyl oxidase (LOX)-dependent collagen crosslinking disrupted tumor progression (Levental *et al.*, 2009). The idea that tensional homeostasis is necessary for normal behavior (Paszek *et al.*, 2005) suggests a possible direction for the development of drug therapies.

1.5 Organization of the thesis

This thesis investigates mechanisms that adherent cells might employ to monitor physical parameters important in regulating cell processes. These parameters go beyond the well-established mechanobiology themes of cell size and shape or substrate rigidity and topography introduced above.

Physical features of the environment are well-known to cause changes in cell behavior. A switch from traditional two-dimensional experimental substrates to more physiologically relevant three-dimensional tissues dramatically changes cell morphology and migration characteristics. In Chapter 2, I test the hypothesis that a migrating cell is able to sense and respond to substrate dimension to control localization. I find that migrating NIH 3T3 fibroblasts use myosin II-dependent traction forces to distinguish between one-dimensional lines and two-dimensional surfaces. I also show that oncogene-transformed fibroblasts are unable to differentiate between one-dimensional and two-dimensional substrates, a mechanosensing defect which may contribute to the invasive behavior observed in transformed cells. This work is published in *Biophysical Journal* (Chang *et al.*, 2013).

An adherent cell utilizes various mechanosensing mechanisms to probe physical aspects of its environment as well as to monitor internal conditions. Detecting mechanical perturbations allows the cell to control functions such as growth and differentiation in proper response to its environment. The goal of Chapter 3 is to demonstrate that the state of cell migration can also function as an input for mechanosensing purposes. I find that a migrating cell has significantly altered cellular mechanical output, focal adhesion dynamics, and internal signaling compared to a stationary cell. This work introduces the concept of migration sensing, in which an

adherent cell is able to regulate important cellular activities based on its migration state.

Force generation, regulation, and transmission to the extracellular environment rely on the cytoskeleton and focal adhesions. Though the role of actin in mechanotransduction is well studied, the mechanism of how microtubules regulate traction output remains elusive. In Chapter 4, I investigate the role of microtubules in migration-dependent regulation of mechanical output. I find that microtubule disruption induces a dramatic increase in cellular traction stress only in stationary cells. Inhibition of GSK3β, which promotes microtubule stabilization and upregulates the interaction between microtubules and CLASP, blocks this increase. These results suggest that microtubule interactions with focal adhesions differs in migrating and stationary cells, and these interactions help control mechanical output.

1.6 References

Alexandrova, Antonina Y., Arnold, Katya, Schaub, Sébastien, Vasiliev, Jury M., Meister, Jean-Jacques, Bershadsky, Alexander D., & Verkhovsky, Alexander B. 2008. Comparative Dynamics of Retrograde Actin Flow and Focal Adhesions: Formation of Nascent Adhesions Triggers Transition from Fast to Slow Flow. *PLoS One*, **3**(9), e3234.

Azioune, Ammar, Storch, Marko, Bornens, Michel, Théry, Manuel, & Piel, Matthieu. 2009. Simple and rapid process for single cell micro-patterning. *Lab Chip*, **9**(11), 1640–1642.

Baker, Brendon M, & Chen, Christopher S. 2012. Deconstructing the third dimension - how 3D culture microenvironments alter cellular cues. *J. Cell Sci.*, **125**(13), 3015–3024.

Balaban, Nathalie Q, Schwarz, Ulrich S, Riveline, Daniel, Goichberg, Polina, Tzur, Gila, Sabanay, Ilana, Mahalu, Diana, Safran, Sam, Bershadsky, Alexander, Addadi, Lia, & Geiger, Benjamin. 2001. Force and focal adhesion assembly: a close relationship studied using elastic micropatterned substrates. *Nat. Cell Biol.*, **3**(5), 466–472.

Beningo, Karen A, & Wang, Yu-Li. 2002. Flexible substrata for the detection of cellular traction forces. *Trends Cell Biol.*, **12**(2), 79–84.

Beningo, Karen A, Dembo, Micah, Kaverina, Irina, Small, J Victor, & Wang, Yu-li. 2001. Nascent focal adhesions are responsible for the generation of strong propulsive forces in migrating fibroblasts. *J. Cell Biol.*, **153**(4), 881–887.

Beningo, Karen A, Dembo, Micah, & Wang, Yu-Li. 2004. Responses of fibroblasts to anchorage of dorsal extracellular matrix receptors. *Proc. Natl. Acad. Sci.*, **101**(52), 18024–18029.

Blakely, Brandon L, Dumelin, Christoph E, Trappmann, Britta, McGregor, Lynn M, Choi, Colin K, Anthony, Peter C, Duesterberg, Van K, Baker, Brendon M, Block, Steven M, Liu, David R, & Chen, Christopher S. 2014. A DNA-based molecular probe for optically reporting cellular traction forces. *Nat. Methods*, **11**(12), 1229–1232.

Brouhard, G. J. 2015. Dynamic instability 30 years later: complexities in microtubule growth and catastrophe. *Mol. Biol. Cell*, **26**(7), 1207–1210.

Burridge, Keith, & Wennerberg, Krister. 2004. Rho and Rac Take Center Stage Review. *Cell*, **116**, 167–179.

Butler, James P, Tolić-Nø rrelykke, Iva Marija, Fabry, Ben, & Fredberg, Jeffrey J. 2002. Traction fields, moments, and strain energy that cells exert on their surroundings. *Am. J. Physiol. Cell Physiol.*, **282**(3), C595–C605.

Califano, Joseph P, & Reinhart-King, Cynthia A. 2010. Exogenous and endogenous force regulation of endothelial cell behavior. *J. Biomech.*, **43**(1), 79–86.

Carisey, Alex, Tsang, Ricky, Greiner, Alexandra M, Nijenhuis, Nadja, Heath, Nikki, Nazgiewicz, Alicja, Kemkemer, Ralf, Derby, Brian, Spatz, Joachim, & Ballestrem, Christoph. 2013. Vinculin regulates the recruitment and release of core focal adhesion proteins in a force-dependent manner. *Curr. Biol.*, **23**(4), 271–281.

Case, Lindsay B, Baird, Michelle A, Shtengel, Gleb, Campbell, Sharon L, Hess, Harald F, Davidson, Michael W, & Waterman, Clare M. 2015. Molecular mechanism of vinculin activation and nanoscale spatial organization in focal adhesions. *Nat. Cell Biol.*, **17**(7), 880–892.

Chang, StephanieS., Guo, Wei-hui, Kim, Youngeun, & Wang, Yu-li. 2013. Guidance of Cell Migration by Substrate Dimension. *Biophys. J.*, **104**(2), 313–321.

Chang, Yuan-Chen, Nalbant, Perihan, Birkenfeld, Jörg, Chang, Zee-Fen, & Bokoch, Gary M. 2008. GEF-H1 Couples Nocodazole-induced Microtubule Disassembly to Cell Contractility via RhoA. *Mol. Biol. Cell*, **19**(5), 2147–2153.

Chen, Christopher S, Mrksich, Milan, Huang, Sui, Whitesides, George M, & Ingber, Donald E. 1997. Geometric Control of Cell Life and Death. *Science*, **276**(5317), 1425–1428.

Chen, Hui, Cohen, Daniel M, Choudhury, Dilshad M, Kioka, Noriyuki, & Craig, Susan W. 2005. Spatial distribution and functional significance of activated vinculin in living cells. *J. Cell Biol.*, **169**(3), 459–470.

Choi, Colin K, Zareno, Jessica, Digman, Michelle A, Gratton, Enrico, & Horwitz, Alan Rick. 2011. Cross-correlated fluctuation analysis reveals phosphorylation-

regulated paxillin-FAK complexes in nascent adhesions. *Biophys. J.*, **100**(3), 583–592.

Choi, Yu Suk, Vincent, Ludovic G, Lee, Andrew R, Kretchmer, Kyle C, Chirasatitsin, Somyot, Dobke, Marek K, & Engler, Adam J. 2012. The alignment and fusion assembly of adipose-derived stem cells on mechanically patterned matrices. *Biomaterials*, **33**(29), 6943–6951.

Chrzanowska-Wodnicka, Magdalena, & Burridge, Keith. 1996. Rho-stimulated Contractiliry Drives the Formation of Stress Fibers and Focal Adhesions. *J. Cell Biol.*, **133**(6), 1403–1415.

Cukierman, Edna, Pankov, Roumen, & Yamada, Kenneth M. 2002. Cell interactions with three-dimensional matrices. *Curr. Opin. Cell Biol.*, **14**(5), 633–639.

Curtis, Adam, & Wilkinson, Chris. 1997. Topographical control of cells. *Biomaterials*, **18**(24), 1573–1583.

Danowski, Barbara A. 1989. Fibroblast contractility and actin organization are stimulated by microtubule inhibitors. *J. Cell Sci.*, **93**(3280), 255–266.

del Rio, Armando, Perez-Jimenez, Raul, Liu, Ruchuan, Roca-Cusachs, Pere, Fernandez, Julio M, & Sheetz, Michael P. 2009. Stretching single talin rod molecules activates vinculin binding. *Science*, **323**(5914), 638–641.

Dembo, Micah, & Wang, Yu-Li. 1999. Stresses at the cell-to-substrate interface during locomotion of fibroblasts. *Biophys. J.*, **76**(4), 2307–2316.

Discher, Dennis E, Janmey, Paul, & Wang, Yu-Li. 2005. Tissue cells feel and respond to the stiffness of their substrate. *Science*, **310**(5751), 1139–1143.

Doyle, Andrew D, Wang, Francis W, Matsumoto, Kazue, & Yamada, Kenneth M. 2009. One-dimensional topography underlies three-dimensional fibrillar cell migration. *J. Cell Biol.*, **184**(4), 481–490.

du Roure, Olivia, Saez, Alexandre, Buguin, Axel, Austin, Robert H, Chavrier, Philippe, Silberzan, Pascal, & Ladoux, Benoit. 2005. Force mapping in epithelial cell migration. *Proc. Natl. Acad. Sci.*, **102**(7), 2390–2395.

Efremov, Yu M, Lomakina, M E, Bagrov, D V, Makhnovskiy, P I, Alexandrova, A Y, Kirpichnikov, M P, & Shaitan, K V. 2014. Mechanical properties of fibroblasts

depend on level of cancer transformation. *Biochim. Biophys. Acta*, **1843**(5), 1013–1019.

Ehrlicher, Allen J, Krishnan, Ramaswamy, Guo, Ming, Bidan, Cécile M, Weitz, David A, & Pollak, Martin R. 2015. Alpha-actinin binding kinetics modulate cellular dynamics and force generation. *Proc. Natl. Acad. Sci.*, **112**(21), 6619–6624.

Engler, Adam J, Griffin, Maureen A, Sen, Shamik, Bönnemann, Carsten G, Sweeney, H Lee, & Discher, Dennis E. 2004. Myotubes differentiate optimally on substrates with tissue-like stiffness: pathological implications for soft or stiff microenvironments. *J. Cell Biol.*, **166**(6), 877–887.

Engler, Adam J, Sen, Shamik, Sweeney, H Lee, & Discher, Dennis E. 2006. Matrix elasticity directs stem cell lineage specification. *Cell*, **126**(4), 677–689.

Etienne-Manneville, Sandrine. 2013. Microtubules in Cell Migration. *Annu. Rev. Cell Dev. Biol.*, **29**(1), 471–499.

Ezratty, Ellen J, Partridge, Michael A, & Gundersen, Gregg G. 2005. Microtubule-induced focal adhesion disassembly is mediated by dynamin and focal adhesion kinase. *Nat. Cell Biol.*, **7**(6), 581–590.

Fraley, Stephanie I, Feng, Yunfeng, Giri, Anjil, Longmore, Gregory D, & Wirtz, Denis. 2012. Dimensional and temporal controls of three-dimensional cell migration by zyxin and binding partners. *Nat. Commun.*, **3**(Mar.), 719.

Frey, Margo T, & Wang, Yu-li. 2009. A photo-modulatable material for probing cellular responses to substrate rigidity. *Soft Matter*, **5**(9), 1918–1924.

Friedland, Julie C, Lee, Mark H, & Boettiger, David. 2009. Mechanically Activated Integrin Switch Controls $\alpha 5\beta 1$ Function. *Science*, **323**(5914), 642–644.

Fu, Jianping, Wang, Yang-Kao, Yang, Michael T, Desai, Ravi A, Yu, Xiang, Liu, Zhijun, & Chen, Christopher S. 2010. Mechanical regulation of cell function with geometrically modulated elastomeric substrates. *Nat. Methods*, **7**(9), 733–736.

Galbraith, Catherine G, Yamada, Kenneth M, & Sheetz, Michael P. 2002. The relationship between force and focal complex development. *J. Cell Biol.*, **159**(4), 695–705.

Ghibaudo, Marion, Trichet, Léa, Le Digabel, Jimmy, Richert, Alain, Hersen, Pascal, & Ladoux, Benoît. 2009. Substrate topography induces a crossover from 2D to 3D behavior in fibroblast migration. *Biophys. J.*, **97**(1), 357–368.

Gittes, F., Mickey, B., Nettleton, J., & Howard, J. 1993. Flexural rigidity of microtubules and actin filaments measured from thermal fluctuations in shape. *J. Cell Biol.*, **120**(4), 923–934.

Gomez, Esther W, Chen, Qike K, Gjorevski, Nikolce, & Nelson, Celeste M. 2010. Tissue geometry patterns epithelial-mesenchymal transition via intercellular mechanotransduction. *J. Cell. Biochem.*, **110**(1), 44–51.

Grinnell, Frederick, Ho, Chin-Han, Tamariz, Elisa, Lee, David J, & Skuta, Gabriella. 2003. Dendritic Fibroblasts in Three-dimensional Collagen Matrices. *Mol. Biol. Cell*, **14**(2), 384–395.

Gundersen, Gregg G, & Bulinski, Jeannette Chloë. 1988. Selective stabilization of microtubules oriented toward the direction of cell migration. *Proc. Natl. Acad. Sci.*, **85**(16), 5946–5950.

Guo, Wei-hui, Frey, Margo T, Burnham, Nancy A, & Wang, Yu-li. 2006. Substrate rigidity regulates the formation and maintenance of tissues. *Biophys. J.*, **90**(6), 2213–2220.

Hamadi, Abdelkader, Bouali, Maya, Dontenwill, Monique, Stoeckel, Herrade, Takeda, Kenneth, & Rondé, Philippe. 2005. Regulation of focal adhesion dynamics and disassembly by phosphorylation of FAK at tyrosine 397. *J. Cell Sci.*, **118**(19), 4415–4425.

Han, Sangyoon J, Oak, Youbean, Groisman, Alex, & Danuser, Gaudenz. 2015. Traction microscopy to identify force modulation in subresolution adhesions. *Nat. Methods*, **12**(7), 653–656.

Harris, Albert K, & Wild, Patricia. 1980. Silicone rubber substrata: a new wrinkle in the study of cell locomotion. *Science*, **208**(4440), 177–179.

Hotulainen, Pirta. 2006. Stress fibers are generated by two distinct actin assembly mechanisms in motile cells. *J. Cell Biol.*, **173**(3), 383–394.

Humphries, Jonathan D, Wang, Pengbo, Streuli, Charles, Geiger, Benny, Humphries,

Martin J, & Ballestrem, Christoph. 2007. Vinculin controls focal adhesion formation by direct interactions with talin and actin. *J. Cell Biol.*, **179**(5), 1043–1057.

Janmey, Paul A, & Miller, R Tyler. 2011. Mechanisms of mechanical signaling in development and disease. *J. Cell Sci.*, **124**(1), 9–18.

Jiang, Xingyu, Bruzewicz, Derek A, Wong, Amy P, Piel, Matthieu, & Whitesides, George M. 2005. Directing cell migration with asymmetric micropatterns. *Proc. Natl. Acad. Sci.*, **102**(4), 975–978.

Kanchanawong, Pakorn, Shtengel, Gleb, Pasapera, Ana M, Ramko, Ericka B, Davidson, Michael W, Hess, Harald F, & Waterman, Clare M. 2010. Nanoscale architecture of integrin-based cell adhesions. *Nature*, **468**(7323), 580–584.

Karakesisoglou, Iakowos, Yang, Yanmin, & Fuchs, Elaine. 2000. An Epidermal Plakin that Integrates Actin and Microtubule Networks at Cellular Junctions. *J. Cell Biol.*, **149**(1), 195–208.

Kaverina, Irina, Rottner, Klemens, & Small, J Victor. 1998. Targeting, capture, and stabilization of microtubules at early focal adhesions. *J. Cell Biol.*, **142**(1), 181–190.

Kaverina, Irina, Krylyshkina, Olga, & Small, J Victor. 1999. Microtubule Targeting of Substrate Contacts Promotes Their Relaxation and Dissociation. *J. Cell Biol.*, **146**(5), 1033–1043.

Kilian, Kristopher A, Bugarija, Branimir, Lahn, Bruce T, & Mrksich, Milan. 2010. Geometric cues for directing the differentiation of mesenchymal stem cells. *Proc. Natl. Acad. Sci.*, **107**(11), 4872–4877.

Kim, Deok-Ho, Han, Karam, Gupta, Kshitiz, Kwon, Keon W, Suh, Kahp-Yang, & Levchenko, Andre. 2009. Mechanosensitivity of fibroblast cell shape and movement to anisotropic substratum topography gradients. *Biomaterials*, **30**(29), 5433–5444.

Kim, Jin-Hong, & Asthagiri, Anand R. 2011. Matrix stiffening sensitizes epithelial cells to EGF and enables the loss of contact inhibition of proliferation. *J. Cell Sci.*, **124**(8), 1280–1287.

Kloxin, April M, Kasko, Andrea M, Salinas, Chelsea N, & Anseth, Kristi S.

2009. Photodegradable Hydrogels for Dynamic Tuning of Physical and Chemical Properties. *Science*, **324**(5923), 59–63.

Kraning-Rush, Casey M, Califano, Joseph P, & Reinhart-King, Cynthia A. 2012. Cellular traction stresses increase with increasing metastatic potential. *PLoS One*, **7**(2), e32572.

Krendel, Mira, Zenke, Frank T, & Bokoch, Gary M. 2002. Nucleotide exchange factor GEF-H1 mediates cross-talk between microtubules and the actin cytoskeleton. *Nat. Cell Biol.*, **4**(4), 294–301.

Krylyshkina, Olga, Kaverina, Irina, Kranewitter, Wolfgang, Steffen, Walter, Alonso, Maria C, Cross, Robert a, & Small, J Victor. 2002. Modulation of substrate adhesion dynamics via microtubule targeting requires kinesin-1. *J. Cell Biol.*, **156**(2), 349–359.

Kumar, Sanjay, Maxwell, Iva Z, Heisterkamp, Alexander, Polte, Thomas R, Lele, Tanmay P, Salanga, Matthew, Mazur, Eric, & Ingber, Donald E. 2006. Viscoelastic retraction of single living stress fibers and its impact on cell shape, cytoskeletal organization, and extracellular matrix mechanics. *Biophys. J.*, **90**(10), 3762–3773.

Kuo, Cheng-Hwa R, Xian, Jian, Brenton, James D, Franze, Kristian, & Sivaniah, Easan. 2012. Complex stiffness gradient substrates for studying mechanotactic cell migration. *Adv. Mater.*, **24**(45), 6059–6064.

Kwak, Tae Kyoung, Lee, Mi-Sook, Ryu, Jihye, Choi, Yoon-Ju, Kang, Minkyung, Jeong, Doyoung, & Lee, Jung Weon. 2012. Cell adhesion-dependent serine 85 phosphorylation of paxillin modulates focal adhesion formation and haptotactic migration via association with the C-terminal tail domain of talin. *J. Biol. Chem.*, **287**(33), 27499–27509.

Lauffenburger, Douglas A, & Horwitz, Alan F. 1996. Cell Migration : A Physically Integrated Molecular Process. *Cell*, **84**(3), 359–369.

Lawson, Christine, Lim, Ssang-Taek, Uryu, Sean, Chen, Xiao Lei, Calderwood, David A., & Schlaepfer, David D. 2012. FAK promotes recruitment of talin to nascent adhesions to control cell motility. *J. Cell Biol.*, **196**(2), 223–232.

Legant, Wesley R, Miller, Jordan S, Blakely, Brandon L, Cohen, Daniel M, Genin,

Guy M, & Chen, Christopher S. 2010. Measurement of mechanical tractions exerted by cells in three-dimensional matrices. *Nat. Methods*, **7**(12), 969–971.

Leight, Jennifer L, Wozniak, Michele A, Chen, Sophia, Lynch, Michelle L, & Chen, Christopher S. 2012. Matrix rigidity regulates a switch between TGF- 1-induced apoptosis and epithelial-mesenchymal transition. *Mol. Biol. Cell*, **23**(5), 781–791.

Levental, Kandice R, Yu, Hongmei, Kass, Laura, Lakins, Johnathon N, Egeblad, Mikala, Erler, Janine T, Fong, Sheri F T, Csiszar, Katalin, Giaccia, Amato, Weninger, Wolfgang, Yamauchi, Mitsuo, Gasser, David L, & Weaver, Valerie M. 2009. Matrix Crosslinking Forces Tumor Progression by Enhancing Integrin Signaling. *Cell*, **139**(5), 891–906.

Li, Bin, Li, Fang, Puskar, Kathleen M, & Wang, James H-C. 2010. Depends on Mechanical Stress Magnitude. *J. Biomech.*, **42**(11), 1622–1627.

Li, Fang, Li, Bin, Wang, Qing-Ming, & Wang, James H-C. 2008. Cell shape regulates collagen type I expression in human tendon fibroblasts. *Cell Motil. Cytoskeleton*, **65**(4), 332–341.

Lo, Chun-Min, Wang, Hong-Bei, Dembo, Micah, & Wang, Yu-Li. 2000. Cell movement is guided by the rigidity of the substrate. *Biophys. J.*, **79**(1), 144–152.

Machacek, Matthias, Hodgson, Louis, Welch, Christopher, Elliott, Hunter, Pertz, Olivier, Nalbant, Perihan, Abell, Amy, Johnson, Gary L, Hahn, Klaus M, & Danuser, Gaudenz. 2009. Coordination of Rho GTPase activities during cell protrusion. *Nature*, **461**(7260), 99–103.

McBeath, Rowena, Pirone, Dana M, Nelson, Celeste M, Bhadriraju, Kiran, & Chen, Christopher S. 2004. Cell shape, cytoskeletal tension, and RhoA regulate stem cell lineage commitment. *Dev. Cell*, **6**(4), 483–495.

McCue, Shannon, Noria, Sabrena, & Langille, B. Lowell. 2004. Shear-induced reorganization of endothelial cell cytoskeleton and adhesion complexes. *Trends Cardiovasc. Med.*, **14**(4), 143–151.

McWhorter, Frances Y, Wang, Tingting, Nguyen, Phoebe, Chung, Thanh, & Liu, Wendy F. 2013. Modulation of macrophage phenotype by cell shape. *Proc. Natl. Acad. Sci.*, **110**(43), 17253–17258.

Menon, Shalini, & Beningo, Karen A. 2011. Cancer Cell Invasion Is Enhanced by Applied Mechanical Stimulation. *PLoS One*, **6**(2), e17277.

Mimori-Kiyosue, Yuko, Grigoriev, Ilya, Lansbergen, Gideon, Sasaki, Hiroyuki, Matsui, Chiyuki, Severin, Fedor, Galjart, Niels, Grosveld, Frank, Vorobjev, Ivan, Tsukita, Shoichiro, & Akhmanova, Anna. 2005. CLASP1 and CLASP2 bind to EB1 and regulate microtubule plus-end dynamics at the cell cortex. *J. Cell Biol.*, **168**(1), 141–153.

Munevar, Steven, Wang, Yu-Li, & Dembo, Micah. 2001. Traction Force Microscopy of Migrating Normal and H-ras Transformed 3T3 Fibroblasts. *Biophys. J.*, **80**(4), 1744–1757.

Nalbant, Perihan, Chang, Yuan-chen, Chang, Zee-fen, & Bokoch, Gary M. 2009. Guanine Nucleotide Exchange Factor-H1 Regulates Cell Migration via Localized Activation of RhoA at the Leading Edge. *Mol. Biol. Cell*, **20**, 4070–4082.

Näthke, Inke S, Adams, Cynthia L, Polakis, Paul, Sellin, Joseph H, & Nelson, W James. 1996. The Adenomatous Polyposis Coli Tumor Suppressor Protein Localizes to Plasma Membrane Sites Involved in Active Cell Migration. *J. Cell Biol.*, **134**(1), 165–179.

Nelson, Celeste M, Khauv, Davitte, Bissell, Mina J, & Radisky, Derek C. 2008. Change in cell shape is required for matrix metalloproteinase-induced epithelial-mesenchymal transition of mammary epithelial cells. *J. Cell. Biochem.*, **105**(1), 25–33.

Oh, Seunghan, Brammer, Karla S, Li, Y S Julie, Teng, Dayu, Engler, Adam J, Chien, Shu, & Jin, Sungho. 2009. Stem cell fate dictated solely by altered nanotube dimension. *Proc. Natl. Acad. Sci.*, **106**(7), 2130–2135.

Palazzo, Alexander F, Eng, Christina H, Schlaepfer, David D, Marcantonio, Eugene E, & Gundersen, Gregg G. 2004. Localized stabilization of microtubules by integrin- and FAK-facilitated Rho signaling. *Science*, **303**(5659), 836–839.

Pasapera, Ana M, Schneider, Ian C, Rericha, Erin, Schlaepfer, David D, & Waterman, Clare M. 2010. Myosin II activity regulates vinculin recruitment to focal adhesions through FAK-mediated paxillin phosphorylation. *J. Cell Biol.*, **188**(6), 877–890.

Paszek, Matthew J, Zahir, Nastaran, Johnson, Kandice R, Lakins, Johnathon N, Rozenberg, Gabriela I, Gefen, Amit, Reinhart-King, Cynthia a, Margulies, Susan S, Dembo, Micah, Boettiger, David, Hammer, Daniel a, & Weaver, Valerie M. 2005. Tensional homeostasis and the malignant phenotype. *Cancer Cell*, **8**(3), 241–254.

Pathak, Amit, & Kumar, Sanjay. 2012. Independent regulation of tumor cell migration by matrix stiffness and confinement. *Proc. Natl. Acad. Sci.*, **109**(26), 10334–10339.

Pelham, Robert J, & Wang, Yu-Li. 1997. Cell locomotion and focal adhesions are regulated by substrate flexibility. *Proc. Natl. Acad. Sci.*, **94**(25), 13661–13665.

Pellegrin, Stéphanie, & Mellor, Harry. 2007. Actin stress fibres. *J. Cell Sci.*, **120**(20), 3491–3499.

Plotnikov, Sergey V, Pasapera, Ana M, Sabass, Benedikt, & Waterman, Clare M. 2012. Force Fluctuations within Focal Adhesions Mediate ECM-Rigidity Sensing to Guide Directed Cell Migration. *Cell*, **151**(7), 1513–1527.

Pollard, Thomas D, & Cooper, John A. 2009. Actin, a central player in cell shape and movement. *Science*, **326**(5957), 1208–1212.

Prager-Khoutorsky, Masha, Lichtenstein, Alexandra, Krishnan, Ramaswamy, Rajendran, Kavitha, Mayo, Avi, Kam, Zvi, Geiger, Benjamin, & Bershadsky, Alexander D. 2011. Fibroblast polarization is a matrix-rigidity-dependent process controlled by focal adhesion mechanosensing. *Nat. Cell Biol.*, **13**(12), 1457–1465.

Rajnicek, Ann M, Britland, Stephen, & McCaig, Colin D. 1997. Contact guidance of CNS neurites on grooved quartz: influence of groove dimensions, neuronal age and cell type. *J. Cell Sci.*, **110**, 2905–2913.

Rape, Andrew D, Guo, Wei-Hui, & Wang, Yu-Li. 2011. The regulation of traction force in relation to cell shape and focal adhesions. *Biomaterials*, **32**(8), 2043–2051.

Reffay, M, Parrini, M C, Cochet-Escartin, O, Ladoux, B, Buguin, A, Coscoy, S, Amblard, F, Camonis, J, & Silberzan, P. 2014. Interplay of RhoA and mechanical forces in collective cell migration driven by leader cells. *Nat. Cell Biol.*, **16**(3), 217–223.

Ren, Xiang-Dong, Kiosses, William B, & Schwartz, Martin A. 1999. Regulation of

the small GTP-binding protein Rho by cell adhesion and the cytoskeleton. *EMBO J.*, **18**(3), 578–585.

Ren, Xiang-Dong, Kiosses, William B, Sieg, David J, Otey, Carol A, Schlaepfer, David D, & Schwartz, Martin A. 2000. Focal adhesion kinase suppresses Rho activity to promote focal adhesion turnover. *J. Cell Sci.*, **113**(Oct.), 3673–3678.

Ridley, Anne J, Schwartz, Martin A, Burridge, Keith, Firtel, Richard A, Ginsberg, Mark H, Borisy, Gary, Parsons, J Thomas, & Horwitz, Alan Rick. 2003. Cell migration: integrating signals from front to back. *Science*, **302**(5651), 1704–1709.

Rolli, Claudio G, Nakayama, Hidekazu, Yamaguchi, Kazuo, Spatz, Joachim P, Kemkemer, Ralf, & Nakanishi, Jun. 2012. Switchable adhesive substrates : Revealing geometry dependence in collective cell behavior. *Biomaterials*, **33**(8), 2409–2418.

Sabass, Benedikt, Gardel, Margaret L, Waterman, Clare M, & Schwarz, Ulrich S. 2008. High resolution traction force microscopy based on experimental and computational advances. *Biophys. J.*, **94**(1), 207–220.

Schwarz, U S, Balaban, N Q, Riveline, D, Bershadsky, A, Geiger, B, & Safran, S A. 2002. Calculation of Forces at Focal Adhesions from Elastic Substrate Data: The Effect of Localized Force and the Need for Regularization. *Biophys. J.*, **83**(3), 1380–1394.

Stehbens, Samantha, & Wittmann, Torsten. 2012. Targeting and transport: How microtubules control focal adhesion dynamics. *J. Cell Biol.*, **198**(4), 481–489.

Stehbens, Samantha J, Paszek, Matthew, Pemble, Hayley, Ettinger, Andreas, Gierke, Sarah, & Wittmann, Torsten. 2014. CLASPs link focal-adhesion-associated microtubule capture to localized exocytosis and adhesion site turnover. *Nat. Cell Biol.*, **16**(6), 561–573.

Stricker, Jonathan, Aratyn-Schaus, Yvonne, Oakes, Patrick W, & Gardel, Margaret L. 2011. Spatiotemporal constraints on the force-dependent growth of focal adhesions. *Biophys. J.*, **100**(12), 2883–2893.

Tan, John L, Tien, Joe, Pirone, Dana M, Gray, Darren S, Bhadriraju, Kiran, & Chen,

Christopher S. 2003. Cells lying on a bed of microneedles: an approach to isolate mechanical force. *Proc. Natl. Acad. Sci.*, **100**(4), 1484–1489.

Teixeira, Ana I, Abrams, George A, Bertics, Paul J, Murphy, Christopher J, & Nealey, Paul F. 2003. Epithelial contact guidance on well-defined micro- and nanostructured substrates. *J. Cell Sci.*, **116**, 1881–1892.

Thakar, Rahul G., Cheng, Qian, Patel, Shyam, Chu, Julia, Nasir, Mansoor, Liepmann, Dorian, Komvopoulos, Kyriakos, & Li, Song. 2009. Cell-shape regulation of smooth muscle cell proliferation. *Biophys. J.*, **96**(8), 3423–3432.

Thievessen, Ingo, Thompson, Peter M, Berlemont, Sylvain, Plevock, Karen M, Plotnikov, Sergey V, Zemljic-Harpf, Alice, Ross, Robert S, Davidson, Michael W, Danuser, Gaudenz, Campbell, Sharon L, & Waterman, Clare M. 2013. Vinculin-actin interaction couples actin retrograde flow to focal adhesions, but is dispensable for focal adhesion growth. *J. Cell Biol.*, **202**(1), 163–177.

Tijore, Ajay, Wen, Feng, Lam, Chee Ren Ivan, Tay, Chor Yong, & Tan, Lay Poh. 2014. Modulating Human Mesenchymal Stem Cell Plasticity Using Micropatterning Technique. *PLoS One*, **9**(11), e113043.

Tojkander, Sari, Gateva, Gergana, & Lappalainen, Pekka. 2012. Actin stress fibers - assembly, dynamics and biological roles. *J. Cell Sci.*, **125**(8), 1855–1864.

Tokuda, Emi Y, Leight, Jennifer L, & Anseth, Kristi S. 2014. Modulation of matrix elasticity with PEG hydrogels to study melanoma drug responsiveness. *Biomaterials*, **35**(14), 4310–4318.

Totsukawa, Go, Yamakita, Yoshihiko, Yamashiro, Shigeko, Hartshorne, David J, Sasaki, Yasuharu, & Matsumura, Fumio. 2000. Distinct Roles of ROCK (Rho-kinase) and MLCK in Spatial Regulation of MLC Phosphorylation for Assembly of Stress Fibers and Focal Adhesions in 3T3 Fibroblasts. *J. Cell Biol.*, **150**(4), 797–806.

Trichet, Léa, Le Digabel, Jimmy, Hawkins, Rhoda J, Vedula, Sri Ram Krishna, Gupta, Mukund, Ribrault, Claire, Hersen, Pascal, Voituriez, Raphael, & Ladoux, Benoit. 2012. Evidence of a large-scale mechanosensing mechanism for cellular adaptation to substrate stiffness. *Proc. Natl. Acad. Sci.*, **109**(18), 6933–6938.

Tse, Justin R, & Engler, Adam J. 2010. Preparation of Hydrogel Substrates with Tunable Mechanical Properties. *Pages 10.16.1–10.16.10 of: Curr. Protoc. Cell Biol.*, vol. 47. Hoboken, NJ, USA: John Wiley & Sons, Inc.

Vats, Kanika, & Benoit, Danielle S W. 2013. Dynamic Manipulation of Hydrogels to Control Cell Behavior: A Review. *Tissue Eng. Part B Rev.*, **19**(6), 455–469.

Vicente-Manzanares, Miguel, Choi, Colin Kiwon, & Horwitz, Alan Rick. 2009. Integrins in cell migration–the actin connection. *J. Cell Sci.*, **122**(2), 199–206.

Vignaud, Timothée, Galland, Rémi, Tseng, Qingzong, Blanchoin, Laurent, Colombelli, Julien, & Théry, Manuel. 2012. Reprogramming cell shape with laser nano-patterning. *J. Cell Sci.*, **125**(9), 2134–2140.

Wang, Hong-Bei, Dembo, Micah, & Wang, Yu-Li. 2000. Substrate flexibility regulates growth and apoptosis of normal but not transformed cells. *Am. J. Physiol. Cell Physiol.*, **279**(5), C1345–C1350.

Wang, Hong-Bei, Dembo, Micah, Hanks, Steven K, & Wang, Yu-li. 2001a. Focal adhesion kinase is involved in mechanosensing during fibroblast migration. *Proc. Natl. Acad. Sci.*, **98**(20), 11295–11300.

Wang, Ning, Naruse, Keiji, Stamenović, Dimitrije, Fredberg, Jeffrey J, Mijailovich, Srboljub M, Tolić-Nø rrelykke, Iva Marija, Polte, Thomas, Mannix, Robert, & Ingber, Donald E. 2001b. Mechanical behavior in living cells consistent with the tensegrity model. *Proc. Natl. Acad. Sci.*, **98**(14), 7765–7770.

Waterman-Storer, Clare M, & Salmon, E. 1999. Positive feedback interactions between microtubule and actin dynamics during cell motility. *Curr. Opin. Cell Biol.*, **11**(1), 61–67.

Watt, Fiona M, Jordan, Peter W, & O'Neill, Charles H. 1988. Cell shape controls terminal differentiation of human epidermal keratinocytes. *Proc. Natl. Acad. Sci.*, **85**(15), 5576–5580.

Wehrle-Haller, Bernhard. 2012. Structure and function of focal adhesions. *Curr. Opin. Cell Biol.*, **24**(1), 116–124.

Weigelt, Britta, Lo, Alvin T, Park, Catherine C, Gray, Joe W, & Bissell, Mina J. 2010. HER2 signaling pathway activation and response of breast cancer cells to

HER2-targeting agents is dependent strongly on the 3D microenvironment. *Breast Cancer Res. Treat.*, **122**(1), 35–43.

Whitesides, George M, Ostuni, Emanuele, Jiang, Xingyu, & Ingber, Donald E. 2001. Soft Lithography in Biology and Biochemistry. *Annu. Rev. Biomed. Eng.*, **3**, 335–373.

Wong, Stephanie, Guo, Wei-Hui, & Wang, Yu-Li. 2014. Fibroblasts probe substrate rigidity with filopodia extensions before occupying an area. *Proc. Natl. Acad. Sci.*, **111**(48), 17176–17181.

Xie, Jingwei, Willerth, Stephanie M, Li, Xiaoran, Macewan, Matthew R, Rader, Allison, Sakiyama-Elbert, Shelly E, & Xia, Younan. 2009. The differentiation of embryonic stem cells seeded on electrospun nanofibers into neural lineages. *Biomaterials*, **30**(3), 354–362.

Young, Jennifer L, & Engler, Adam J. 2011. Hydrogels with time-dependent material properties enhance cardiomyocyte differentiation in vitro. *Biomaterials*, **32**(4), 1002–1009.

Zaidel-Bar, Ronen, Milo, Ron, Kam, Zvi, & Geiger, Benjamin. 2007. A paxillin tyrosine phosphorylation switch regulates the assembly and form of cell-matrix adhesions. *J. Cell Sci.*, **120**(1), 137–148.

Zhang, Douglas, & Kilian, Kristopher A. 2013. The effect of mesenchymal stem cell shape on the maintenance of multipotency. *Biomaterials*, **34**(16), 3962–3969.

Zhang, Jian, Guo, Wei-Hui, & Wang, Yu-Li. 2014a. Microtubules stabilize cell polarity by localizing rear signals. *Proc. Natl. Acad. Sci.*, **111**(46), 16383–16388.

Zhang, Yun, Ge, Chenghao, Zhu, Cheng, & Salaita, Khalid. 2014b. DNA-based digital tension probes reveal integrin forces during early cell adhesion. *Nat. Commun.*, **5**(Oct.), 5167.

Zouani, Omar F, Chanseau, Christel, Brouillaud, Brigitte, Bareille, Reine, Deliane, Florent, Foulc, Marie-Pierre, Mehdi, Ahmad, & Durrieu, Marie-Christine. 2012. Altered nanofeature size dictates stem cell differentiation. *J. Cell Sci.*, **125**(5), 1217–1224.

Chapter 2

Guidance of Cell Migration by Substrate Dimension

There is increasing evidence to suggest that physical parameters, including substrate rigidity, topography, and cell geometry, play an important role in cell migration. As there are significant differences in cell behavior when cultured in 1D, 2D, or 3D environments, we hypothesize that migrating cells are also able to sense the dimension of the environment as a guidance cue. NIH 3T3 fibroblasts were cultured on micropatterned substrates where the path of migration alternates between 1D lines and 2D rectangles. We found that 3T3 cells had a clear preference to stay on 2D rather than 1D substrates. Cells on 2D surfaces generated stronger traction stress than did those on 1D surfaces, but inhibition of myosin II caused cells to lose their sensitivity to substrate dimension, suggesting that myosin-II-dependent traction forces are the determining factor for dimension sensing. Furthermore, oncogene-transformed fibroblasts are defective in mechanosensing while generating similar traction forces on 1D and 2D surfaces. Dimension sensing may be involved in guiding cell migration for both physiological functions and tissue engineering, and for maintaining normal cells in their home tissue.

2.1 Introduction

Cell migration is essential for many biological processes, including development and wound healing. Migration also plays a key role in cancer metastasis and tissue engineering. The process of cell migration involves tightly regulated cycles of polarization, cytoplasmic protrusion, and adhesion formation and detachment (Ridley *et al.*, 2003) guided by environmental cues. Although early work emphasized the role of chemical gradients, it is becoming evident that physical features of the substrate play an equally important role in guiding cell migration.

The effects of physical cues have been demonstrated in a variety of contexts. It has been known for decades that cells migrate preferentially along grooves on a substrate, a phenomenon referred to as contact guidance (Curtis & Wilkinson, 1997). Other surface topography, such as pillars, also affect cell shape and migration (Ghibaudo *et al.*, 2009; Frey *et al.*, 2006; Han *et al.*, 2012). Migrating fibroblasts also respond to substrate rigidity by moving toward stiffer substrates, and to stretching forces by reorienting in the direction of tensile forces (Lo *et al.*, 2000). By micropatterning adhesion areas, it was further discovered that spreading area and cell shape can profoundly affect traction forces (Rape *et al.*, 2011), differentiation (McBeath *et al.*, 2004), growth (Singhvi *et al.*, 1994), and apoptosis (Chen *et al.*, 1997).

Accumulating evidence indicates that adhesive cells respond profoundly to the dimension of adhesive surfaces. Most conventional studies have been performed in 2D environments, on either charged plastic or glass surfaces. Adhesive cells under such conditions form prominent actin bundles (stress fibers), large wedge-shaped focal adhesions, and broad lamellipodia (Hakkinen *et al.*, 2011). In contrast, cells migrating along narrow lines form fewer interior stress fibers but strong peripheral actin

bundles and small punctuate adhesion structures (Doyle *et al.*, 2009). Furthermore, centrosomes in cells on 1D substrate typically trail the nucleus (Doyle *et al.*, 2009), whereas centrosomes on 2D surfaces are typically located in front of the nucleus (Doyle *et al.*, 2009; Luxton & Gundersen, 2011). Cells in 3D extracellular matrices (ECMs) are often stellar in shape and share many characteristics with cells in 1D (Doyle *et al.*, 2009; Fraley *et al.*, 2012), likely due to the fibrillar structure of many ECM proteins.

Physical cues must be sensed by cells with some form of physical interactions. Traction forces, myosin-II-dependent mechanical forces exerted by adhesive cells on the substrate (Dembo & Wang, 1999; Legant *et al.*, 2010), were believed to be the driving force for cell migration (Munevar *et al.*, 2001a). However, there is increasing evidence to suggest that the role they play in sensing the physical environment and guiding cell migration (Lo *et al.*, 2000) is at least equal in importance. The concentration of active traction forces near the leading edge, where protrusion and steering of cell migration take place, supports this view (Dembo & Wang, 1999; Munevar *et al.*, 2001a). Traction forces may be used for probing the stiffness of the substrate based on the deformability of the material upon mechanical stress. Cell shape and size can also be measured based on the amount of traction force required to maintain a mechanical equilibrium (Rape *et al.*, 2011; Wang *et al.*, 2002). A similar mechanism may be used to detect whether a cell is spreading over 2D surfaces or stretching along a 1D line.

Given the sensitivity of cell structures to substrate dimension, we hypothesized that migrating cells may be able to use dimension as a guidance cue. However, most studies of cell migration have focused on cells migrating in a homogeneous dimension, whereas any systematic investigation of dimension-mediated guidance must place cells on substrates with changing dimension. In this study, we created such an environment

by micropatterning flexible polyacrylamide surfaces with alternating 1D lines and 2D rectangles of identical adhesiveness, which allowed us both to detect dimensional preference during cell migration and to measure the underlying traction stress. We further investigate whether dimension sensing might be impaired in transformed cells.

2.2 Methods and Materials

2.2.1 Preparation of Polyacrylamide Gels

Patterned polyacrylamide hydrogels were prepared as described previously (Rape *et al.*, 2011). A 0.1% solution of 50 Bloom gelatin was activated with 3.6 mg/mL sodium m-periodate (Sigma-Aldrich, St. Louis, MO) at room temperature for 30 min. A polydimethylsiloxane stamp was fabricated by standard soft lithography techniques and incubated with the activated gelatin solution for 45 min. Excess solution was blown away under a nitrogen stream and the stamp was brought into contact with a small glass coverslip for 5 min.

Polyacrylamide was prepared with a final concentration of 5% acrylamide (Bio-Rad, Hercules, CA), 0.1% bis-acrylamide (Bio-Rad), and a 1:2000 dilution of 0.2 μm fluorescent beads (Molecular Probes, Carlsbad, CA). Initiators ammonium persulfate (Sigma-Aldrich) and N,N,N',N' tetra-methylethylenediamine (Bio-Rad) were added to the acrylamide solution after degassing, and a 30 μL drop was pipetted onto a large coverslip activated with Bind-Silane (GE Healthcare, Waukesha, WI). The small stamped coverslip carrying activated gelatin was placed pattern-side down onto the acrylamide drop. After polymerization was complete, the top coverslip was gently removed. Patterned polyacrylamide hydrogels were mounted into chamber dishes, sterilized under ultraviolet light for 30 min, and incubated in cell culture media for 1 h at 37°C. The final gel had an estimated Young's modulus of 3.5 kPa.

2.2.2 Cell Culture and Microscopy

NIH 3T3 cells and PAP2 cells (Dr. Ann Chambers, London Regional Cancer Program, Ontario, Canada) were maintained in Dulbecco's modified Eagle's medium (Life Technologies, Carlsbad, CA) supplemented with 10% donor adult bovine serum (Thermo Scientific, Waltham, MA), 2mM L-glutamine, 50 μg/mL streptomycin, and 50 U/mL penicillin (Life Technologies). Cells were treated with 10 μM blebbistatin (Calbiochem, San Diego, CA) for 1 h to inhibit myosin contractility. In some experiments, cells were treated with 30 μM mitomycin (Calbiochem) for 2 h to inhibit mitosis.

Phase-contrast images of migrating cells were collected with a Nikon Eclipse Ti microscope using a 10X N.A. 0.3 Plan Fluor air objective (Nikon, Tokyo, Japan). Images were collected every 10 min for a period of 20 h. To avoid the influence that neighboring cells might have on migration, only single cells were counted. For quantification of migration parameters, phase-contrast images were collected using a 20X N.A. 0.5 Plan Fluor air objective (Nikon) every 2 min for a period of 6 h. Persistence is given as a ratio of net migration distance divided by the total pathlength.

Cells seeded on patterned substrates were fixed in 4% formaldehyde (Thermo) and stained with phalloidin (Molecular Probes, Eugene, OR), and antibodies against vinculin (Santa Cruz Biotechnology, Santa Cruz, CA) or Ser^{19}- phosphorylated myosin regulatory light chain (MRLC, Cell Signaling Technology, Danvers, MA). Fluorescence images were collected using a 100X oil immersion lens. Focal adhesion size was quantified by thresholding each image and creating a binary mask in ImageJ (National Institutes of Health, Bethesda, MD). Fluorescence intensity was measured

by subtracting the average background intensity and summing the total intensity over each cell using custom software.

2.2.3 Traction Force Microscopy

Phase-contrast images of single cells adhered to the pattern were collected with a Nikon Eclipse Ti microscope using a 40X N.A. 0.75 Plan Fluor air objective (Nikon). Fluorescent images of the embedded beads near the surface of the hydrogel were taken before and after cells were removed with 0.05% Trypsin-EDTA (Life Technologies) to remove traction forces. Cell outlines were manually drawn and bead displacement fields computed using custom software. Traction stress maps were computed using the LIBTRC package (Dr. Micah Dembo, Boston University, Boston, MA (Dembo & Wang, 1999)).

2.2.4 Statistical Analysis

The mean±SE was determined, and unpaired two-tailed t-tests were performed using the Analysis ToolPak in Microsoft Excel. To determine the significance of cell distribution in 2D versus 1D, the chi-square statistic was calculated and the corresponding p-value was obtained in Microsoft Excel. The number of cells observed for each experiment is indicated in the figure captions.

2.3 Results

2.3.1 Fibroblasts preferentially localize in 2D areas over 1D lines

To test the hypothesis that the dimension of the adhesive environment is able to guide cell migration, we designed micropatterned substrates such that migrating cells encounter alternating 1D and 2D environments. We define 1D as a strip sufficiently narrow to confine the trajectory of the nucleus along a straight line. Our pattern consisted of 50×100 μm rectangular 2D regions connected by 1D lines 10 μm in width and 400 μm length (Figure 2.1A). Substrates were generated by micropatterning gelatin on the surface of nonadhesive polyacrylamide sheets. Inadvertently we found that fluorescent polystyrene beads became more concen- trated in areas conjugated with gelatin than in areas without gelatin, thereby allowing easy detection of the micropattern (Figure 2.1B).

NIH 3T3 cells were allowed to adhere on the micropatterned substrate, and their

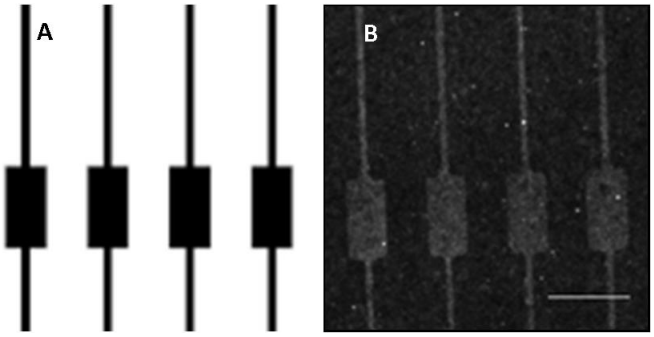

FIGURE 2.1. Micropattern with alternating 1D lines and 2D rectangles. The surface of polyacrylamide hydrogels is conjugated with gelatin in a defined micropattern (A), which is easily detected due to the concentration of fluorescent beads (B). Scale bar, 100 μm.

migration was recorded with time-lapse phase contrast microscopy. Preference between 1D and 2D regions was determined by counting the number of cells that were able to move across the dimension border versus those switching directions. We found that 100% of the cells entered 2D rectangular areas as they approached from a 1D line. These cells migrated persistently along the original direction (Table 2.2) until the frontal process exited the 2D region and entered the 1D line on the opposite side. The majority of these cells (63%, N = 62) then reversed the direction of migration and broke the persistence (Figure 2.2*A*). The response consequently caused cells to localize preferentially in 2D areas over time, such that the percentage of cells in 2D areas increased from 38% (N = 684) upon initial adhesion to 66% (N = 685) after 24 h of incubation (Figure 2.2*C*). This localization is not affected by cell proliferation, as similar results were obtained with cells maintained without or with mitomycin to inhibit mitosis. (Figure A.1).

2.3.2 Involvement of myosin II and traction forces in dimension sensing

Due to the implication of myosin-II-dependent traction forces in sensing various physical cues, we hypothesized that the response to substrate dimension is dependent on traction forces. If true, a decrease in traction forces should reduce the cells ability to sense dimension. To test this hypothesis, we treated cells on micropatterned substrates with a potent inhibitor of myosin II ATPase, blebbistatin (Straight *et al.*, 2003; Kovács *et al.*, 2004). Cells treated with 10 μM blebbistatin maintained both their motility and persistence along 1D lines (Doyle *et al.*, 2009; Guo & Wang, 2012), as well as their ability to enter from 1D into 2D regions. However, the majority of cells (72%,N = 36) continued with the migration and exited into 1D lines at the opposite

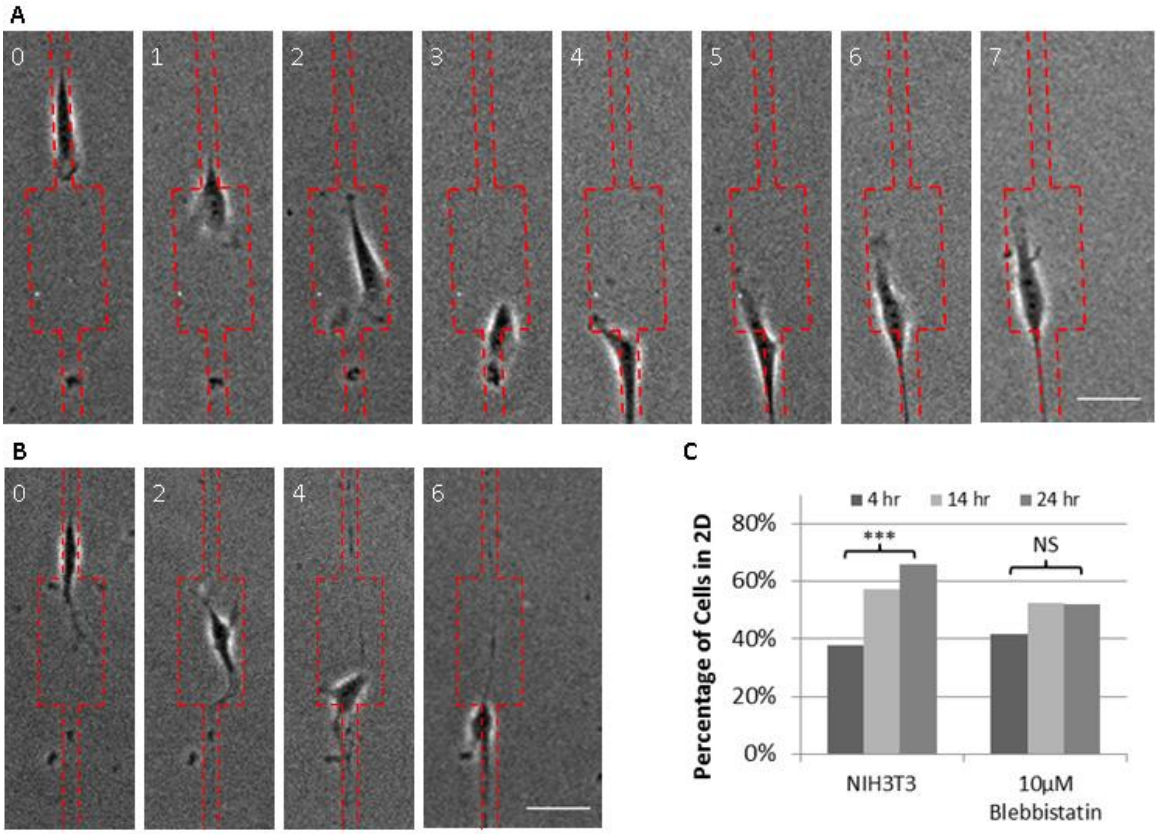

FIGURE 2.2. Different responses to the 1D-2D interface between normal and blebbistatin-treated cells. (*A*) An NIH 3T3 cell migrating along 1D line enters a 2D area, then moves deeply into the 1D exit on the opposite side of the rectangle before turning around. (*B*) In contrast, a cell treated with 10 μM blebbistatin for 30 min enters the 2D area from a 1D line and exits through the 1D line on the opposite side. Red dotted lines indicate the borders of micropatterning. Numbers indicate time in hours. Scale bar, 50μm. (*C*, *left*) As a result of the perferential localization on 2D areas, an increasing percentage of NIH 3T3 cells becomes localized on 2D areas over a period of 24 hours after seeding. N = 684, 701, and 685 cells at 3, 14, and 24 hours, respectively (Chi-square test, * $p<0.0001$). (*C*, *right*) Cells treated with blebbistatin to inihibit myosin II show no significant accumulation on 2D areas. N = 226, 202, and 194 blebbistatin-treated cells at 3, 14, and 24 hours, respectively. The experiment was performed with cells treated with mitomycin.

end (Figure 2.2*B*). Consistent with this finding, myosin-II-inhibited cells failed to show preferred localization on 2D areas after 24 h of incubation (Figure 2.2*C*), in contrast to control cells. The percentage of cells in 2D areas showed an insignificant change from 42% (N = 226) initially to 49% (N = 184).

A simple way for cells to detect the dimension border is to generate stronger traction forces on 2D surfaces than on 1D lines, which may bias both the direction of translocation and the strength of adhesive resistance due to inside-out signaling (Discher *et al.*, 2005). To test this hypothesis, we quantified traction stress using traction-force microscopy (Dembo & Wang, 1999). Comparisons were made based on the 95^{th} percentile of traction stress, i.e., the top 5% of traction stress exerted by each cell. This measurement is used to avoid the complication due to different cell areas, though measurements of average traction stress show similar trends as 95^{th} percentile stress (Figure A.2). As shown in Figure 2.3, *A and B*, cells migrating on 2D rectangles generated 42% higher 95^{th} percentile traction stress (801 ± 65 Pa) than cells along 1D lines (564 ± 54 Pa; p=0.004). Time-lapse traction force microscopy confirmed the increase in traction stress as cells cross the border from 1D to 2D (Figure 2.3, *C and D*). In contrast, blebbistatin-treated cells showed not only a large decrease in magnitude, but also similar traction stresses on 2D and 1D substrates (270 ± 28 and 247 ± 32 Pa, respectively), consistent with the hypothesis that dimension sensing is driven by differential traction forces.

To test whether cells exhibited stronger adhesion on 2D than on 1D, we examined the morphology and total area of focal adhesions. As shown in Figure 2.4*A*, cells on 2D areas formed large, elongated focal adhesions throughout the cell body, whereas cells on 1D lines showed adhesions mainly at the leading edge. The number of focal adhesions and total area of focal adhesions were significantly higher on 2D than on 1D,

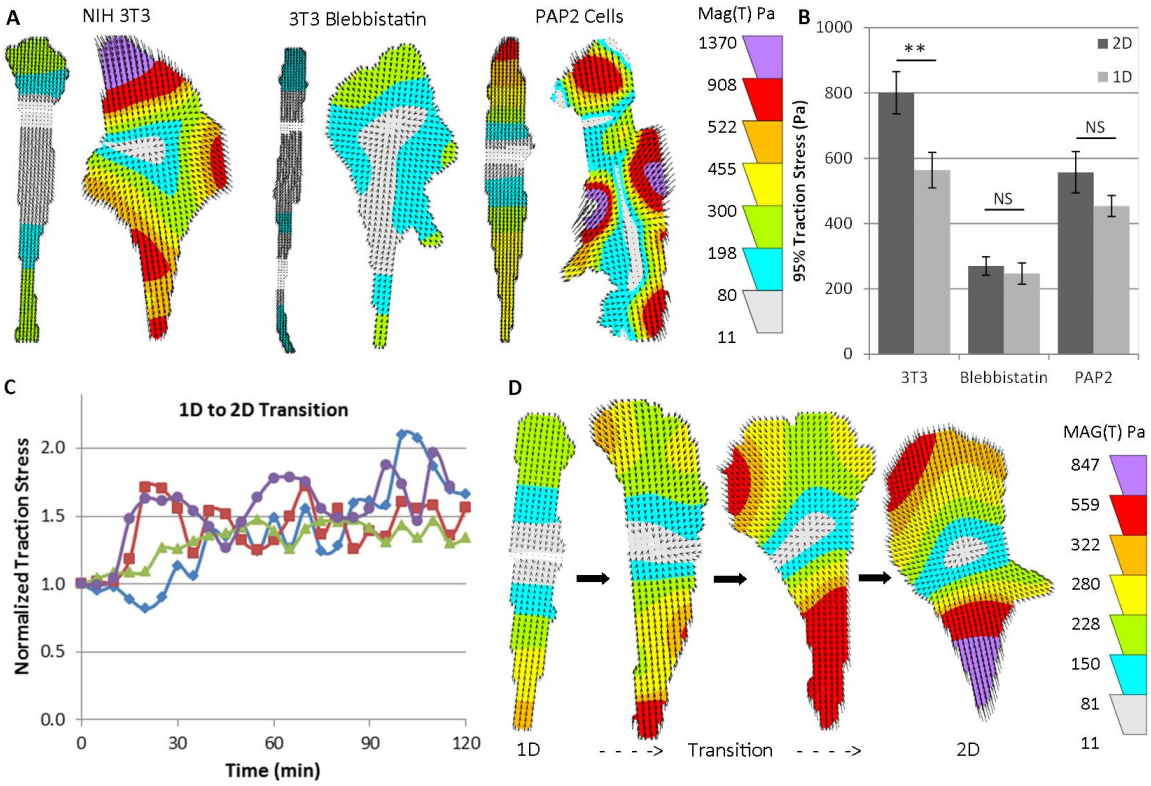

FIGURE 2.3. Traction stress measurements of cells migrating along 1D lines or on 2D rectangles. (*A*) The distribution of traction stress is shown as both vectors (*small arrows*) and heat maps (*color-coded regions*). Bar graph shows the top 5% traction stress under different conditions (*B*). A significant difference between 2D and 1D is seen for control cells but not for blebbistatin treated cells or PAP2 cells. N=18,13,18 for control, blebbistatin, and PAP2 cells on 2D rectangles, respectively. N=17,13,19 for the corresponding measurements along 1D lines,. Error bars represent the mean ± SE (t-test, ** p=0.004). (*C and D*) Normalized traction stress of four cells (the time immediately before the cell reaches the 1D-2D interface is set as 0, and the corresponding traction stress is set as 1) and traction stress heat maps (*D*) show an increase as cells migrate from 1D to 2D.

and the average focal adhesion size was 14% larger in 2D under the present condition (Figure 2.4*B*). Staining with fluorescent phalloidin indicated that cells spread on 2D regions form thick stress fibers across the cell body, whereas cells on 1D lines show a strong actin cortex along the cell border but few stress fibers (Figure 2.5*A*).

As myosin II activities are regulated by the phosphorylation of its regulatory light chain at Ser^{19} and Thr^{18} (Tan *et al.*, 1992), we stained cells on 1D and 2D with antibodies specific for MRLC monophosphorylated at Ser^{19}. Phosphorylated myosin II generally colocalizes along the actin stress fibers. Interestingly, cells in 2D regions showed a strong concentration of phosphomyosin along stress fibers over the nucleus, referred to previously as the nuclear cap (Figure 2.5*A*). Staining of cells on 1D showed both weaker staining along stress fibers and fewer stress fibers, and only 25% of cells showed nuclear caps. Quantification of fluorescence intensity shows significantly more phosphorylated MRLC in cells spread on 2D surfaces compared to cells on 1D lines (Figure 2.5*B*). Blebbistatin-treated cells showed few actin stress fibers and small punctate focal adhesions along the edges on both 1D and 2D substrates (Figures 2.4*A* and 2.5*A*). These results suggest a mechanism that limits traction-force generation based on physical constraints of the substrate.

2.3.3 Defective dimension sensing in oncogene-transformed fibroblasts

As metastatic invasion may be caused by defects in migration guidance, we asked whether dimension sensing might be affected in transformed cells, using H-*ras*-transformed mouse fibroblasts, the PAP2 line, as a model system (Bondy *et al.*, 1985). The NIH 3T3 cells used in this study are the parental cell line of PAP2

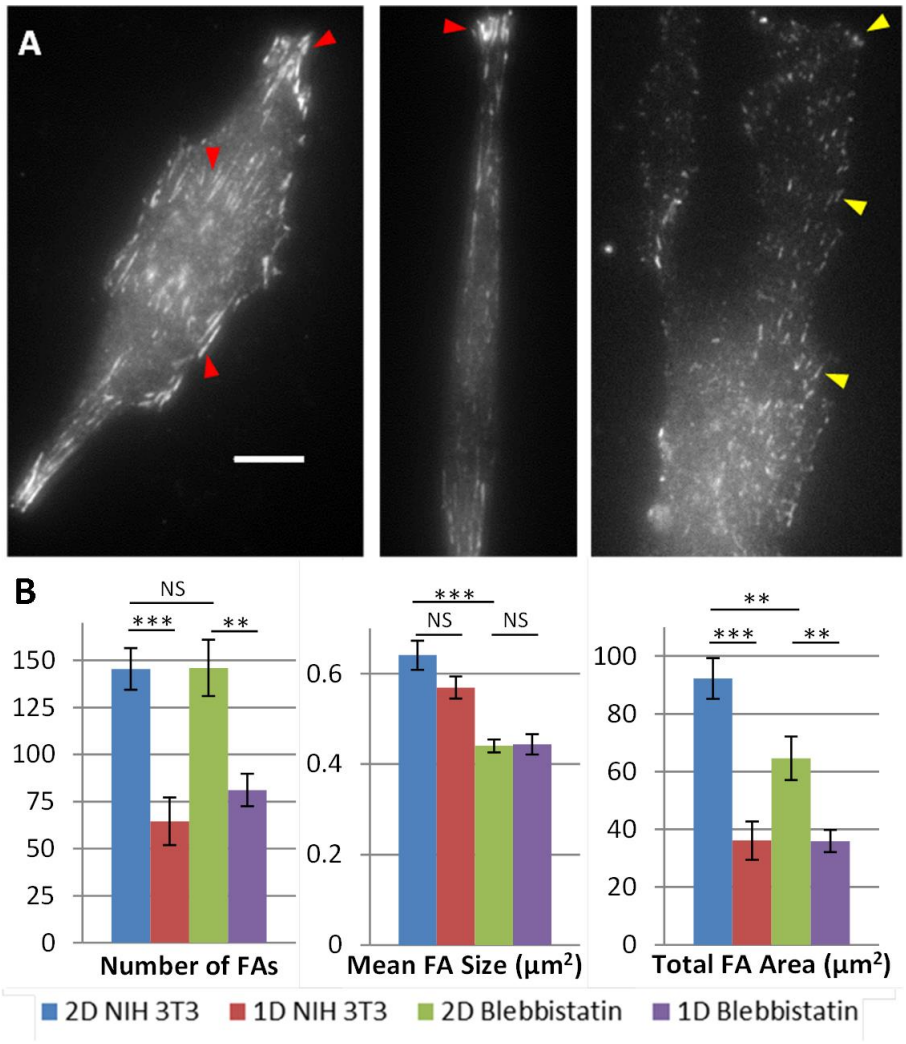

FIGURE 2.4. Size and number of focal adhesions along 1D lines and in 2D regions. (*A*) Immunofluorescence images of vinculin for NIH 3T3 cells show a larger number and/or size of focal adhesions in a 2D region than along a 1D line and after treatment with 10 μM blebbistatin. Arrows indicate elongated focal adhesions;arrowheads show small punctate adhesions in the cell treated with blebbistatin. Bar, 10 μm. (*B*) Bar graphs show average number of focal adhesions, focal adhesion size, and total focal adhesion area. Error bars represent the mean $\pm$ SE. ** indicates $p < 0.01$; *** indicates $p<0.001$

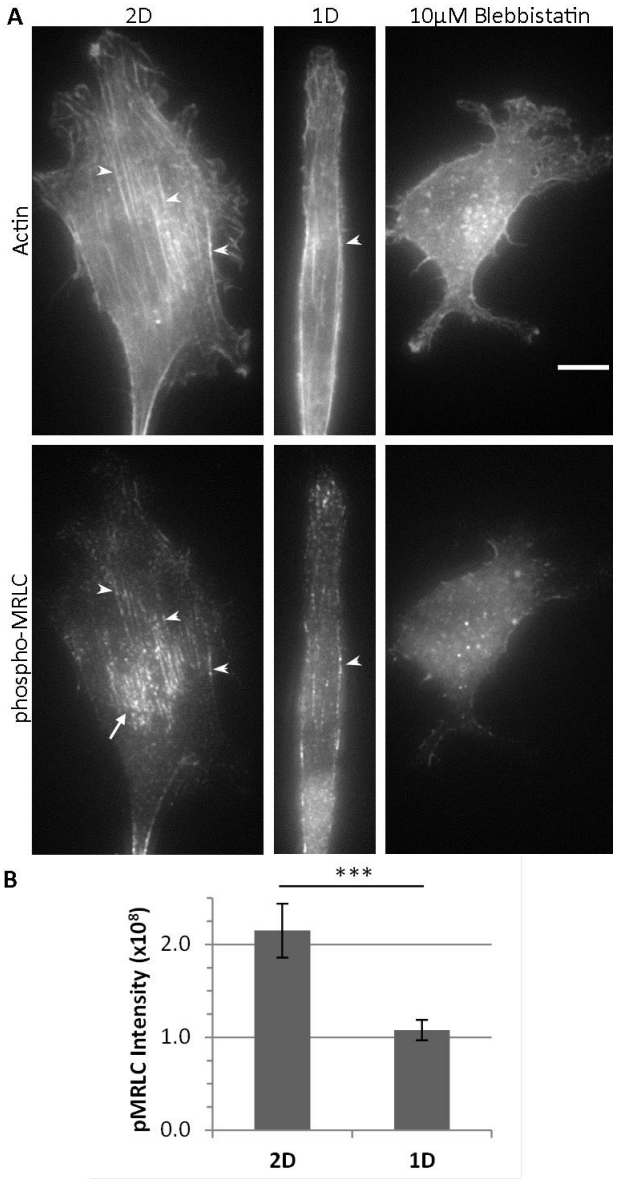

FIGURE 2.5. Stress fiber formation and myosin II activity differs between 1D and 2D. (*A*) Fluorescence images show the distribution of actin filaments and phosphorylated MRLC of NIH 3T3 cells in a 2D region, along a 1D line, and after treatment with 10 μM blebbistatin. Arrowheads indicate co-localization between phosphorylated MRLC and actin fibers. Arrow shows phosphorylated MRLC enrichment around the nucleus. Stress fibers are prominent in 2D regions, whereas cortical actin bundles are prominent in 1D. Treatment with blebbistatin causes the disassembly of both forms of actin bundles. Scale bar, 10 μm. (*B*) Bar graph shows that MRLC is phosphorylated at a significantly higher level when cells are spread on 2D surfaces compared to cells along 1D lines. Intensity is given in arbitrary units. N = 16,25 cells on 2D and 1D respectively. *** indicates p = 0.001.

cells. Previous studies have shown that PAP2 cells generate disorganized traction stresses (Munevar *et al.*, 2001b), such that the shape and migration of these cells are poorly coordinated with the direction of traction forces, whereas normal migrating cells showed a well-defined long axis, with strong traction forces concentrated along the anterior border of the axis (Munevar *et al.*, 2001b). Furthermore, the growth and apoptosis of PAP2 cells were nonresponsive to substrate stiffness (Wang *et al.*, 2000), in contrast to normal fibroblasts, suggesting that their mechanosensing may be defective.

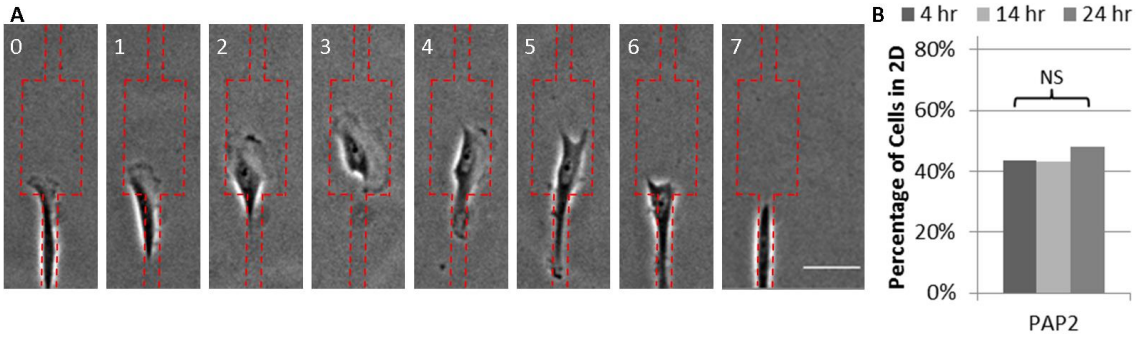

FIGURE 2.6. Lack of preference of *ras*-transformed NIH 3T3 fibroblasts (PAP2 cells) for localization in a 2D region. (*A*) A cell enters a 2D area from a 1D line but turns around to reenter the 1D line. Dotted lines indicate the border of the micropattern. Numbers indicate time in hours. Scale bar, 50 μm. (*B*) Consistent with the lack of dimensional preference, PAP2 cells show no significant accumulation on 2D areas over time. N = 333, 351, and 386 cells at 3, 14, and 24 hours, respectively.

Time-lapse recording indicated that, as in the case of 3T3 cells, PAP2 cells migrated persistently along 1D lines and rarely switched direction. However, much like blebbistatin-treated cells, H-*ras*-transformed cells are more likely to exit 2D areas into 1D lines than are normal 3T3 cells (Table 2.1). This defect is also reflected in the lack of accumulation in 2D areas over time (Figure 2.6*B*). Moreover, a significant

	Stays in rectangle	Leaves rectangle	
Control	63% (39)	37% (23)	
Blebbistatin	28% (10)	72% (26)	**
PAP2	26% (10)	74% (29)	***

TABLE 2.1. Quantification of migration direction as cells approach 1D from 2D rectangles. The 2D area was 50 μm wide and the 1D area was 10 μm wide. In contrast to control 3T3 fibroblasts, which prefer to localize in 2D rectangular areas, the majority of blebbistatin-treated cells and PAP2 cells readily leave 2D areas and migrate into 1D lines (chi-squared test with Yates correction, **p = 0.0017, ***p = 0.0006). Only single cells that migrated into the 2D region were counted. Cells that remained in the rectangle for more than 6 h were counted as staying.

percentage of these cells reversed the polarity upon the initial entry from 1D into a 2D area (31%, N = 39) and exited along the line of entry (Figure 2.6*A*). This reversal of direction was rarely observed with NIH 3T3 cells with or without blebbistatin treatment.

To determine whether the defect of PAP2 cells in dimension sensing was related to abnormal generation of traction forces, we measured traction stress of PAP2 cells along 1D lines and on 2D areas. As shown in Figure 2.3*B*, traction stress decreased significantly compared to normal cells on 2D regions, but not along 1D lines. As a result, there was a smaller (23%) difference between the traction stress produced on 1D lines and that produced on 2D rectangles (454 $\pm$ 32 Pa vs. 557 $\pm$ 63 Pa, respectively; p = 0.08), compared to 3T3 cells. These data suggest that defects in the generation and/or regulation of traction forces may play an important role in the defect of dimension sensing for transformed cells, which may in turn contribute to their invasive behavior.

2.4 Discussion

Elastic polyacrylamide hydrogels have been used extensively for testing cellular response to substrate rigidity and for measuring traction stress (Lo *et al.*, 2000; Beningo & Wang, 2002). A new method for high-resolution micropatterning of polyacrylamide surfaces further allowed the control of cell shape and migration and analyses of cellular responses to geometric parameters (Rape *et al.*, 2011). In this study, we have applied these methods to test the sensitivity of cell migration to substrate dimension. Although true 1D lines rarely occur in vivo, they may be used as a simplified model for 3D migration because of the similarity in cell morphology, likely due to the fibrillar nature of the extracellular matrix. Recent work has investigated the effect of line width and substrate stiffness on cell migration (Pathak & Kumar, 2012). Here, we focus on cellular behavior at the border between 1D lines and 2D surfaces, by forcing NIH 3T3 fibroblasts to migrate between micropatterned alternating 1D and 2D environments. The striking morphological and structural differences, including lamellipodia, actin structures, and substrate adhesions, suggest that cells may show a preferential localization between 1D and 2D environments.

We found that when migrating cells encountered a transition from1D to 2D, 100% of them entered the 2D area, which may be due in part to the strong persistence while migrating along 1D. In contrast, when cells encountered a transition from 2D to 1D, only a minority of them were able to continue into 1D lines. This difference cannot be explained by a difference in persistence, since the majority of these cells turned around only after a large portion of the cell had entered the 1D region where the persistence is higher than on 2D (Figure 2.2*A* and Table A.1). Moreover, 3T3 cells rarely turned around when migrating across the length of 2D rectangles (Figure

2.2*A*). This active reversal of polarity supports the argument that the cells exhibit a real preference for 2D.

Two observations suggest that the preference for 2D over 1D is driven by differential traction forces. First, we found that cells generate stronger traction stresses when migrating on 2D surfaces than when moving along 1D lines. Although active traction forces at the front are always balanced by passive anchorage forces at the rear (Dembo & Wang, 1999) (Figure 2.3, *A and D*), these active forces are stronger when the frontal region is in a 2D region than when it is along a 1D line. The bias may then steer migration toward 2D. Second, the preference for 2D vanished when actomyosin contractility was pharmacologically blocked by blebbistatin, supporting the idea that the increase in traction forces on 2D is responsible for the preferential localization. Morphologically, cells treated with blebbistatin became elongated without a broad leading edge, resembling cells in 1D even after entering into 2D surfaces (Frey *et al.*, 2006). Therefore, guidance by substrate dimension may be explained by the difference in size of the leading edge between 1D and 2D, which may differentially increase traction forces on 2D surfaces. Given the narrow leading edges for cells in most 3D ECMs (Cukierman *et al.*, 2001), one could further predict that cells also prefer to localize on 2D surfaces when given a choice between 2D and 3D fibrous matrices.

The increase in traction stress on 2D is coupled to increases in focal adhesions and stress fibers. The maturation of focal adhesions, generation of traction forces, and assembly of stress fibers are likely coupled by positive feedback to reinforce each other (Eyckmans *et al.*, 2011; Oakes *et al.*, 2012). Thus the difference in traction force generation may be attributed to the lower physical constraint for cell spreading on 2D than on 1D, which would allow the positive feedback to continue and brings traction forces to a higher level. Our results further confirm those of previous reports that focal

adhesion size and traction forces are limited by geometric contraints of adhesion areas (Rape *et al.*, 2011). Myosin II inhibition eliminates the effect of substrate dimension, as focal adhesions are unable to mature and grow in size regardless of the size of adhesion area. Furthermore, the intriguing localization of phosphorylated myosin II in nuclear caps of cells in 2D suggests strong contractility of stress fibers in the region above the nucleus, which may send forces along stress fibers to reach the associated focal adhesions at the cell anterior to mediate mechanosensing (Kim *et al.*, 2012). In addition, it has been reported that microtubules may play a central role in regulating the actin cytoskeleton when cells are migrating in a confined channel (Balzer *et al.*, 2012). Observations from our group also showed that treatment with nocodazole inhibits cell migration along lines, yet blebbistatin and Y-27632 do not negatively affect migration speed (Guo & Wang, 2012). Thus, microtubule polymerization may provide at least some driving forces for 1D migration, whereas 2D migration requires primarily actin-myosin II contractility. These different mechanisms may generate different magnitudes of traction stress and cause the bias in cell localization.

As demonstrated by the preferential accumulation of cells on 2D surfaces over time, dimension sensitivity may be involved in concentrating cells at the destination during both physiological and pathological processes. Adhesive ligands in multicellular organisms may be either concentrated along a network of fibers, creating a 1D-like environment, or distributed over a tissue surface, generating a 2D-like environment. The creation of such 2D surfaces may take place during embryonic development and wound healing, whereas 1D or 3D migration may occur during processes such as tumor metastasis (Friedl & Gilmour, 2009). Other elements, such as soluble factors, immobile ligands, substrate rigidity, and mechanical forces, may play equally important roles and would allow multiple ways to regulate the destination of migration

in a cell-type-specific manner.

We suspect that defects in dimension sensitivity may play a role in metastatic invasion, causing cancerous cells to leave their 2D home environment to invade into the surrounding fibrous connective tissue. Supporting this hypothesis, we found that *ras*-transformed 3T3 fibroblasts (PAP2) showed no dimension preference. Although PAP2 cells were as persistent as 3T3 cells when migrating along 1D lines (Table 2.2), many of them turned around when entering from 1D lines into 2D surfaces. This behavior was coupled to highly disorganized morphology and protrusive activities on 2D surfaces, with multiple protrusions seemingly competing against one another for the control of cell polarity (Munevar *et al.*, 2001b). Traction stresses of PAP2 cells were also weaker and highly disorganized on 2D surfaces (Munevar *et al.*, 2001b). Therefore, in addition to the smaller difference in traction stress between 2D and 1D, the unstable protrusions on 2D surfaces may prove less effective in guiding cell localization than the persistent migration imposed by 1D lines. A possible explanation of the defect at the molecular level may be the ability of *ras* to activate the PI3 kinase (Castellano & Downward, 2011), which is in turn involved in the formation of lamellipodia from filopodia on 2D surfaces (Welf *et al.*, 2012). In transformed cells, the formation of multiple competing protrusions may be attributed to a loss of regulatory control of *ras*.

Consistent with the idea that traction forces drive dimension sensitivity, PAP2 cells generated similar traction stress in 1D and 2D environments. Interestingly, traction stress of PAP2 cells along 1D lines did not decrease significantly compared to nontransformed fibroblasts, supporting the idea that transformation may not affect the initial protrusion but instead may impair the subsequent expansion, stabilization, and force generation of lamellipodia on 2D surfaces. The lack of difference in

traction stress between 1D and 2D may contribute to the defect in dimension sensing and the invasive behavior of transformed cells. Conversely, migration defects of transformation may be suppressed when cells are confined to a 1D environment.

Traction forces actively generated near the leading edge are ideally suited for guiding cell migration (Dembo & Wang, 1999; Legant *et al.*, 2010; Munevar *et al.*, 2001a). The magnitude and pattern of traction forces, coupled to mechanical responses of the environment upon cellular probing, may allow cells to respond to both external parameters such as rigidity and internal parameters such as cell shape, size, and migrating state. Dimension sensing represents a novel addition to this collection of sensing mechanisms. Detailed knowledge of these force-dependent responses may facili- tate not only the design of scaffolds for engineering artificial tissues, but also clinical interventions of diseases, such as cancer, that depend on cell migration.

2.5 References

Balzer, Eric M, Tong, Ziqiu, Paul, Colin D, Hung, Wei-Chien, Stroka, Kimberly M, Boggs, Amanda E, Martin, Stuart S, & Konstantopoulos, Konstantinos. 2012. Physical confinement alters tumor cell adhesion and migration phenotypes. *FASEB J.*, **26**(10), 4045–4056.

Beningo, Karen A, & Wang, Yu-Li. 2002. Flexible substrata for the detection of cellular traction forces. *Trends Cell Biol.*, **12**(2), 79–84.

Bondy, Gregory P, Wilson, Sylvia, & Chambers, Ann F. 1985. Experimental Metastatic Ability of H-ras-transformed NIH3T3 Cells. *Cancer Res.*, **45**, 6005–6009.

Castellano, Esther, & Downward, Julian. 2011. RAS Interaction with PI3K: More Than Just Another Effector Pathway. *Genes Cancer*, **2**(3), 261–274.

Chen, Christopher S, Mrksich, Milan, Huang, Sui, Whitesides, George M, & Ingber, Donald E. 1997. Geometric Control of Cell Life and Death. *Science*, **276**(5317), 1425–1428.

Cukierman, Edna, Pankov, Roumen, Stevens, Daron R, & Yamada, Kenneth M. 2001. Taking cell-matrix adhesions to the third dimension. *Science*, **294**(5547), 1708–1712.

Curtis, Adam, & Wilkinson, Chris. 1997. Topographical control of cells. *Biomaterials*, **18**(24), 1573–1583.

Dembo, Micah, & Wang, Yu-Li. 1999. Stresses at the cell-to-substrate interface during locomotion of fibroblasts. *Biophys. J.*, **76**(4), 2307–2316.

Discher, Dennis E, Janmey, Paul, & Wang, Yu-Li. 2005. Tissue cells feel and respond to the stiffness of their substrate. *Science*, **310**(5751), 1139–1143.

Doyle, Andrew D, Wang, Francis W, Matsumoto, Kazue, & Yamada, Kenneth M. 2009. One-dimensional topography underlies three-dimensional fibrillar cell migration. *J. Cell Biol.*, **184**(4), 481–490.

Eyckmans, Jeroen, Boudou, Thomas, Yu, Xiang, & Chen, Christopher S. 2011. A hitchhiker's guide to mechanobiology. *Dev. Cell*, **21**(1), 35–47.

Fraley, Stephanie I, Feng, Yunfeng, Giri, Anjil, Longmore, Gregory D, & Wirtz, Denis. 2012. Dimensional and temporal controls of three-dimensional cell migration by zyxin and binding partners. *Nat. Commun.*, **3**(Mar.), 719.

Frey, Margo T, Tsai, Irene Y, Russell, Thomas P, Hanks, Steven K, & Wang, Yu-Li. 2006. Cellular responses to substrate topography: role of myosin II and focal adhesion kinase. *Biophys. J.*, **90**(10), 3774–3782.

Friedl, Peter, & Gilmour, Darren. 2009. Collective cell migration in morphogenesis, regeneration and cancer. *Nat. Rev. Mol. Cell Biol.*, **10**(7), 445–457.

Ghibaudo, Marion, Trichet, Léa, Le Digabel, Jimmy, Richert, Alain, Hersen, Pascal, & Ladoux, Benoît. 2009. Substrate topography induces a crossover from 2D to 3D behavior in fibroblast migration. *Biophys. J.*, **97**(1), 357–368.

Guo, Wei-Hui, & Wang, Yu-Li. 2012. A Three-Component Mechanism for Fibroblast Migration with a Contractile Cell Body that Couples a Myosin II-Independent Propulsive Anterior to a Myosin II-Dependent Resistive Tail. *Mol. Biol. Cell*, **23**(Mar.), 1657–1663.

Hakkinen, Kirsi M, Harunaga, Jill S, Doyle, Andrew D, & Yamada, Kenneth M. 2011. Direct comparisons of the morphology, migration, cell adhesions, and actin cytoskeleton of fibroblasts in four different three-dimensional extracellular matrices. *Tissue Eng. Part A*, **17**(5-6), 713–724.

Han, Sangyoon J, Bielawski, Kevin S, Ting, Lucas H, Rodriguez, Marita L, & Sniadecki, Nathan J. 2012. Decoupling Substrate Stiffness, Spread Area, and Micropost Density: A Close Spatial Relationship between Traction Forces and Focal Adhesions. *Biophys. J.*, **103**(4), 640–648.

Kim, Dong-Hwee, Khatau, Shyam B, Feng, Yunfeng, Walcott, Sam, Sun, Sean X, Longmore, Gregory D, & Wirtz, Denis. 2012. Actin cap associated focal adhesions and their distinct role in cellular mechanosensing. *Sci. Rep.*, **2**(555).

Kovács, Mihály, Tóth, Judit, Hetényi, Csaba, Málnási-Csizmadia, András, & Sellers, James R. 2004. Mechanism of blebbistatin inhibition of myosin II. *J. Biol. Chem.*, **279**(34), 35557–35563.

Legant, Wesley R, Miller, Jordan S, Blakely, Brandon L, Cohen, Daniel M, Genin,

Guy M, & Chen, Christopher S. 2010. Measurement of mechanical tractions exerted by cells in three-dimensional matrices. *Nat. Methods*, **7**(12), 969–971.

Lo, Chun-Min, Wang, Hong-Bei, Dembo, Micah, & Wang, Yu-Li. 2000. Cell movement is guided by the rigidity of the substrate. *Biophys. J.*, **79**(1), 144–152.

Luxton, G W Gant, & Gundersen, Gregg G. 2011. Orientation and function of the nuclear-centrosomal axis during cell migration. *Curr. Opin. Cell Biol.*, **23**(5), 579–588.

McBeath, Rowena, Pirone, Dana M, Nelson, Celeste M, Bhadriraju, Kiran, & Chen, Christopher S. 2004. Cell shape, cytoskeletal tension, and RhoA regulate stem cell lineage commitment. *Dev. Cell*, **6**(4), 483–495.

Munevar, Steven, Wang, Yu-Li, & Dembo, Micah. 2001a. Distinct roles of frontal and rear cell-substrate adhesions in fibroblast migration. *Mol. Biol. Cell*, **12**(12), 3947–3954.

Munevar, Steven, Wang, Yu-Li, & Dembo, Micah. 2001b. Traction Force Microscopy of Migrating Normal and H-ras Transformed 3T3 Fibroblasts. *Biophys. J.*, **80**(4), 1744–1757.

Oakes, Patrick W, Beckham, Yvonne, Stricker, Jonathan, & Gardel, Margaret L. 2012. Tension is required but not sufficient for focal adhesion maturation without a stress fiber template. *J. Cell Biol.*, **196**(3), 363–74.

Pathak, Amit, & Kumar, Sanjay. 2012. Independent regulation of tumor cell migration by matrix stiffness and confinement. *Proc. Natl. Acad. Sci.*, **109**(26), 10334–10339.

Rape, Andrew D, Guo, Wei-Hui, & Wang, Yu-Li. 2011. The regulation of traction force in relation to cell shape and focal adhesions. *Biomaterials*, **32**(8), 2043–2051.

Ridley, Anne J, Schwartz, Martin A, Burridge, Keith, Firtel, Richard A, Ginsberg, Mark H, Borisy, Gary, Parsons, J Thomas, & Horwitz, Alan Rick. 2003. Cell migration: integrating signals from front to back. *Science*, **302**(5651), 1704–1709.

Singhvi, Rahul, Kumar, Amit, Lopez, Gabriel P, Stephanopoulos, Gregory N, Wang, Daniel I C, Whitesides, George M, & Ingber, Donald E. 1994. Engineering cell shape and function. *Science*, **264**(5159), 696–698.

Straight, Aaron F, Cheung, Amy, Limouze, John, Chen, Irene, Westwood, Nick J, Sellers, James R, & Mitchison, Timothy J. 2003. Dissecting Temporal and Spatial Control of Cytokinesis with a Myosin II Inhibitor. *Science*, **299**(5613), 1743–1747.

Tan, John L, Ravid, Shoshana, & Spudich, James A. 1992. Control of Nonmuscle Myosins by Phosphorylation. *Annu. Rev. Biochem.*, **61**(1), 721–759.

Wang, Hong-Bei, Dembo, Micah, & Wang, Yu-Li. 2000. Substrate flexibility regulates growth and apoptosis of normal but not transformed cells. *Am. J. Physiol. Cell Physiol.*, **279**(5), C1345–C1350.

Wang, Ning, Ostuni, Emanuele, Whitesides, George M, & Ingber, Donald E. 2002. Micropatterning tractional forces in living cells. *Cell Motil. Cytoskeleton*, **52**(2), 97–106.

Welf, Erik S, Ahmed, Shoeb, Johnson, Heath E, Melvin, Adam T, & Haugh, Jason M. 2012. Migrating fibroblasts reorient directionality by a metastable, PI3K-dependent mechanism. *J. Cell Biol.*, **197**(1), 105–114.

Chapter 3

Migration State Regulates Cellular Mechanical Output and Signaling Activities

Adherent cells are known to probe the physical parameters of their environment, including substrate rigidity and topography. Additionally, cells are able to monitor their internal states such as shape and spread area. These physical conditions are known to have profound effects on cellular functions including growth and differentiation. Here, we demonstrate that the state of migration can also regulate important cellular activities. We find that non-migrating cells generate traction stress two-fold higher than migrating cells. Traction stresses are also less dynamic and more peripherally localized in stationary cells than in migrating cells, which mirrors the reduced dynamics and peripheral localization of focal adhesions,. The observations may be explained by the presence of an active zone of traction force generation near the front, where focal adhesions in migrating cells remain for a much shorter period of time than in stationary cells. Paxillin phosphorylation is enhanced in stationary cells compared to migrating cells, indicating that internal signaling and downstream activities are also affected by migration state. These results suggest that migration state generates signals to control cellular mechanical and chemical activities. We propose that migration-dependent regulation assists cells in controlling their states of growth and differentiation as a function of location and extent of anchorage to the environment.

3.1 Introduction

Recent studies indicate adherent cells are highly sensitive to internal and external physical states in addition to chemical signals. For example, elongated shape (Kilian *et al.*, 2010), large spread area (McBeath *et al.*, 2004), and rigid substrates (Engler *et al.*, 2006) were all found to favor osteogenic differentiation while opposite conditions favor adipogenic or neurogenic differentiations.

Interestingly, conditions that favor osteogenic differentiation also promote the generation of stronger actomyosin-dependent traction forces on the substrate. Cells generate stronger traction forces on stiff substrates than cells on soft substrates (Lo *et al.*, 2000; Trichet *et al.*, 2012). In addition, spread cells exert stronger traction forces than cells confined to small areas (Wang *et al.*, 2002; Rape *et al.*, 2011). Cell geometry, such as aspect ratio (Rape *et al.*, 2011), and substrate dimension (Baker & Chen, 2012; Chang *et al.*, 2013) have also been shown to profoundly affect traction force generation. Although myosin II-dependent traction forces are commonly considered to be generated for the purpose of driving cell migration (Dembo & Wang, 1999; Morin *et al.*, 2014), they also serve the purpose of probing the external or internal physical state (Discher *et al.*, 2005; Prager-Khoutorsky *et al.*, 2011). In addition, lineage specification during stem cell differentiation has been shown to be dependent on myosin-II activity (Engler *et al.*, 2006), likely through the crosstalk between inside-out and outside-in signaling to activate mechanotransduction pathways. Defective regulation of traction forces is also thought to contribute to metastatic potential of cancer cells. Traction forces are often disorganized in transformed cells (Munevar *et al.*, 2001), and traction forces have been shown to increase with increasing metastatic potential in a number of cancer models (Kraning-Rush *et al.*, 2012).

These observations suggest that regulation or manipulation of traction forces may serve as a universal approach for controlling cell differentiation, and that traction force generation may serve as a handle to identify conditions that affect cell differentiation and possibly other important activities. In this study, we find that the state of cell migration has a profound effect on the generation of traction forces and the phosphorylation state of paxillin, a known marker of mechanotransduction. Our results further suggest that cell migration affects focal adhesion dynamics, possibly through mechanical cross-talk between newly formed and pre-existing focal adhesions, which may in turn alter adhesion dependent signaling.

3.2 Methods and Materials

3.2.1 Substrate Preparation

Micropatterned polyacrylamide hydrogels were prepared as described previously (Rape *et al.*, 2011). Briefly, a polydimethylsiloxane stamp was incubated for 45 min with a 0.1% (w/v) gelatin solution that had been activated with 3.6 mg/mL sodium periodate (Sigma, St. Louis, MO). The stamp was dried using N_2 gas then lightly pressed onto a small glass coverslip. A freshly prepared solution of 5% acrylamide and 0.1% bis-acrylamide (Bio-Rad, Hercules, CA) was degassed; 0.2 μm fluorescent beads (Molecular Probes, Carlsbad, CA) were added at a 1:2000 dilution if the substrate was to be used for traction force microscopy. After addition of the initiators ammonium persulfate (Sigma) and N,N,N',N'-tetramethylethane-1,2-diamine (EMD Millipore, Billerica, MA), a 30 μL drop was pipetted onto a large coverslip pre-treated with Bind-Silane (GE Healthcare, Little Chalfont, United Kingdom). The small stamped coverslip was immediately placed pattern-side down onto the acrylamide drop. After complete acrylamide polymerization, the top coverslip was carefully removed. Micropatterned polyacrylamide hydrogel substrates were mounted into chamber dishes, sterilized under ultraviolet light for 30 min, and incubated in cell culture media for 1 h at 37°C before use. The final gel had an estimated Young's modulus of 3.5 kPa (Tse & Engler, 2010).

Glass substrates micropatterned with linear acrylamide were prepared as described previously (Guo & Wang, 2010). Briefly, a coverslip was treated with Bind-Silane. Standard photolithography techniques were used to pattern areas designated for cell adhesion with SPR 220.3 positive photoresist (Microchem, Newton, MA). The remaining glass surface was made non-adhesive by grafting linear polyacrylamide to

the Bind-Silane-activated surface. The photoresist was then stripped away using Remover 1165 (Microchem), and the exposed glass surface was incubated with 10 μg/mL fibronectin (Sigma) for 1 h.

3.2.2 Cell Culture

NIH 3T3 cells (ATCC, Manassas, VA) were cultured in Dulbecco's modified Eagle's medium (Life Technologies, Carlsbad, CA) supplemented with 10% donor adult bovine serum (Thermo Scientific, Waltham, MA), 2 mM L-glutamine, 50 μg/mL streptomycin, and 50 U/mL penicillin (Life Technologies); cells were maintained under 5% CO_2 at 37°C. The mCherry-paxillin construct was kindly provided by Dr. Michael Davidson (Florida State University). Cells were transfected using the Amaxa Nucleofector (Lonza, Walkersville, MD) system following the manufacturer's instructions.

3.2.3 Traction Force Microscopy

Phase contrast images of single cells spread on a uniformly-coated polyacrylamide gel or across a micropatterned island were collected with a Nikon Eclipse Ti microscope using a 40X N.A. 0.75 PlanFluor dry objective (Nikon, Tokyo, Japan) and an Andor iXon CCD camera and custom software. Fluorescence images of the embedded beads near the surface of the hydrogel were taken before and after cells were removed with 0.05% Trypsin-EDTA (Life Technologies). For time-lapse recordings, paired phase-contrast images of the cell and fluorescence images of the underlying beads were collected every 10 min for 4 h. For high resolution tracking of substrate strain, phase contrast images of the cell and corresponding fluorescence images of underlying beads

were collected using a 100X N.A. 1.3 Plan Fluor oil immersion objective (Nikon) at a frequency of 4 min for 2 h. Cell outlines were manually drawn, and bead displacement fields were computed using custom software. Color maps of traction force-induced strain were generated using MATLAB. Traction stress was computed using LIBTRC software package (Prof. Micah Dembo, Boston University).

3.2.4 TIRF Microscopy and Focal Adhesion Analysis

Cells expressing mCherry-paxillin were plated on glass substrates incubated with fibronectin. Total internal reflection fluorescence (TIRF) images of focal adhesions in cells spread on either a micropatterned or an unpatterned coverslip were collected with a Nikon Eclipse Ti microscope using a 100X N.A. 1.49 Apo TIRF oil immersion objective (Nikon) and an Andor iXon CCD camera. mCherry was excited using a 561-nm laser (Coherent, Santa Clara, CA) and images were collected every 4 min for 2 h. The area of focal adhesion was quantified using the Focal Adhesion Analysis Server (Berginski & Gomez, 2013). Lifetime of focal adhesions that formed at the leading edge of migrating cells and at the corners of stationary cells was manually measured using time-lapse images.

3.2.5 Focal Adhesion Immunostaining

Cells seeded on micropatterned polyacrylamide substrates were fixed in 4% formaldehyde (Thermo Scientific) and stained with mouse monoclonal antibodies against vinculin (Santa Cruz Biotechnology, Dallas, TX) and rabbit polyclonal antibodies against Tyr^{118}-phosphorylated paxillin (Cell Signaling Technology, Danvers, MA). Fluorescence images were collected using a 100X N.A. 1.3 Plan Fluor

oil immersion objective. Average background intensity was subtracted from each image using custom software, and fluorescence intensity of p-paxillin was divided by that of vinculin measured at ten focal adhesions in each cell located near the leading edge with the strongest p-paxillin fluorescence signal. Focal adhesions were segmented to create a mask in ImageJ. The masks were used in creating color heat maps of the ratio of p-paxillin against vinculin fluorescence in MATLAB.

3.3 Results

3.3.1 Traction force generation differs between stationary and migrating cells

To investigate how traction force generation is regulated during cell migration, we applied traction force microscopy to NIH 3T3 cells plated on elastic polyacrylamide gels of 3.5 kPa, conjugated with gelatin on the surface to facilitate cell adhesion. Micropatterning of bound gelatin allowed precise control of cell size, shape, and migration state (Figure 3.1, *A*-*C*). Traction force generation was assessed based on the magnitude of 95^{th} percentile traction stress (Rape *et al.*, 2011), which focuses on regions of high mechanical activity.

Cells on a uniformly-coated surface were able to migrate freely and exerted a traction stress of 356±25.6 Pa. Similarly, cells migrating along micropatterned strips of gelatin exerted a traction stress of 370±22.4 Pa. In contrast, when gelatin was micropatterned as 50×50 μm square islands, confined stationary NIH 3T3 cells exerted a traction stress of 718±124 Pa (Figure 3.1*D*). The two-fold difference was unexpected since traction stress is known to be sensitive to spreading size and aspect ratio (Rape *et al.*, 2011), and unconfined cells often spread to a larger size and show a higher aspect ratio than cells on 50×50 μm islands.

To further control for the effect of cell size and shape, we micropatterned gelatin as teardrop shaped islands to mimic the shape and size of typical migrating cells. Cells spread on these islands exerted a traction stress of 850±81.9 Pa, similar to cells on square islands, which argues against the effect of cell shape or spreading area and indicates that migration state is able to regulate traction force generation.

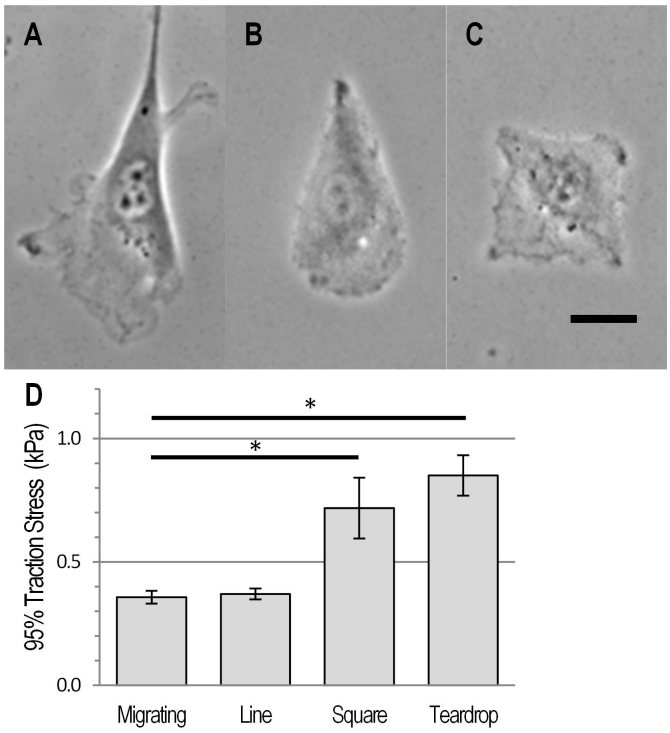

FIGURE 3.1. Traction force generation differs between migrating and stationary cells. While NIH3T3 cells migrate freely on a gel with a uniform coating of gelatin (A), micropatterning of gelatin as islands results in cells that are confined to a teardrop (B) or square (C) shape. Scale bar, 20 μm. Stationary cells exert approximately twice the traction stress of that for migrating cells regardless of shape (D). N = 18, 15, 15, 15 for migrating on unpatterned surfaces, migrating on a line, stationary square, and stationary teardrop-shaped cells respectively. * indicates $p<0.05$.

3.3.2 Traction force generation is dependent on cell migration speed

To further investigate the dynamic relationship between cell migration and traction force generation, we applied time-lapse traction force microscopy to cells migrating on linear strips of finite length. Cell migration paused for a variable period of time at the end of the strip before the cell reversed its direction of migration. A typical recording showed that traction stress increased approximately two-fold after the cell stopped at the end of the strip (Figure 3.2, *A and B*), mirroring the two-fold difference in traction stress observed between separate migrating and confined cells.

This finding suggests that the output of traction forces may function as a speedometer for migrating cells, with the magnitude of stress controlled dynamically by the speed. We therefore performed a scatter plot analysis using a collection of 24 cells migrating at speeds ranging between 0 and 48 μm/hr along adhesive strips 30 μm in width. As shown in Figure 3.2*C*, traction stress, ranging between 300 and 900 Pa, was negatively correlated with the speed of migration even though these cells shared a similar shapes. Thus, traction force regulation is a dynamic process that is in part regulated by the speed of cell migration.

3.3.3 Traction force distribution differs between stationary and migrating cells

Previous studies showed that in migrating cells, the distribution of traction forces did not match the distribution of total focal adhesions; rather, they more closely reflected newly-formed focal adhesions near the leading edge (Beningo *et al.*, 2001;

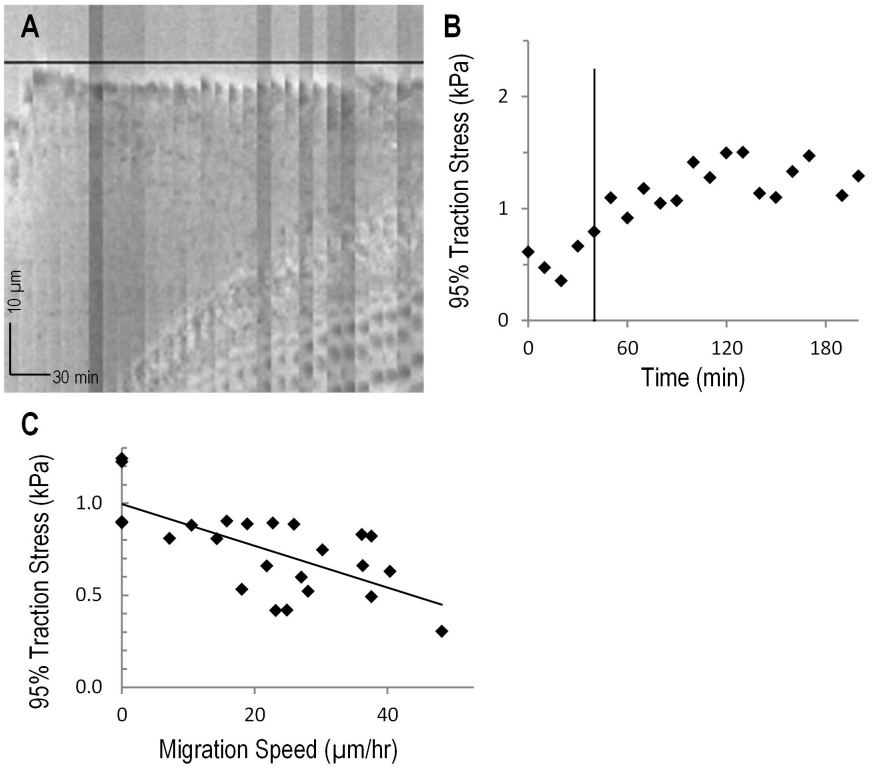

FIGURE 3.2. Traction force generation is regulated by cell migration state. Kymograph along the main axis shows a migrating NIH3T3 cell as it stops at the end of a 30 μm wide adhesive strip of finite length (A). Horizontal black line indicates the end of micropatterned strip. Traction stress increases when the cell stops migrating (B). Vertical black line indicates the time when cell reaches the end of the strip. Scatter plot analysis indicates that traction stress is negatively correlated with cell migration speed (C).

Stricker *et al.*, 2011). In stationary square-shaped cells, focal adhesions were found throughout the cell while maximal traction stress was localized at the corners (Wang *et al.*, 2002).

We employed high magnification imaging to map traction forces at a high resolution. As the high magnification precluded imaging of the entire cell for the computation of traction stress, maximal traction forces were located relative to the edge of the cell based on substrate displacements. For stationary cells confined to square islands, peak traction forces were located at the corners and along the very edge of these cells, as shown in the heat maps in Figure 3.3. Notably, high substrate strain persists at the corners for long periods of time (*kymograph*, Figure 3.3*B*). In contrast, for cells migrating either on an unpatterned surface or along a 30 m wide linear strip, maximal substrate displacement was located as far as 15 μm behind the leading edge. The region of maximal substrate displacement moved forward during cell migration, maintaining a constant distance from the leading edge, which resulted in a wave of high substrate strain that followed the leading edge of migrating cells (*kymograph*, Figure 3.3*A*). These observations suggest that cell migration affects the location of maximal traction force relative to the edge of the cell. The generation of traction forces may be determined by the distance of focal adhesions from the leading edge, a distance which increases in migration cells but remains constant in stationary cells.

3.3.4 Focal adhesion dynamics differ between stationary cells and migrating cells

Traction forces are generated by contractility of the actomyosin cytoskeleton and transmitted to the substrate through integrins at focal adhesions (Beningo *et al.*,

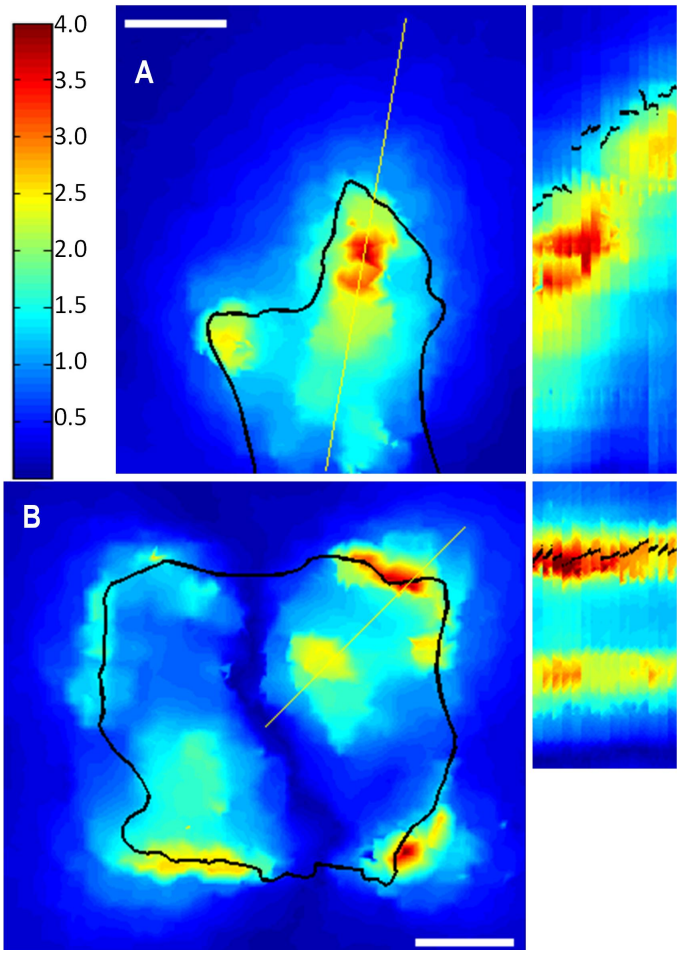

FIGURE 3.3. Substrate displacement maps reveal the location of maximal traction forces relative to the leading edge. Heat maps depict substrate displacement caused by migrating (A) and stationary (B) cells. Scale bar, 10 μm. Black line represents cell outline. Yellow line indicates region of interest for generating kymographs (*right panels*), which suggest steady association of maximal traction forces with the very edge of stationary cells and a constant distance between maximal traction forces and the leading edge in migrating cells. Traction strain also lasts longer in stationary cells than in migrating cells. Kymograph duration, 1 hour.

2001; Geiger *et al.*, 2009; Vicente-Manzanares *et al.*, 2009). We suspected that the difference in traction stresses between migrating and stationary cells may be related to differences in the dynamics of focal adhesions. Using NIH 3T3 cells expressing mCherry-paxillin, we examined focal adhesions in cells plated on fibronectin-coated glass coverslips with TIRF microscopy (Figure 3.4, *A nad B*). Stationary cells on coverslips were confined within areas surrounded by grafted linear polyacrylamide as a blocking agent (Guo & Wang, 2010).

Measurements of focal adhesions revealed an average size of 0.52 μm^2 in stationary cells and 0.47 μm^2 in migrating cells, suggesting that focal adhesions were able to reach a larger size possibly for sustaining larger traction forces in stationary cells. Focal adhesions at the corners of square shaped cells, where the strongest traction forces were localized, were particularly prominent; these corner adhesions had an average size of 0.62 μm^2 with some exceeding 4 μm^2 in size (Figure 3.4*C*).

Time-lapse recording of migrating cells showed typical focal adhesion dynamics described previously, forming at the leading edge and remaining largely stationary relative to the substrate (Figure 3.4*B*). As the cell migrated forward, focal adhesions became localized to the cell interior, many of which disassembled over the course of an hour. In contrast, focal adhesions in confined cells remained stationary relative to both the cell and substrate over a period longer than two hours. A small fraction of focal adhesions then detached from the edge and moved across a long distance towards the interior of the cell. As described in a previous report, such long-range movement of focal adhesions relative to the substrate appeared to take place only in non-migrating cells, possibly due to strong traction forces dislodging the focal adhesion or manipulating ECM protein conformation (Smilenov *et al.*, 1999).

The difference in dynamics is also evident in the significantly increased focal adhesion

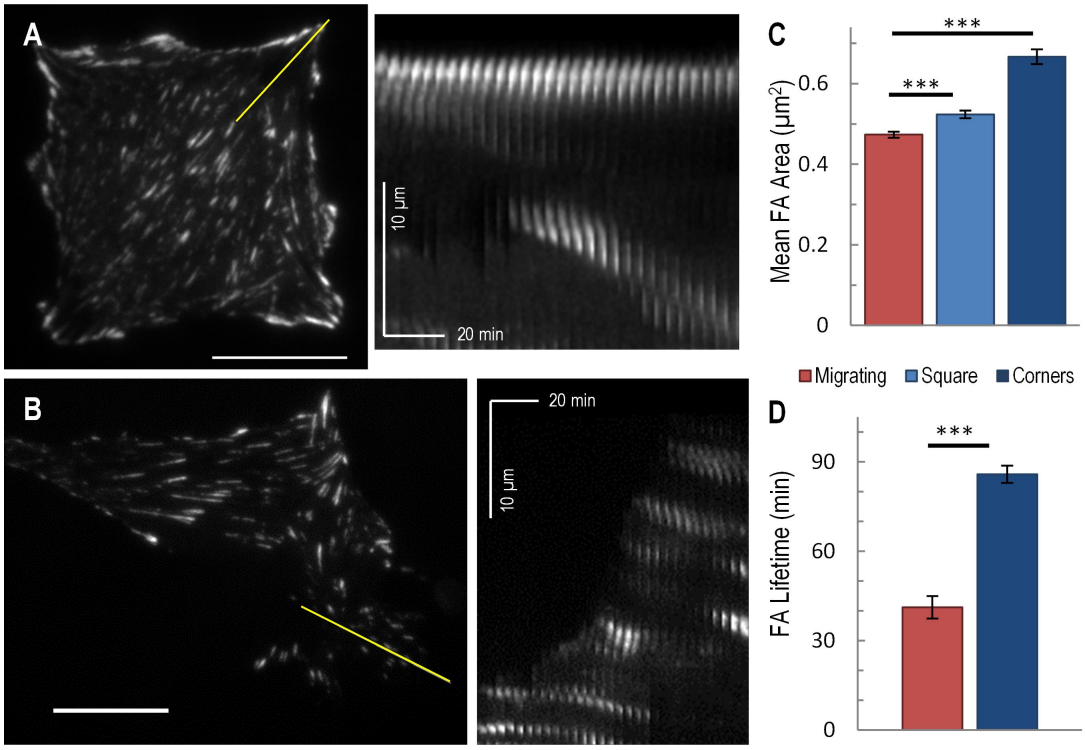

FIGURE 3.4. Focal adhesions are more dynamic in migrating than in stationary cells. Stationary (A) and migrating (B) NIH3T3 cells expressing mCherry-paxillin are imaged with TIRF microscopy. Yellow line indicates region of interest for generating kymographs. Scale bar, 20 μm. Stationary cells have larger, more stable focal adhesions than migrating cells, with particularly large adhesions at the corners (C). N = 4772, 4603, 1927 focal adhesions in migrating, square, and square corners respectively. Focal adhesions at the corners of square stationary cells have longer lifetimes than focal adhesions at the leading edge of migrating cells (D). N = 80, 35 FAs in migrating and stationary cells respectively. *** indicates $p<0.001$.

lifetime in stationary cells (Figure 3.4*D*). We suggest that different dynamic states of focal adhesions may be responsible for differential traction force generation. In stationary cells, strong traction forces were maintained stably at stable focal adhesions at the edge. In migrating cells, peak traction forces were associated only transiently at focal adhesions at a certain distance from the leading edge and continuous shifted to younger focal adhesions in front as the cell migrated forward.

3.3.5 Paxillin phosphorylation differs between stationary and migrating cells

To determine if the differences in mechanical activities and focal adhesion dynamics are associated with differences in signaling activities, we compared the level of paxillin phosphorylation between migrating and stationary cells. Phosphorylation of Tyr^{118} on paxillin is believed to represent part of the mechanism for transducing mechanical signals in conjunction with the recruitment of FAK to adhesion sites (Zaidel-Bar *et al.*, 2007; Choi *et al.*, 2011). NIH 3T3 cells on 3.5 kPa polyacrylamide gels were fixed and stained with polyclonal antibodies against paxillin phosphorylated at tyrosine-118 and with monoclonal antibodies against vinculin. Fluorescence intensity of phosphorylated paxillin was normalized against vinculin fluorescence intensity by ratio imaging.

As shown in Figure 3.5, phosphorylated paxillin was concentrated near the leading edge of migrating cells and along the edges of stationary cells. The intensity ratio was 68% higher in focal adhesions at the corners of stationary cells than those near the leading edge of migrating cells (Figure 3.5*I*), suggesting a higher extent of paxillin phosphorylation. These results indicate that focal adhesions in stationary cells and

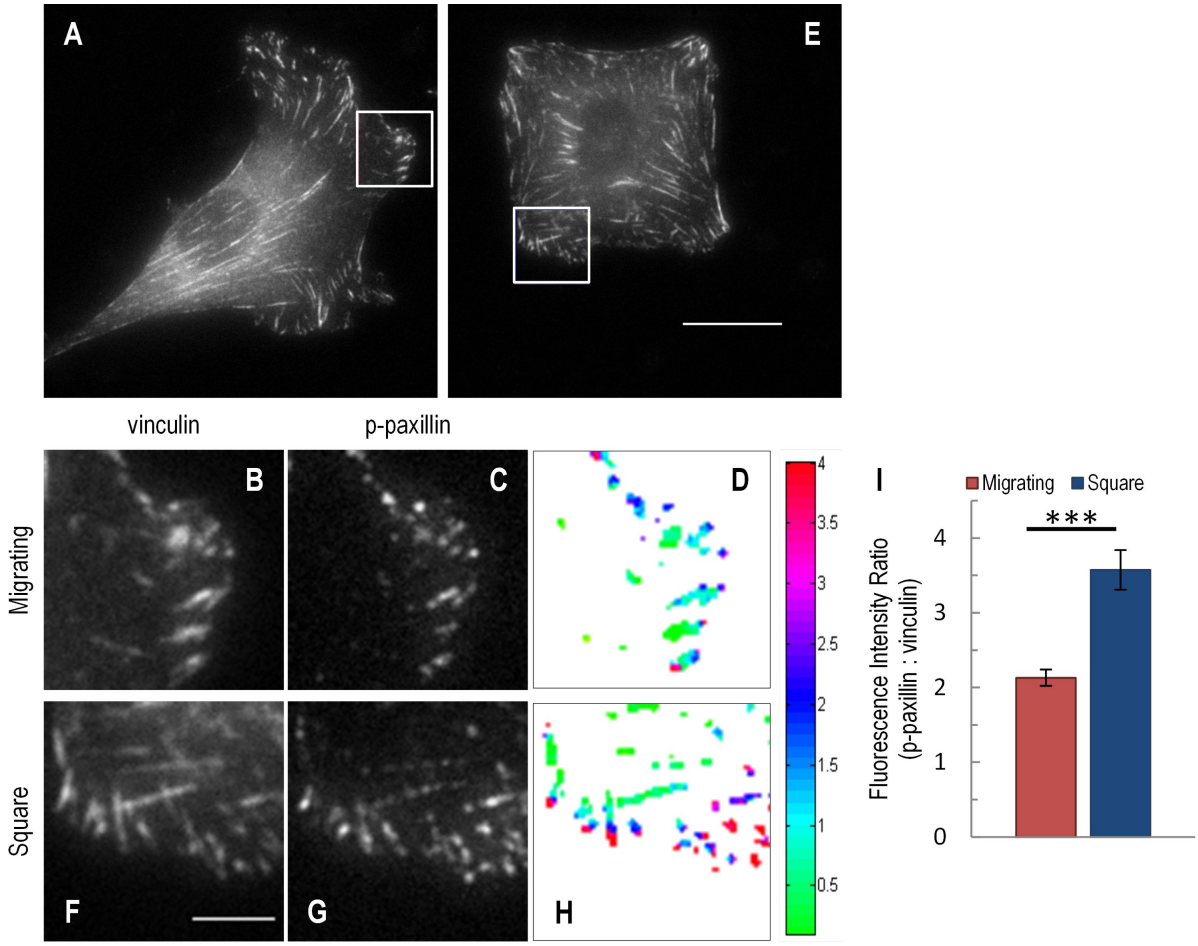

FIGURE 3.5. Paxillin phosphorylation depends on migration state. Vinculin staining shows focal adhesions in migrating (*A*) and stationary (*E*) cells. Scale bar, 20 μm. Boxed regions of interest in migrating (*B-D*) and stationary cells (*F-H*) are enlarged to show vinculin (*B,F*), phosphorylated paxillin (*C,G*), and color heat maps of the ratio of intensities between phosphorylated paxillin and vinculin (*D,H*). Scale bar, 5 μm. Bar graph (*I*) shows that the ratio of intensities of phosphorylated paxillin against vinculin is higher for focal adhesions at the corners in stationary cells than focal adhesions at the leading edge in migrating cells. N = 230, 300 focal adhesions in migrating and stationary cells respectively. *** indicates $p<0.001$.

migrating cells are in different signaling states, which may affect downstream events such as cell growth and differentiation.

3.4 Discussion

We used micropatterning of elastic polyacrylamide hydrogels to simultaneously control cell migration and measure traction force generation. We found that cells confined to adhesive islands exerted traction stress two times higher than migrating cells. Moreover, cells migrating along a linear strip showed a two-fold increase in traction stress when they reached the end of the strip. A scatter plot of traction stress against migration speed further revealed an inverse relationship. These observations indicate that traction force generation can serve as readout for the cell to determine its migration speed.

The inverse relationship between traction stress and migration speed may seem counterintuitive if one considers traction forces only as a means for driving cell migration. However, traction forces have now been implicated as a means both for probing mechanical properties of the environment and for sensing the cell's own physical status. Adherent cells exert traction forces through filopodia to probe substrate rigidity (Wong *et al.*, 2014). Moreover, traction stress increases with cell area and aspect ratio, which may be understood mechanically as a means for maintaining the shape of an elastic object (Rape *et al.*, 2011). The cell may in turn use the magnitude of traction forces generated for detecting its own physical state for the purpose of regulating important activities such as differentiation.

The dependence of traction forces on migration speed cannot be explained by differences in cell shape or size, as cells confined to a teardrop-shaped island, which resembles the natural shape of migrating cells, exhibit similarly strong traction stress as square stationary cells. Moreover, traction stress increases two-fold when the cell stopped at the end of a linear track without showing an increase in spreading area,

supporting the idea that cells are able to regulate traction force output based on migration state.

We suspect that the difference in traction force generation between migrating and stationary cells may be directly related to the difference in focal adhesion dynamics. Relative to the frame of a stationary cell, most focal adhesions remain stationary. In contrast, focal adhesions form continuously at the leading edge then move toward the cell center relative to the frame of a migrating cell. In addition, a large fraction of focal adhesions disassemble within minutes in migrating cells, while focal adhesions in stationary cells are more stable, which may then allow both the focal adhesion and associated stress fibers to grow to a larger size than in migrating cells.

An additional clue comes from the location of peak traction forces as determined by the maximal substrate deformation, which are positioned at the very edge of stationary cells but are several micrometers behind the leading edge in migrating cells. A closely related trend in traction force distribution has been reported by Gardel and colleagues, who found that the traction force exerted through leading focal adhesions in rapidly protruding cells increased transiently then decreased as the cell center migrated toward the focal adhesion. In contrast, traction forces remained high at focal adhesions that stayed close to the cell edge. (Stricker *et al.*, 2011).

The distribution of traction stress is known to mirror the location of newly-formed focal adhesions rather than that of total focal adhesions (Beningo *et al.*, 2001; Stricker *et al.*, 2011). Previous speculations have leaned toward an age-based mechanism, where focal adhesions lose their mechanical activities as they mature over time (Zaidel-Bar *et al.*, 2004). Our observations are instead more compatible with a position-based mechanism, where traction forces build up within a narrow active zone near the leading edge then drop as soon as the leading edge protrudes away from the

focal adhesion. Thus, in stationary cells, traction forces reach a high level as focal adhesions at the leading edge remain trapped within the active zone. Conversely, in migrating cells, newly formed focal adhesions traverse through the active zone, where they are allowed to build up traction forces for only a finite period of time. Mathematically, the magnitude of maximal traction stress, T_{max}, may be expressed as a function of the width of the active zone, w, the speed of protrusion, v, and the rate of change of traction stress, $\mathrm{d}T/\mathrm{d}t$, in the active zone, which shows that maximal traction stress increases with decreasing speed.

$$T_{max} = \frac{w}{v}\frac{\mathrm{d}T}{\mathrm{d}t} \tag{3.1}$$

We ask what might be responsible for the creation of an active zone for traction force buildup. Since focal adhesions are responsive to mechanical forces, one possibility is that traction forces generated by newly formed focal adhesions at the leading edge may affect focal adhesions that fall behind. Such rearward traction forces exerted on the substrate at the very front would cause forward-pointing counter forces to pull the rest of the cell forward. These counter forces, when exerted on the actin cytoskeleton behind the leading edge, would act to cancel out contractile forces on the focal adhesion, which may cause a decrease in traction forces and possibly disassembly of the focal adhesion (Figure 3.6).

The width of the active zone should then be inversely related to the rate of focal adhesion formation per unit distance protrusion, $\mathrm{d}FA/\mathrm{d}x$, as

$$\frac{1}{w} = \frac{\mathrm{d}FA}{\mathrm{d}x}. \tag{3.2}$$

Substituting Equation 3.2 into Equation 3.1 and taking into account $v = \mathrm{d}x/\mathrm{d}t$ leads

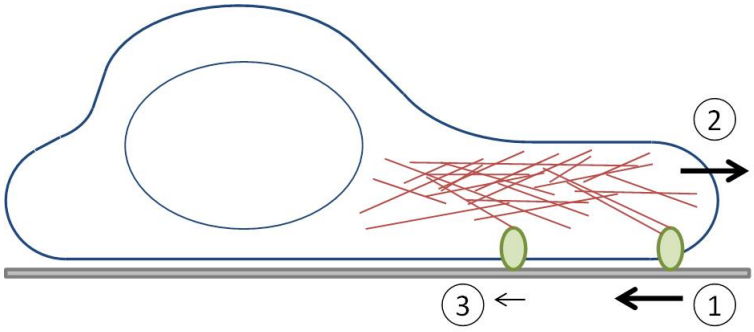

FIGURE 3.6. Schematic of possible mechanical interactions responsible for migration sensing. (*1*) New focal adhesions at the leading edge generate inward traction force on the substrate. (*2*) Outward counter forces drive forward migration and also counteract inward actomyosin forces on more interior focal adhesions. (*3*) Decrease in inward contractile forces causes a decrease in traction forces at interior adhesions.

to the expression

$$T_{max} = \frac{\frac{\mathrm{d}T}{\mathrm{d}t}}{v\frac{\mathrm{d}FA}{\mathrm{d}x}} = \frac{\mathrm{d}T}{\mathrm{d}FA}. \tag{3.3}$$

Thus the maximal traction stress depends on traction stress buildup per focal adhesion formed. This set of expressions also explains the dependence of both the magnitude and location of maximal traction stress on the speed of cell migration.

In summary, we have uncovered a way for adherent cells to detect their state of migration, which we term *migration sensing*. As previously demonstrated for cell size and shape, we show that the physical act of migration also serves to modulate the magnitude of traction forces, which may in turn regulate intracellular chemical activities through mechanosensitive proteins located at the sites of matrix adhesions. As cell size and shape have been shown to play a pivotal role in regulating stem cell differentiation (McBeath *et al.*, 2004; Kilian *et al.*, 2010), we suspect that migration sensing plays a similarly important role. For example, during tissue formation, it may make sense to suppress differentiation while a cell is migrating, a restraint which

is lifted only when the cell has arrived at the destination and is ready to perform physiological functions. Likewise, defects in migration sensing may cause cancer cells to lose such regulation, as well as the control over their growth activities and differentiation state.

3.5 References

Baker, Brendon M, & Chen, Christopher S. 2012. Deconstructing the third dimension - how 3D culture microenvironments alter cellular cues. *J. Cell Sci.*, **125**(13), 3015–3024.

Beningo, Karen A, Dembo, Micah, Kaverina, Irina, Small, J Victor, & Wang, Yu-li. 2001. Nascent focal adhesions are responsible for the generation of strong propulsive forces in migrating fibroblasts. *J. Cell Biol.*, **153**(4), 881–887.

Berginski, Matthew E, & Gomez, Shawn M. 2013. The Focal Adhesion Analysis Server: a web tool for analyzing focal adhesion dynamics. *F1000Research*, **2**, 68.

Chang, StephanieS., Guo, Wei-hui, Kim, Youngeun, & Wang, Yu-li. 2013. Guidance of Cell Migration by Substrate Dimension. *Biophys. J.*, **104**(2), 313–321.

Choi, Colin K, Zareno, Jessica, Digman, Michelle A, Gratton, Enrico, & Horwitz, Alan Rick. 2011. Cross-correlated fluctuation analysis reveals phosphorylation-regulated paxillin-FAK complexes in nascent adhesions. *Biophys. J.*, **100**(3), 583–592.

Dembo, Micah, & Wang, Yu-Li. 1999. Stresses at the cell-to-substrate interface during locomotion of fibroblasts. *Biophys. J.*, **76**(4), 2307–2316.

Discher, Dennis E, Janmey, Paul, & Wang, Yu-Li. 2005. Tissue cells feel and respond to the stiffness of their substrate. *Science*, **310**(5751), 1139–1143.

Engler, Adam J, Sen, Shamik, Sweeney, H Lee, & Discher, Dennis E. 2006. Matrix elasticity directs stem cell lineage specification. *Cell*, **126**(4), 677–689.

Geiger, Benjamin, Spatz, Joachim P, & Bershadsky, Alexander D. 2009. Environmental sensing through focal adhesions. *Nat. Rev. Mol. Cell Biol.*, **10**(1), 21–33.

Guo, Wei-hui, & Wang, Yu-li. 2010. Micropatterning cell-substrate adhesions using linear polyacrylamide as the blocking agent. *Chap. 3, pages 43–52 of:* Goldman, Robert D, Swedlow, Jason R, & Spector, David L (eds), *Live Cell Imaging A Lab. Man.*, second edn., vol. 2011. Cold Spring Harbor Laboratory Press.

Kilian, Kristopher A, Bugarija, Branimir, Lahn, Bruce T, & Mrksich, Milan. 2010.

Geometric cues for directing the differentiation of mesenchymal stem cells. *Proc. Natl. Acad. Sci.*, **107**(11), 4872–4877.

Kraning-Rush, Casey M, Califano, Joseph P, & Reinhart-King, Cynthia A. 2012. Cellular traction stresses increase with increasing metastatic potential. *PLoS One*, **7**(2), e32572.

Lo, Chun-Min, Wang, Hong-Bei, Dembo, Micah, & Wang, Yu-Li. 2000. Cell movement is guided by the rigidity of the substrate. *Biophys. J.*, **79**(1), 144–152.

McBeath, Rowena, Pirone, Dana M, Nelson, Celeste M, Bhadriraju, Kiran, & Chen, Christopher S. 2004. Cell shape, cytoskeletal tension, and RhoA regulate stem cell lineage commitment. *Dev. Cell*, **6**(4), 483–495.

Morin, Timothy R, Ghassem-Zadeh, Sean A, & Lee, Juliet. 2014. Traction force microscopy in rapidly moving cells reveals separate roles for ROCK and MLCK in the mechanics of retraction. *Exp. Cell Res.*, **326**(2), 280–294.

Munevar, Steven, Wang, Yu-Li, & Dembo, Micah. 2001. Traction Force Microscopy of Migrating Normal and H-ras Transformed 3T3 Fibroblasts. *Biophys. J.*, **80**(4), 1744–1757.

Prager-Khoutorsky, Masha, Lichtenstein, Alexandra, Krishnan, Ramaswamy, Rajendran, Kavitha, Mayo, Avi, Kam, Zvi, Geiger, Benjamin, & Bershadsky, Alexander D. 2011. Fibroblast polarization is a matrix-rigidity-dependent process controlled by focal adhesion mechanosensing. *Nat. Cell Biol.*, **13**(12), 1457–1465.

Rape, Andrew D, Guo, Wei-Hui, & Wang, Yu-Li. 2011. The regulation of traction force in relation to cell shape and focal adhesions. *Biomaterials*, **32**(8), 2043–2051.

Smilenov, Lubomir B, Mikhailov, Alexei, Pelham, Robert J, Marcantonio, Eugene E, & Gundersen, Gregg G. 1999. Focal adhesion motility revealed in stationary fibroblasts. *Science*, **286**, 1172–1174.

Stricker, Jonathan, Aratyn-Schaus, Yvonne, Oakes, Patrick W, & Gardel, Margaret L. 2011. Spatiotemporal constraints on the force-dependent growth of focal adhesions. *Biophys. J.*, **100**(12), 2883–2893.

Trichet, Léa, Le Digabel, Jimmy, Hawkins, Rhoda J, Vedula, Sri Ram Krishna, Gupta, Mukund, Ribrault, Claire, Hersen, Pascal, Voituriez, Raphael, & Ladoux,

Benoit. 2012. Evidence of a large-scale mechanosensing mechanism for cellular adaptation to substrate stiffness. *Proc. Natl. Acad. Sci.*, **109**(18), 6933–6938.

Tse, Justin R, & Engler, Adam J. 2010. Preparation of Hydrogel Substrates with Tunable Mechanical Properties. *Pages 10.16.1–10.16.10 of: Curr. Protoc. Cell Biol.*, vol. 47. Hoboken, NJ, USA: John Wiley & Sons, Inc.

Vicente-Manzanares, Miguel, Choi, Colin Kiwon, & Horwitz, Alan Rick. 2009. Integrins in cell migration–the actin connection. *J. Cell Sci.*, **122**(2), 199–206.

Wang, Ning, Ostuni, Emanuele, Whitesides, George M, & Ingber, Donald E. 2002. Micropatterning tractional forces in living cells. *Cell Motil. Cytoskeleton*, **52**(2), 97–106.

Wong, Stephanie, Guo, Wei-Hui, & Wang, Yu-Li. 2014. Fibroblasts probe substrate rigidity with filopodia extensions before occupying an area. *Proc. Natl. Acad. Sci.*, **111**(48), 17176–17181.

Zaidel-Bar, R, Cohen, M, Addadi, L, & Geiger, B. 2004. Hierarchical assembly of cellmatrix adhesion complexes. *Biochem. Soc. Trans.*, **32**(3), 416–420.

Zaidel-Bar, Ronen, Milo, Ron, Kam, Zvi, & Geiger, Benjamin. 2007. A paxillin tyrosine phosphorylation switch regulates the assembly and form of cell-matrix adhesions. *J. Cell Sci.*, **120**(1), 137–148.

Chapter 4

Microtubules Regulate Cellular Mechanical Output in a Migration Dependent Manner

In adherent cells, interactions between cytoskeletal filaments and focal adhesions are the foundation for the generation of traction forces, which function to propel cell migration and to probe the physical condition of the environment. The effects of actomyosin contractility and focal adhesion dynamics on traction forces have been well studied, but the role of microtubules is less understood. Here, we demonstrate that microtubules regulate cellular mechanical output in a manner that depends on migration state. Microtubule depolymerization causes a dramatic increase in traction stress output only in non-migrating cells. The difference in responses between migrating and stationary cells may be caused by differences in the organization or dynamics of microtubules. Inhibition of glycogen synthase kinase 3β, which is known to directly affect microtubule associated proteins and dynamics of the microtubule plus end, prevents nocodazole-induced traction stress increase in stationary cells without affecting the mechanical output of migrating cells. These results suggest that microtubules and focal adhesions interact in migrating cells but not in stationary cells to modulate mechanotransduction. We propose that the structure and function of the microtubule network changes in response to migration behavior, which may in turn serve as part of the sensing mechanisms to regulate cellular mechanical activities.

4.1 Introduction

Focal adhesions serve not only as a physical link between the cell and the extracellular matrix, but also as a mechanosensing unit capable of initiating signaling cascades in response to mechanical forces (Vicente-Manzanares *et al.*, 2009). As cytoskeletal elements are known to interact with focal adhesions both physically and chemically through signaling intermediates (Bershadsky *et al.*, 2003; Parsons *et al.*, 2010), differences in cytoskeletal architecture may facilitate the response of focal adhesion dynamics and traction generation to the state of migration reported in Chapter 3.

In comparison to the role of the actomyosin network, knowledge of the role of microtubules in traction force regulation remains rudimentary. Early work observed that microtubule disruption caused and increase in cell contractility and suggested that microtubule dynamics may somehow weaken actin organization or contractility (Danowski, 1989). More recent studies have reported an increase in traction forces after microtubule depolymerization (Rape *et al.*, 2011a), which may be driven by an increase in Rho activity upon microtubule disruption (Ren *et al.*, 1999; Chang *et al.*, 2008). Other studies note that microtubule growth corresponds with focal adhesion disassembly (Ezratty *et al.*, 2005) in migrating cells.

Structurally, microtubules are composed of 13 proto-filaments arranged cylindrically around a hollow core, yielding a longer persistence length and higher mechanical strength than actin (Gittes *et al.*, 1993). In a purely mechanical model referred to as the tensegrity model, microtubules have been viewed as struts responsible for compressive strength to the cell (Wang *et al.*, 2001). In comparison, actin and intermediate filaments are often described as providing tensile strength to the cell cytoskeleton. In combination, the microtubule network may help a cell maintain its

shape against actomyosin contractility and membrane perturbations associated with protrusion/retraction during migration.

Beyond its tensegrity function, microtubules are also known to be involved in a number of signaling pathways which affect the generation of traction force. Microtubules have been shown to bind GEF-H1, a guanine nucleotide exchange factor that activates Rho (Krendel *et al.*, 2002), suggesting that microtubule polymerization regulates Rho activity through sequestration (Nalbant *et al.*, 2009). Microtubule polymerization after nocodazole washout was shown to increase Rac1 activity, suggesting that dynamic microtubules are important for lamellipodial protrusions (Waterman-Storer & Salmon, 1999). Additional studies have revealed a link between microtubule stability and FAK activity (Palazzo *et al.*, 2004), which may directly affect focal adhesion stability.

Additional modalities of microtubule function may involve the transport of cargo and/or the interaction between plus ends with structures such as focal adhesions. Microtubule associated proteins act as adapters between the microtubule and other important cellular structures. A number of molecular motors are associated with microtubules; dynein and kinesin drive polarized delivery of cargo towards and away from the centrosome, respectively (Sheetz, 1996). Other proteins, including EB1 and CLASP, localize specifically to the growing tips of microtubules (Stehbens & Wittmann, 2012; Etienne-Manneville, 2013), which have been implicated in helping a growing microtubule target the cell cortex (Gundersen *et al.*, 2004) and focal adhesions (Stehbens & Wittmann, 2012). The nature of microtubule organization and growth enable polarization of intracellular trafficking and implicate microtubules in generating spatial patterns of the intracellular signals required for directed migration (Zhang *et al.*, 2014).

By monitoring the output of traction forces, we show in this chapter that microtubule function is dependent on migration state — stationary cells are much more sensitive to the disassembly of microtubules than migrating cells. We further suggest that physical interactions between microtubule tips and focal adhesions may play a role in this difference.

4.2 Methods and Materials

4.2.1 Substrate Preparation

Micropatterned polyacrylamide hydrogels were prepared as described previously (Rape *et al.*, 2011b). Briefly, a polydimethylsiloxane stamp was incubated for 45 min with a 0.1% (w/v) gelatin solution that had been activated with 3.6 mg/mL sodium periodate (Sigma, St. Louis, MO). The stamp was dried using N_2 gas then lightly pressed onto a small glass coverslip. A freshly prepared solution of 5% acrylamide and 0.1% bis-acrylamide (Bio-Rad, Hercules, CA) was degassed; 0.2 μm fluorescent beads (Molecular Probes, Carlsbad, CA) were added at a 1:2000 dilution if the substrate was to be used for traction force microscopy. After addition of the initiators ammonium persulfate (Sigma) and N,N,N',N'-tetramethylethane-1,2-diamine (EMD Millipore, Billerica, MA), a 30 μL drop was pipetted onto a large coverslip pre-treated with Bind-Silane (GE Healthcare, Little Chalfont, United Kingdom). The small stamped coverslip was immediately placed pattern-side down onto the acrylamide drop. After complete acrylamide polymerization, the top coverslip was carefully removed. Micropatterned polyacrylamide hydrogel substrates were mounted into chamber dishes, sterilized under ultraviolet light for 30 min, and incubated in cell culture media for 1 h at 37°C before use. The final gel had an estimated Young's modulus of 3.5 kPa (Tse & Engler, 2010).

Glass substrates micropatterned with linear acrylamide were prepared as described previously (Guo & Wang, 2010). Briefly, a coverslip was treated with Bind-Silane. Standard photolithography techniques were used to pattern areas designated for cell adhesion with SPR 220.3 positive photoresist (Microchem, Newton, MA). The remaining glass surface was made non-adhesive by grafting linear polyacrylamide to

the Bind-Silane-activated surface. The photoresist was then stripped away using Remover 1165 (Microchem), and the exposed glass surface was incubated with 10 μg/mL fibronectin (Sigma) for 1 h.

4.2.2 Cell Culture

NIH 3T3 cells (ATCC, Manassas, VA) were cultured in Dulbecco's modified Eagle's medium (Life Technologies, Carlsbad, CA) supplemented with 10% donor adult bovine serum (Thermo Scientific, Waltham, MA), 2 mM L-glutamine, 50 μg/mL streptomycin, and 50 U/mL penicillin (Life Technologies); cells were maintained under 5% CO_2 at 37°C. Cells were treated with 10 μM nocodazole (Sigma) for 30 min to depolymerize microtubules. Cells were treated with 20 mM lithium chloride (Sigma) or 20 μM SB216763 (Tocris Bioscience, Minneapolis, MN) at time of seeding to inhibit GSK3β.

4.2.3 Traction Force Microscopy

Phase contrast images of single cells spread on a uniformly-coated polyacrylamide gel or across a micropatterned island were collected with a Nikon Eclipse Ti microscope using a 40X N.A. 0.75 PlanFluor dry objective (Nikon, Tokyo, Japan) and an Andor iXon CCD camera (Belfast, United Kingdom) and custom software. Fluorescence images of the embedded beads near the surface of the hydrogel were taken before and after cells were removed with 0.05% Trypsin-EDTA (Life Technologies). For time-lapse recordings, paired phase-contrast images of the cell and fluorescence images of the underlying beads were collected every 10 min for 4 h. Cell outlines were manually drawn, and bead displacement fields were computed using custom software. Traction

stress was computed using LIBTRC software package (Prof. Micah Dembo, Boston University).

4.2.4 Immunofluorescence and Image Analysis

Cells seeded on micropatterned polyacrylamide substrates were fixed in using a solution of 0.5% glutaraldehyde (Sigma) and 0.3% Triton X-100 (Sigma) for 1 min followed by 1% glutaraldehyde for 15 min. Glutaraldehyde autofluorescence was quenched with fresh 0.5 mg/mL $NaBH_4$ (Sigma) for 5 min. The fixed samples were stained with mouse monoclonal antibodies against α-tubulin (Sigma) and rhodamine-phalloidin (Life Technologies). Fluorescence images were collected using a 100X N.A. 1.3 PlanFluor oil immersion objetctive (Nikon).

Microtubule orientation was measured using the OrientationJ plugin (Rezakhaniha *et al.*, 2012) for ImageJ (National Institutes of Health, Bethesda, MD). OrientationJ evaluates the local orientation, coherency, and energy of every pixel in an image by calculating the structure tensor, which is the matrix representation of partial derivatives. Local orientation was measured in the OrientationJ Distribution panel. Default threshold values were used: Gaussian window $\sigma = 1$, Min. Coherency = 0%, Min. Energy = 0%. These thresholds mean that orientation value from every pixel is reported. The orientation value of each pixel is weighted by the coherency value to give more importance to highly oriented structures and less importance to pixels in more uniform regions. The weighted histogram of orientation distribution is returned in both graph and list form. For each migrating cell, the major axis was manually measured in ImageJ; the corresponding orientation histogram list was adjusted such that this value was set as 0°. Similarly, the major axis of teardrop shaped cells was

used as the 0° reference, while one of the straight sides in square cells was selected to use as the 0° reference. Orientation distributions of 20 cells of each shape were averaged.

4.3 Results

4.3.1 Microtubule depolymerization dramatically increases traction stress in stationary cells

We used traction stress exerted on the substrate as a readout of cellular mechanical activities. As shown in Chapter 3, stationary cells showed a two-fold stronger traction stress than migrating cells. To explore the role of microtubules in traction force generation, microtubules were depolymerized using 10 μM nocodazole, which removes the microtubule network almost entirely within minutes. Immunofluorescence images of cells fixed and stained after 30 minutes of nocodazole treatment show only short fragments of α-tubulin (Figure 4.1A). In contrast, the actin network remained intact. Traction force microscopy of nocodazole-treated cells showed surprising differences between migrating and stationary cells. In migrating cells, 95^{th} percentile traction stress increased 67%, but stationary cells experienced a dramatic 400% increase in traction stress (Figure 4.1C). Given the well-documented upregulation of Rho activity upon nocodazole treatment (Waterman-Storer & Salmon, 1999; Chang *et al.*, 2008), an increase in traction forces may be expected. However the dramatic difference in the increase of traction stress between migrating and stationary cells was puzzling and may be indicative of. a poorly understood regulatory function of microtubules.

The effects of nocodazole were readily reversible. Immunofluorescence images of cells 30 minutes after nocodazole washout show that the microtubule network regrew to reach a level and structure similar to that before treatment (Figure 4.1B). To determine if the changes in traction stress were also reversible, we employed time-lapse traction force microscopy to follow the changes before nocodazole, during

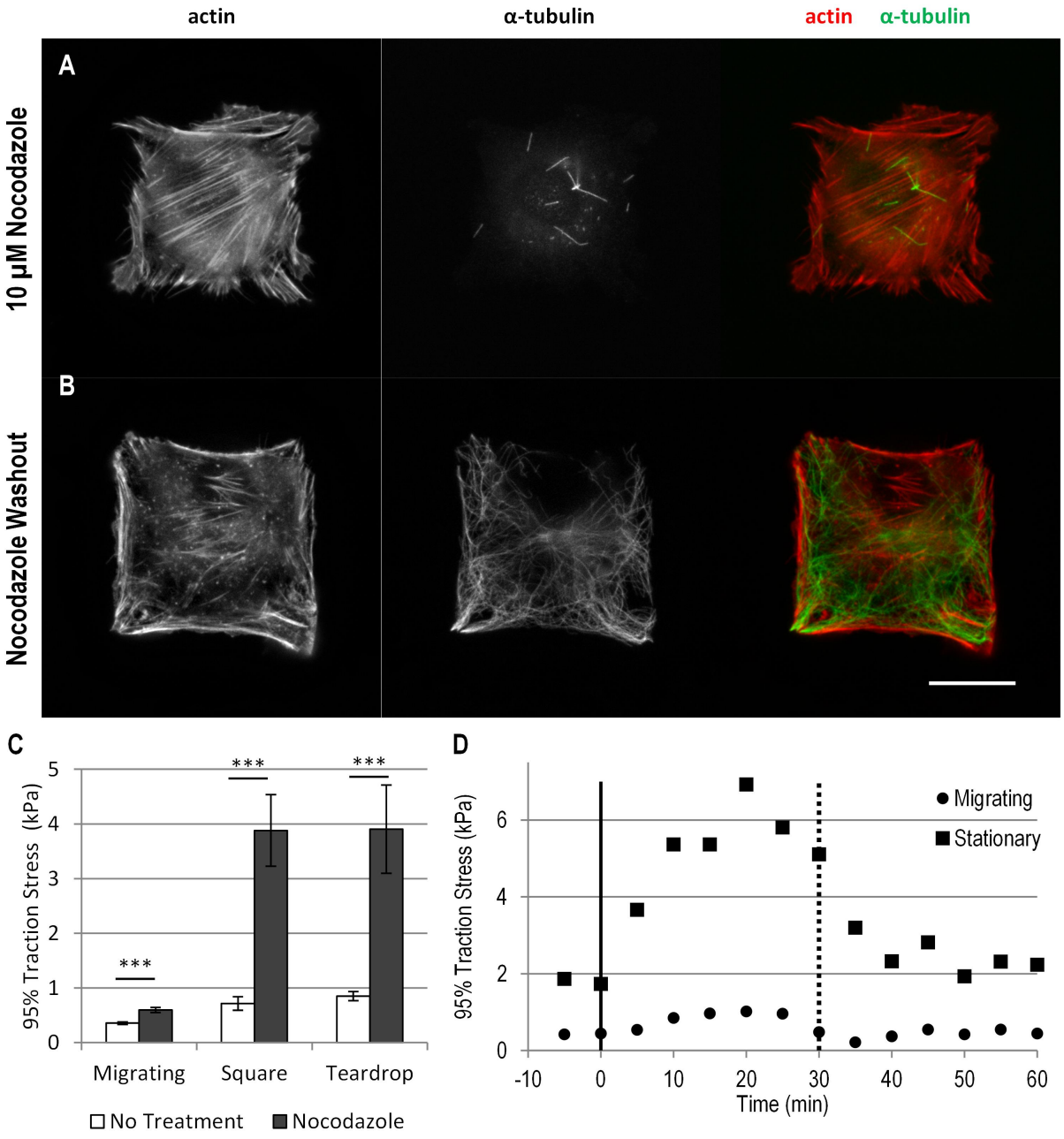

FIGURE 4.1. Stationary cells are more sensitive to microtubule depolymerization. Immunofluorescence images of actin and microtubules in a stationary cell after treatment with 10 μM nocodazole for 30 min (A) and 30 min after washout of nocodazole (B). Nocodazole causes traction stress to increase dramatically only in stationary cells (C). N = 18, 15, 14 for migrating, square, and teardrop cells respectively. *** indicates $p < 0.001$. Nocodazole washout returns traction stress to pre-nocodazole levels (D).

treatment, and after washout (Figure 4.1*D*). The time course in stationary cells shows an immediate and dramatic increase in traction stress after nocodazole treatment. Upon nocodazole washout, traction stress returns to pre-nocodazole levels within 30 minutes. A similar time course also occurred in migrating cells, although the changes are more gradual. Of particular note, traction stress in stationary cells remained higher than traction stress in migrating cells even after drug washout and microtubule regrowth. Thus, the presence of a microtubule network is not enough to explain the difference in traction force regulation between migrating and stationary cells.

4.3.2 Migration state affects microtubule network organization

To investigate the organization of the cytoskeleton, cells migrating freely on an unpatterned coverglass and cells confined to islands micropatterned with linear acrylamide were fixed and stained with antibodies against α-tubulin to visualize microtubules and with rhodamine-phalloidin to visualize actin (Figure 4.2, *A and B*). Microtubule orientation was quantified using the ImageJ plugin OrientationJ, which computes the structure tensor for each pixel to obtain local orientation properties (Rezakhaniha *et al.*, 2012).

Immunofluorescence images of -tubulin show microtubules extending radially from the centrosome located near the cell nucleus. In migrating cells, microtubule orientation shows a large peak in the direction of the cell's major axis, which corresponds with the migration direction. In stationary cells, the microtubule orientation is much more random (Figure 4.2*C*). This random orientation is especially noticeable at the corners of square stationary cells where individual microtubule filaments curve away at the

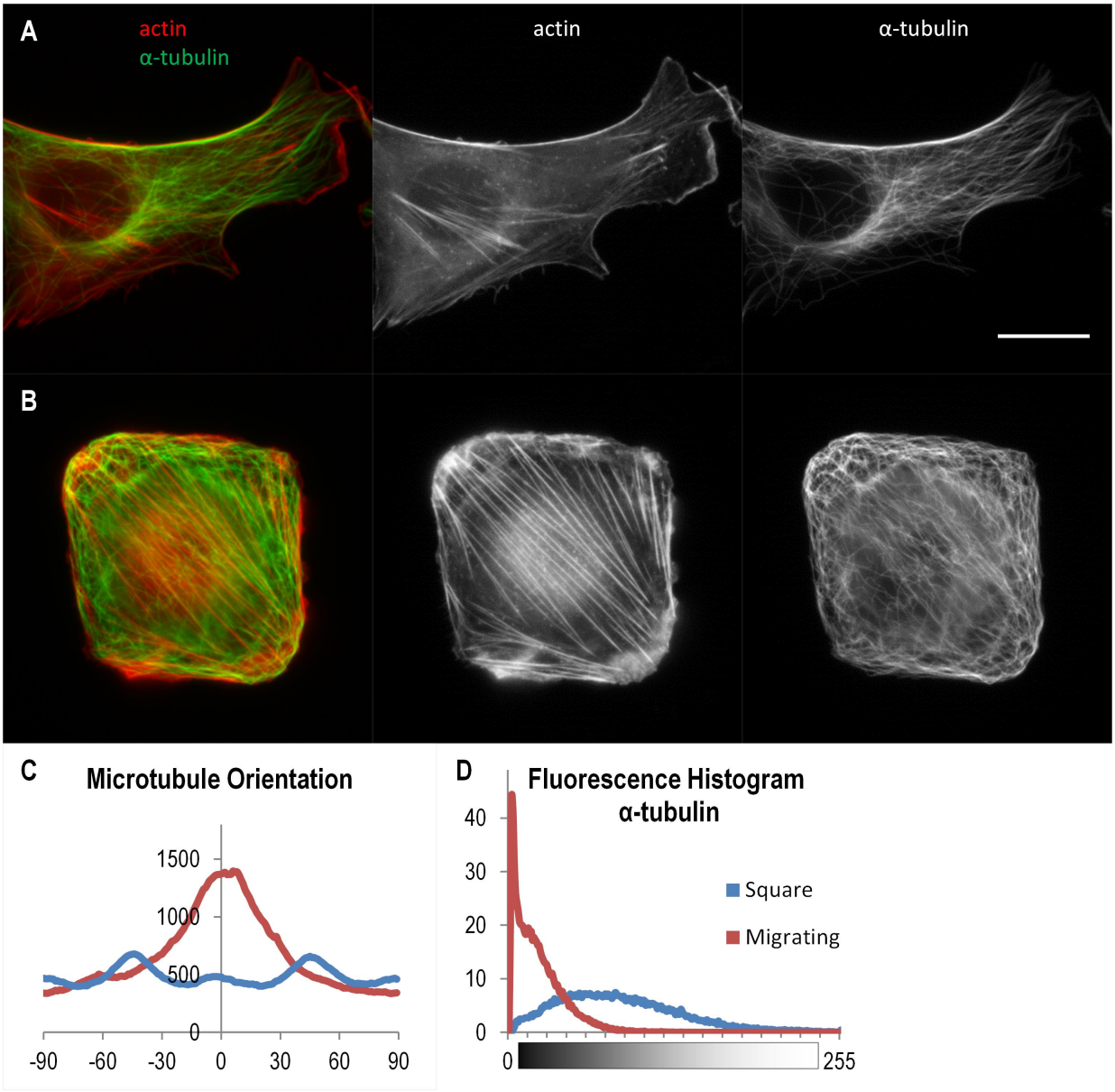

FIGURE 4.2. Microtubule network differs between migrating and stationary cells. Immunofluorescence images of actin and microtubules in migrating (A) and stationary (B) cells. Bar, 20 μm. Orientation analysis of α-tubulin in migrating cells, with 0° set along the long axis of each cell, shows that microtubules are oriented towards the leading edge (*C, red line*). Orientation analysis in stationary cells shows that microtubules are randomly oriented and not organized in any particular direction (*C, blue line*). Fluorescence histogram near regions of strong traction stress (leading edge in migrating cells and corners in square stationary cells) indicates that very few microtubules are found at the leading edge of migrating cells, but α-tubulin is readily found at the corners of stationary cells (D). N = 20 cells for both migrating and stationary conditions.

cell edge rather than pointing straight towards membrane. Notably, microtubules do not extend to the leading edge of migrating cells as seen in merged images of actin and α-tubulin. In contrast, microtubules are present at the very edges of stationary cells. These observations were confirmed by measuring the average gray value of α-tubulin fluorescence at the leading edge of migrating cells and at the corners of stationary cells (Figure 4.2*D*). A value of 0 would indicate no fluorescence, while 255 indicates maximum fluorescence at every pixel in the region of interest. Migrating cells have an average gray value of 21.9 at the leading edge, compared with 84.1 for the corner of stationary cells indicating that migrating cells are deficient in microtubules near the leading edge, which may explain the reduced sensitivity to microtubule depolymerization. NIH 3T3 fibroblasts cultured on micropatterned teardrop-shaped islands have similar microtubule orientation and α-tubulin fluorescence as stationary cells on square islands (Figure A.4). Thus, the microtubule orientation and density at the cell edge are dependent on migration state, not cell shape.

4.3.3 GSK3β inhibition prevents nocodazole-induced traction increase

Previous studies have shown that physical interaction between focal adhesions and the growing tips of microtubules, an interaction facilitated by proteins that bind both to microtubules and to focal adhesion proteins, can lead to focal adhesion disassembly and enhanced cell migration (Kaverina *et al.*, 1999; Ezratty *et al.*, 2005). Among such proteins, CLASP is known to be involved in microtubule stabilization and focal adhesion disassembly, and CLASP activity is suppressed by glycogen synthase kinase 3β (GSK3β) as shown in Figure 4.3*A* (Kumar *et al.*, 2009; Sun *et al.*, 2009). Therefore, to test whether a difference in the interactions between microtubule tips and focal

adhesions plays a role in traction force regulation, we treated migrating or stationary cells with known GSK3β inhibitors of LiCl or SB216376 to upregulate CLASP activity.

NIH 3T3 cells treated with 20 mM LiCl or 20 μM SB216763 show no change in 95^{th} percentile traction stress if the cells are unconfined and migrating. The increase in traction stress induced by microtubule depolymerization in migrating GSK3β inhibited and control cells was also indistinguishable. In contrast, stationary cells exert significantly lower traction stress upon GSK3β inhibition compared to untreated control cells (Figure 4.3B). In addition, nocodazole treatment of GSK3β-inhibited stationary cells failed to induce the four-fold traction stress increase as seen in control cells (Figure 4.3C). In fact, the traction stress of stationary cells treated with LiCl is nearly identical to the traction stress exerted by migrating cells. These results suggest that CLASP-facilitated microtubule-focal adhesion interaction is deficient in stationary cells, which may contribute to increased traction force generation.

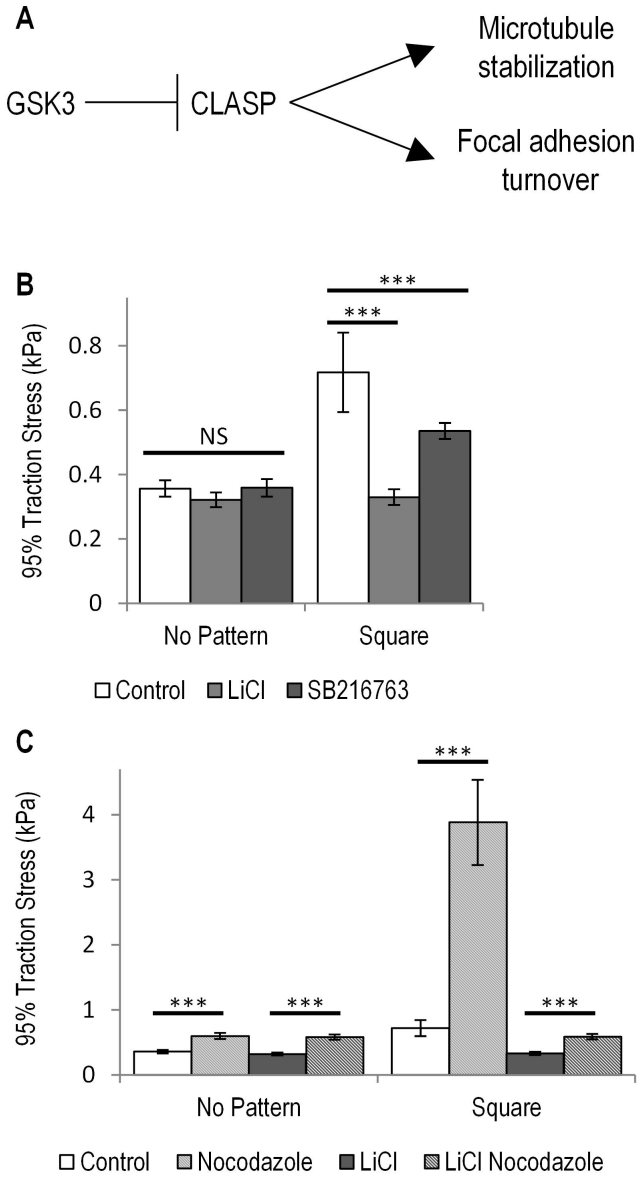

FIGURE 4.3. GSK3β inhibition blocks nocodazole-induced traction increase. Schematic shows how GSK3β activity affects microtubule stabilization and focal adhesion turnover via CLASP (A). Treatment with 20 mM LiCl or 20 μM SB216763 causes no change in traction stress in migrating cells, but decreases traction stress output in stationary cells (B). N = 18, 26, 28 migrating cells and 15, 26, 28 stationary cells under control, LiCl, and SB216763 treatment respectively; *** indicates $p<0.001$. Nocodazole treatment does not cause a dramatic increase in traction stress for stationary cells treated with LiCl (C). N = 18, 26, 15, 25 for control migrating, LiCl migrating, control stationary, and LiCl stationary cells respectively.

4.4 Discussion

We found that depolymerization of microtubules caused a four-fold increase in traction stress only in stationary cells; migrating cells showed an increase of less than one fold when treated with nocodazole. Immunofluorescence images showed that the microtubule network in stationary cells is more randomly oriented than in migrating cells, where microtubules point preferentially towards the leading edge. Microtubule plus end tips were previously observed to be concentrated at active protrusion sites, and are thought to be involved in Rac1 activation (Waterman-Storer & Salmon, 1999). Further, the dramatic nocodazole-induced increase of traction stress in stationary cells was blocked upon the inhibition of GSK3β. These results point to a role for microtubules in regulating traction force generation in response to cell migration.

The fact that traction output in migrating cells is less sensitive to microtubule depolymerization may be explained by the lower density of microtubules in the leading edge, where traction forces are actively generated. However, this still leaves the question of why the microtubule network is different between migrating and stationary cells in the first place. The higher traction stress in stationary cells even after nocodazole washout implies that the microtubule network changes function when migration stops.

Reports that show an increase in stable microtubules in migrating cells at the edge of a scratch wound (Gundersen & Bulinski, 1988) hint that microtubule dynamics change with migration behavior. Stable microtubules, marked by post-translational modification of α-tubulin to remove the terminal tyrosine and expose glutamine (Gundersen *et al.*, 1984), may act selectively as tracks to transport molecules towards or away from the leading edge. Potential cargo molecules may include

clathrin- or caveolin-mediated endocytotic vesicles to transport adhesion molecules away (Stehbens & Wittmann, 2012) or matrix metalloprotease (MMP) to facilitate ECM degradation and release of matrix-integrin connections (Stehbens *et al.*, 2014). Kaverina and colleagues have also reported that interaction with focal adhesions can contribute to microtubule stabilization (Kaverina *et al.*, 1998). Combined with our unpublished observation that migrating cells are more likely to have stable microtubules than stationary cells (Figure A.5), we speculate that microtubules do not target focal adhesions when a cell stops migrating and experience more frequent catastrophe. This lack of microtubule stabilization may interfere with focal adhesion disassembly mechanisms in stationary cells.

Then what is the role of microtubules in migrating cells compared to their role in stationary cells? Why does microtubule depolymerization cause such a dramatic traction stress increase in only stationary cells? We propose a working model to explain the role of microtubules in migration-dependent traction force generation. In migrating cells, interaction between microtubules and focal adhesions targets focal adhesions for disassembly (Figure 4.4*A*). Moderate traction force generation is necessary for efficient migration. The combination of adhesion disassembly and the continual protrusion of the lamellipodial actin network contributes to traction force generation that is controlled — neither so low that it cannot sustain migration not so high that the traction impedes migration. In stationary cells, downregulated microtubule-focal adhesion interaction allows focal adhesions to grow to a larger size and persist for longer times as reported in Chapter 3. It is also possible that the increased focal adhesion lifetime allows more time for focal adhesions to form strong connections with the actomyosin network and generate stronger traction forces. In this case, the microtubule network bears more tensile stress than microtubules in

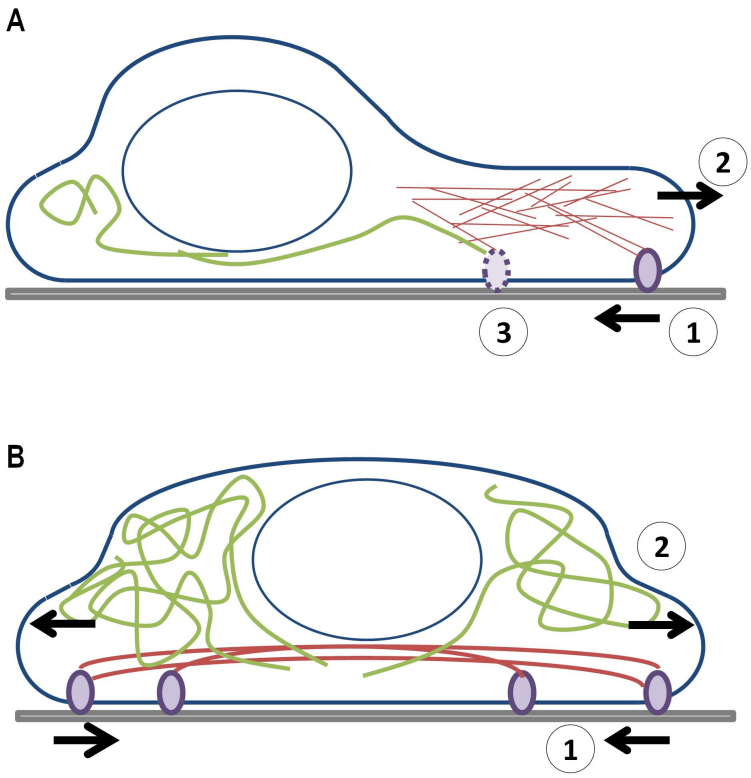

FIGURE 4.4. Schematic of the possible role of microtubules in regulating traction forces. In a migrating cell (*A*), traction forces are exerted via focal adhesions (*1*), counteracting forces generated by the actomyosin network drive forward migration (*2*), and microtubule filaments target focal adhesions for disassembly (*3*). In a stationary cell (*B*), strong traction forces are exerted on the substrate via focal adhesions connected to thick stress fibers (*1*), and microtubules counteract the inward-pointing forces by acting as structural resistance (*2*).

migrating cells (Figure 4.4*B*). Thus when the microtubule network is disrupted in stationary cells, the cell contractile structure no longer meets any resistance and exerts very high traction stress on the substrate through focal adhesions that remain intact. Migrating cells have less pre-stress, so a disruption in the tensile-bearing microtubule network results in smaller increase in traction stress.

The shift in microtubule-focal adhesion interactions may be rooted in the change in focal adhesion properties we reported in Chapter 3. As focal adhesion dynamics and

signaling are affected by migration state, microtubule affinity may also be affected. A difference in microtubule orientation and stability may be a consequence of such a change, leading to a difference in microtubule targeting of focal adhesions. An alternative mechanism may even argue that focal adhesions in stationary cells are more sensitive to microtubules than focal adhesions in migrating cells. In the absence of microtubules, focal adhesions exert more mechanical output in stationary cells than in migrating cells. Microtubule regrowth would cause greater suppression of traction stress in stationary cells than in migrating cells.

In reality, it is likely that microtubules regulate traction generation through a combination of physical and chemical mechanisms. Physically, microtubules may counterbalance against contractile forces, target focal adhesions, and provide a highway for polarized transport of inhibitory molecules, all of which are known to change dynamically in response to migration. Chemically, a change in migration behavior may affect the balance between GTPases Rho and Rac, both of which play essential but antagonistic roles in cell migration (Burridge & Wennerberg, 2004; Machacek *et al.*, 2009). Wittmann and Waterman-Storer have speculated a local downregulation in GSK3β activity by Rac1 may control microtubule-focal adhesion interactions in the lamella of migrating cells (Wittmann & Waterman-Storer, 2005). In this case, our mechanism would suggest that stationary cells have lost this activity gradient. Other studies have suggested that dynamic microtubules locally regulate Rac activity (Waterman-Storer & Salmon, 1999) as well as Rho activity at the leading edge of migrating cells via GEF-H1 (Nalbant *et al.*, 2009). It still remains to be proven how exactly migration state affects the interactions between the growing tips of microtubules and focal adhesions to regulate traction force generation.

4.5 References

Bershadsky, Alexander D, Balaban, Nathalie Q, & Geiger, Benjamin. 2003. Adhesion-dependent cell mechanosensitivity. *Annu. Rev. Cell Dev. Biol.*, **19**, 677–695.

Burridge, Keith, & Wennerberg, Krister. 2004. Rho and Rac Take Center Stage Review. *Cell*, **116**, 167–179.

Chang, Yuan-Chen, Nalbant, Perihan, Birkenfeld, Jörg, Chang, Zee-Fen, & Bokoch, Gary M. 2008. GEF-H1 Couples Nocodazole-induced Microtubule Disassembly to Cell Contractility via RhoA. *Mol. Biol. Cell*, **19**(5), 2147–2153.

Danowski, Barbara A. 1989. Fibroblast contractility and actin organization are stimulated by microtubule inhibitors. *J. Cell Sci.*, **93**(3280), 255–266.

Etienne-Manneville, Sandrine. 2013. Microtubules in Cell Migration. *Annu. Rev. Cell Dev. Biol.*, **29**(1), 471–499.

Ezratty, Ellen J, Partridge, Michael A, & Gundersen, Gregg G. 2005. Microtubule-induced focal adhesion disassembly is mediated by dynamin and focal adhesion kinase. *Nat. Cell Biol.*, **7**(6), 581–590.

Gittes, F., Mickey, B., Nettleton, J., & Howard, J. 1993. Flexural rigidity of microtubules and actin filaments measured from thermal fluctuations in shape. *J. Cell Biol.*, **120**(4), 923–934.

Gundersen, Gregg G, & Bulinski, Jeannette Chloë. 1988. Selective stabilization of microtubules oriented toward the direction of cell migration. *Proc. Natl. Acad. Sci.*, **85**(16), 5946–5950.

Gundersen, Gregg G, Kalnoski, Michael H, & Bulinski, Jeannette Chloë. 1984. Distinct populations of microtubules: tyrosinated and nontyrosinated alpha tubulin are distributed differently in vivo. *Cell*, **38**(3), 779–789.

Gundersen, Gregg G, Gomes, Edgar R, & Wen, Ying. 2004. Cortical control of microtubule stability and polarization. *Curr. Opin. Cell Biol.*, **16**(1), 106–112.

Guo, Wei-hui, & Wang, Yu-li. 2010. Micropatterning cell-substrate adhesions using linear polyacrylamide as the blocking agent. *Chap. 3, pages 43–52 of:* Goldman,

Robert D, Swedlow, Jason R, & Spector, David L (eds), *Live Cell Imaging A Lab. Man.*, second edn., vol. 2011. Cold Spring Harbor Laboratory Press.

Kaverina, Irina, Rottner, Klemens, & Small, J Victor. 1998. Targeting, capture, and stabilization of microtubules at early focal adhesions. *J. Cell Biol.*, **142**(1), 181–190.

Kaverina, Irina, Krylyshkina, Olga, & Small, J Victor. 1999. Microtubule Targeting of Substrate Contacts Promotes Their Relaxation and Dissociation. *J. Cell Biol.*, **146**(5), 1033–1043.

Krendel, Mira, Zenke, Frank T, & Bokoch, Gary M. 2002. Nucleotide exchange factor GEF-H1 mediates cross-talk between microtubules and the actin cytoskeleton. *Nat. Cell Biol.*, **4**(4), 294–301.

Kumar, Praveen, Lyle, Karen S, Gierke, Sarah, Matov, Alexandre, Danuser, Gaudenz, & Wittmann, Torsten. 2009. GSK3β phosphorylation modulates CLASPmicrotubule association and lamella microtubule attachment. *J. Cell Biol.*, **184**(6), 895–908.

Machacek, Matthias, Hodgson, Louis, Welch, Christopher, Elliott, Hunter, Pertz, Olivier, Nalbant, Perihan, Abell, Amy, Johnson, Gary L, Hahn, Klaus M, & Danuser, Gaudenz. 2009. Coordination of Rho GTPase activities during cell protrusion. *Nature*, **461**(7260), 99–103.

Nalbant, Perihan, Chang, Yuan-chen, Chang, Zee-fen, & Bokoch, Gary M. 2009. Guanine Nucleotide Exchange Factor-H1 Regulates Cell Migration via Localized Activation of RhoA at the Leading Edge. *Mol. Biol. Cell*, **20**, 4070–4082.

Palazzo, Alexander F, Eng, Christina H, Schlaepfer, David D, Marcantonio, Eugene E, & Gundersen, Gregg G. 2004. Localized stabilization of microtubules by integrin- and FAK-facilitated Rho signaling. *Science*, **303**(5659), 836–839.

Parsons, J Thomas, Horwitz, Alan Rick, & Schwartz, Martin A. 2010. Cell adhesion: integrating cytoskeletal dynamics and cellular tension. *Nat. Rev. Mol. Cell Biol.*, **11**(9), 633–643.

Rape, Andrew, Guo, W.-h., & Wang, Y.-l. 2011a. Microtubule depolymerization

induces traction force increase through two distinct pathways. *J. Cell Sci.*, **124**(24), 4233–4240.

Rape, Andrew D, Guo, Wei-Hui, & Wang, Yu-Li. 2011b. The regulation of traction force in relation to cell shape and focal adhesions. *Biomaterials*, **32**(8), 2043–2051.

Ren, Xiang-Dong, Kiosses, William B, & Schwartz, Martin A. 1999. Regulation of the small GTP-binding protein Rho by cell adhesion and the cytoskeleton. *EMBO J.*, **18**(3), 578–585.

Rezakhaniha, R, Agianniotis, A, Schrauwen, J T C, Griffa, A, Sage, D, Bouten, C V C, van de Vosse, F N, Unser, M, & Stergiopulos, N. 2012. Experimental investigation of collagen waviness and orientation in the arterial adventitia using confocal laser scanning microscopy. *Biomech. Model. Mechanobiol.*, **11**(3-4), 461–473.

Sheetz, M P. 1996. Microtubule motor complexes moving membranous organelles. *Cell Struct. Funct.*, **21**(5), 369–373.

Stehbens, Samantha, & Wittmann, Torsten. 2012. Targeting and transport: How microtubules control focal adhesion dynamics. *J. Cell Biol.*, **198**(4), 481–489.

Stehbens, Samantha J, Paszek, Matthew, Pemble, Hayley, Ettinger, Andreas, Gierke, Sarah, & Wittmann, Torsten. 2014. CLASPs link focal-adhesion-associated microtubule capture to localized exocytosis and adhesion site turnover. *Nat. Cell Biol.*, **16**(6), 561–573.

Sun, Tong, Rodriguez, Marbelys, & Kim, Leung. 2009. Glycogen synthase kinase 3 in the world of cell migration. *Dev. Growth Differ.*, **51**(9), 735–742.

Tse, Justin R, & Engler, Adam J. 2010. Preparation of Hydrogel Substrates with Tunable Mechanical Properties. *Pages 10.16.1–10.16.10 of: Curr. Protoc. Cell Biol.*, vol. 47. Hoboken, NJ, USA: John Wiley & Sons, Inc.

Vicente-Manzanares, Miguel, Choi, Colin Kiwon, & Horwitz, Alan Rick. 2009. Integrins in cell migration–the actin connection. *J. Cell Sci.*, **122**(2), 199–206.

Wang, Ning, Naruse, Keiji, Stamenović, Dimitrije, Fredberg, Jeffrey J, Mijailovich, Srboljub M, Tolić-Nø rrelykke, Iva Marija, Polte, Thomas, Mannix, Robert, & Ingber, Donald E. 2001. Mechanical behavior in living cells consistent with the tensegrity model. *Proc. Natl. Acad. Sci.*, **98**(14), 7765–7770.

Waterman-Storer, Clare M, & Salmon, E. 1999. Positive feedback interactions between microtubule and actin dynamics during cell motility. *Curr. Opin. Cell Biol.*, **11**(1), 61–67.

Wittmann, Torsten, & Waterman-Storer, Clare M. 2005. Spatial regulation of CLASP affinity for microtubules by Rac1 and GSK3beta in migrating epithelial cells. *J. Cell Biol.*, **169**(6), 929–939.

Zhang, Jian, Guo, Wei-Hui, & Wang, Yu-Li. 2014. Microtubules stabilize cell polarity by localizing rear signals. *Proc. Natl. Acad. Sci.*, **111**(46), 16383–16388.

Chapter 5

Conclusion and Future Directions

5.1 Traction forces in mechanosensing

Traction forces are involved in both inside-out and outside-in signaling (Discher *et al.*, 2005). Internal actomyosin contractility is transmitted through focal adhesions to produce traction forces on the extracellular substrate. These forces are instrumental for both maintaining substrate adhesions (Friedland *et al.*, 2009) and driving cell migration (Beningo *et al.*, 2001; Ridley *et al.*, 2003). At the same time, the cell uses traction forces to probe the external environment, a process crucial for such tasks as sensing substrate rigidity (Lo *et al.*, 2000; Wong *et al.*, 2014) and topographical cues (Frey *et al.*, 2006). In this thesis, I showed that traction forces can also be used for sensing substrate dimension, a case of outside-in signaling. Conversely, in an example resembling inside-out signaling, traction forces can be used as a readout of migration state.

Providing binding sites for both extracellular matrix proteins and cytoskeletal filaments, focal adhesions play a central role for signaling in both directions. Previous studies have reported that traction increases with focal adhesion size (Galbraith *et al.*, 2002), that large tractions are produced by new adhesions at the front of a migrating cell (Beningo *et al.*, 2001), and that traction magnitude depends on focal adhesion location (Stricker *et al.*, 2011). It is clear that traction forces and focal adhesions follow a complex relationship that remains to be fully characterized.

Both physical mechanisms and chemical pathways participate in the regulation of traction forces. Physically, the cellular tensegrity model suggests that traction stresses are generated by actin contractility and resisted by microtubules (Ingber, 2003). Chemically, Rho family GTPases play the most prominent roles in regulating traction forces, particularly the interplay between RhoA and Rac1 (Burridge & Wennerberg,

2004). Proper regulation of traction forces and its associated signaling pathways contribute to normal cell and tissue functions including wound healing and cell differentiation (Engler *et al.*, 2006). On the other hand, loss of regulatory control may contribute to increased cancer metastasis (Munevar *et al.*, 2001; Paszek *et al.*, 2005) or other pathologies like cardiovascular disease (Janmey & Miller, 2011). Knowledge of how mechanics affect cell behavior provides a powerful approach complementary to chemical approaches in regenerative medicine and in the development of cancer therapies.

5.2 Summary of the thesis

5.2.1 Migrating cells use traction forces to sense substrate dimension

In Chapter 2, I showed that migrating cells are able to sense and respond to a change in substrate dimension. Specifically, when NIH 3T3 fibroblasts encounter an interface between a one-dimensional line and two-dimensional surface, they preferentially localize to the two-dimensional surface. I found that cells on one-dimensional lines generate lower traction forces than cells on two-dimensional surfaces. Smaller focal adhesions and less phosphorylated myosin light chain kinase further indicate the decrease in mechanical output in 1D cells compared to cells on a 2D surface. These results suggest that migrating fibroblasts use traction forces to differentiate substrate dimension. We refer to this phenomenon as *dimension sensing*.

Cell migration on two-dimensional surfaces is known to differ drastically from cell migration through a three-dimensional matrix; 2D migration usually depends on actomyosin contractility (Lauffenburger & Horwitz, 1996) while migration through a 3D matrix utilizes an array of migration modes including amoeboid-like behavior and/or MMP activity (Zaman *et al.*, 2006; Friedl *et al.*, 2012). Use of three-dimensional substrates is ideal for recreating the most physiological environment, however tracking and imaging individual cells in three dimensions remains challenging. Recent studies have revealed a number of similarities in one-dimensional and three-dimensional migration (Doyle *et al.*, 2009). Notably, cells migrating on one-dimensional thin lines and in three-dimensional-like matrices have fewer stress fibers and smaller focal adhesions. Even the fibrillar structure of

many three-dimensional matrices recalls one-dimensional tracks. Together, these observations imply that 1D substrates may be used as a simplified model for studying 3D migration.

Interestingly, fibroblasts transformed with the *ras* oncogene were unable to sense substrate dimension. I showed that PAP2 cells generate similar levels of traction stress regardless of substrate dimension, and as a result they do not localize preferentially to two-dimensional surfaces. Combined with previous reports that PAP2 cells display increased metastatic potential (Bondy *et al.*, 1985) and abnormal organization of traction forces (Munevar *et al.*, 2001), my results suggest that abnormal control of traction forces contributes to invasive behavior and cancer progression.

5.2.2 Cell migration regulates mechanical output

In Chapter 3, I found that the magnitude, dynamics, and localization of traction forces depend on migration state. In migrating cells, traction stress is low, and maximal substrate strain occurs behind the leading edge. In stationary cells, traction stress is high, and maximal substrate strain occurs directly at the cell edge. Additionally, I revealed an inverse relationship between traction stress and migration speed. The change in mechanical output is mirrored in focal adhesion size and dynamics. Stationary cells form larger focal adhesion plaques that maintain the same location for long periods of time, especially at the corners of squares where the highest substrate strains were observed. Migrating cells continuously form new focal adhesions at the leading edge which have a shorter lifetime. Migration state affects paxillin phosphorylation, as focal adhesions at the corners of stationary cells have greater phospho-paxillin fluorescence intensity than focal adhesions at the leading edge of

migrating cells. I proposed that aligned assembly and disassembly of adhesions define an active zone where traction forces are generated. In stationary cells, the lack of adhesion disassembly allows traction forces to build up within the active zone. In migrating cells, the active zone moves forward with the leading edge, limiting the amount of time for traction buildup at a particular focal adhesion. Thus migration state plays a role in controlling cell behavior, including mechanical output and signaling activities.

5.2.3 Microtubules regulate traction forces in a migration-dependent manner

In Chapter 4, I reported that disruption of the microtubule network by nocodazole treatment affects traction forces differently in migrating and stationary cells. Migrating cells experience a 67% increase in traction stress while stationary cells experience a 400% increase. Regrowth of the microtubule network after nocodazole washout lowers traction stress to the same level as untreated cells. Notably, washout does not lower traction stress in stationary cells to the same level as migrating cells even though others have reported that nocodazole washout induces disassembly of focal adhesions (Ezratty *et al.*, 2005). This result indicates that microtubules behave differently depending on migration state. Indeed, I found that the microtubule network differs in migrating and stationary cells with respect to fiber orientation and targeting to the cell edge. Additionally, inhibition of GSK3β lowers traction stress in stationary cells. Based on these results, I proposed a mechanism in which interactions between microtubules and focal adhesions are altered based on migration state to regulate traction forces.

5.3 Future directions

5.3.1 Focal adhesion dynamics in the absence of microtubules

In Chapter 3, I linked changes in mechanical output in migrating and stationary cells to focal adhesion dynamics. Our group has previously reported an increase in traction stress after microtubule disruption (Rape *et al.*, 2011). It has also been reported that disruption of the microtubule network results in larger, more stable focal adhesions (Liu *et al.*, 1998). These reports are in agreement with my proposal that larger, more stable focal adhesions are linked to stronger traction forces. In Chapter 4, I reported that the traction output of cells lacking a microtubule network is also dependent on migration state. I suspect that focal adhesion dynamics may similarly be involved in the difference in mechanical output. A simple way to test this hypothesis is to monitor focal adhesion dynamics in nocodazole-treated cells with TIRF microscopy, similar to the procedure described in Chapter 3. Future experiments could also investigate whether microtubules affect the mechanical connections between focal adhesions.

5.3.2 Regulation of focal adhesion-microtubule interaction

In Chapter 4, I presented evidence that inhibition of GSK3β in stationary cells reduces their traction stress; in essence, stationary cells behaved like migrating cells with respect to their mechanical output and response to microtubule depolymerization. GSK3β targets multiple substrates which affect microtubules and focal adhesions including CLASP, APC, and ACF7 (Stehbens & Wittmann, 2012). A recent study implicated the GSK3β substrate CLASP in regulating microtubule-adhesion

interaction to promote focal adhesion disassembly (Stehbens *et al.*, 2014). It is also possible that inhibition of GSK3β works to modulate traction forces in a microtubule-independent manner. Some studies have implicated GSK3β in regulating focal adhesion dynamics directly (Bianchi *et al.*, 2005; Kobayashi *et al.*, 2006). Importantly, I inhibited GSK3β during initial cell seeding for the experiments reported in Chapter 4. This perhaps conditions focal adhesions in stationary cells to have altered dynamics such that the effect of microtubules is unimportant. However, the dramatic increase in traction stress after microtubule depolymerization in normal stationary cells suggests that microtubules play an important role in regulating mechanical output.

More work needs to be done to determine how GSK3β inhibition affects the regulation of traction forces. I speculated that interactions between microtubules and focal adhesions play an important role in modulating traction forces. If CLASPs regulate this interaction, there should be a difference in CLASP activity and/or localization between migrating and stationary cells. Future work should fully characterize microtubule-focal adhesion interactions to address the hypothesis that migration state affects microtubule-focal adhesion interactions.

5.3.3 Applying knowledge of mechanosensing to problems in biomedical engineering

This thesis presented work with single cells migrating individually on hydrogels or confined on microislands of defined shape. It remains to be seen how such research translates to experiments with large groups of cells or even multiple cell types. Additionally, the jump from cell behavior on 2D surfaces to cell behavior in 3D matrices or *in vivo* tissues needs more investigation. Directing cell migration and/or

controlling cell shape to manipulate internal cell mechanics continue to be attractive approaches for regenerative medicine so it is important to understand the both the behavior of single cells and the interactions between cells.

The relationship between mechanobiology and cancer continues to be of great interest and may provide answers to some frustrating aspects of cancer research. Why do some cell masses remain benign while another metastasizes? My results suggest that invasive cells have mechanosensing defects. Others have reported that cancer cells generate higher traction forces with increasing metastatic potential (Kraning-Rush *et al.*, 2012). The values reported for highly metastatic cell lines are similar to my measurements of average traction stress in PAP2 cells (Figure A.2) but are lower than traction stress in normal NIH 3T3 fibroblasts. During EMT, a previously stationary epithelial cell gains migratory/invasive ability. However, these traction stress measurements indicate that invasive cells lie on a spectrum between an epithelial and a truly fibroblastic morphology. This may result in a traction force regulatory system that is rudimentary in comparison to normal mesenchymal cells.

Then are defects in physical sensing simply indicators of disease, or can they even contribute to disease? The upregulation in tumor cells of molecules known to play vital roles in mechanosensing such as FAK (Owens *et al.*, 1995) and RhoA (Horiuchi *et al.*, 2003) suggest that this may be the case. The development of new cancer therapies may also benefit from basic knowledge about mechanosensing, as drug efficacy may be affected.

5.4 References

Beningo, Karen A, Dembo, Micah, Kaverina, Irina, Small, J Victor, & Wang, Yu-li. 2001. Nascent focal adhesions are responsible for the generation of strong propulsive forces in migrating fibroblasts. *J. Cell Biol.*, **153**(4), 881–887.

Bianchi, Mariarita, De Lucchini, Stefania, Marin, Oriano, Turner, David L, Hanks, Steven K, & Villa-Moruzzi, Emma. 2005. Regulation of FAK Ser-722 phosphorylation and kinase activity by GSK3 and PP1 during cell spreading and migration. *Biochem. J.*, **391**(2), 359–370.

Bondy, Gregory P, Wilson, Sylvia, & Chambers, Ann F. 1985. Experimental Metastatic Ability of H-ras-transformed NIH3T3 Cells. *Cancer Res.*, **45**, 6005–6009.

Burridge, Keith, & Wennerberg, Krister. 2004. Rho and Rac Take Center Stage Review. *Cell*, **116**, 167–179.

Discher, Dennis E, Janmey, Paul, & Wang, Yu-Li. 2005. Tissue cells feel and respond to the stiffness of their substrate. *Science*, **310**(5751), 1139–1143.

Doyle, Andrew D, Wang, Francis W, Matsumoto, Kazue, & Yamada, Kenneth M. 2009. One-dimensional topography underlies three-dimensional fibrillar cell migration. *J. Cell Biol.*, **184**(4), 481–490.

Engler, Adam J, Sen, Shamik, Sweeney, H Lee, & Discher, Dennis E. 2006. Matrix elasticity directs stem cell lineage specification. *Cell*, **126**(4), 677–689.

Ezratty, Ellen J, Partridge, Michael A, & Gundersen, Gregg G. 2005. Microtubule-induced focal adhesion disassembly is mediated by dynamin and focal adhesion kinase. *Nat. Cell Biol.*, **7**(6), 581–590.

Frey, Margo T, Tsai, Irene Y, Russell, Thomas P, Hanks, Steven K, & Wang, Yu-Li. 2006. Cellular responses to substrate topography: role of myosin II and focal adhesion kinase. *Biophys. J.*, **90**(10), 3774–3782.

Friedl, Peter, Sahai, Erik, Weiss, Stephen, & Yamada, Kenneth M. 2012. New dimensions in cell migration. *Nat. Rev. Mol. Cell Biol.*, **13**(11), 743–747.

Friedland, Julie C, Lee, Mark H, & Boettiger, David. 2009. Mechanically Activated Integrin Switch Controls $\alpha 5\beta 1$ Function. *Science*, **323**(5914), 642–644.

Galbraith, Catherine G, Yamada, Kenneth M, & Sheetz, Michael P. 2002. The relationship between force and focal complex development. *J. Cell Biol.*, **159**(4), 695–705.

Horiuchi, Akiko, Imai, Tsutomu, Wang, Cuiju, Ohira, Satoshi, Feng, Yuzhen, Nikaido, Toshio, & Konishi, Ikuo. 2003. Up-Regulation of Small GTPases, RhoA and RhoC, Is Associated with Tumor Progression in Ovarian Carcinoma. *Lab. Investig.*, **83**(6), 861–870.

Ingber, Donald E. 2003. Tensegrity I. Cell structure and hierarchical systems biology. *J. Cell Sci.*, **116**(7), 1157–1173.

Janmey, Paul A, & Miller, R Tyler. 2011. Mechanisms of mechanical signaling in development and disease. *J. Cell Sci.*, **124**(1), 9–18.

Kobayashi, Tsuyoshi, Hino, Shin-ichiro, Oue, Naohide, Asahara, Toshimasa, Zollo, Massimo, Yasui, Wataru, & Kikuchi, Akira. 2006. Glycogen Synthase Kinase 3 and h-prune Regulate Cell Migration by Modulating Focal Adhesions. *Mol. Cell. Biol.*, **26**(3), 898–911.

Kraning-Rush, Casey M, Califano, Joseph P, & Reinhart-King, Cynthia A. 2012. Cellular traction stresses increase with increasing metastatic potential. *PLoS One*, **7**(2), e32572.

Lauffenburger, Douglas A, & Horwitz, Alan F. 1996. Cell Migration : A Physically Integrated Molecular Process. *Cell*, **84**(3), 359–369.

Liu, Betty P, Chrzanowska-Wodnicka, Magdalena, & Burridge, Keith. 1998. Microtubule depolymerization induces stress fibers, focal adhesions, and DNA synthesis via the GTP-binding protein Rho. *Cell Adhes. Commun.*, **5**, 249–255.

Lo, Chun-Min, Wang, Hong-Bei, Dembo, Micah, & Wang, Yu-Li. 2000. Cell movement is guided by the rigidity of the substrate. *Biophys. J.*, **79**(1), 144–152.

Munevar, Steven, Wang, Yu-Li, & Dembo, Micah. 2001. Traction Force Microscopy of Migrating Normal and H-ras Transformed 3T3 Fibroblasts. *Biophys. J.*, **80**(4), 1744–1757.

Owens, Lewis V, Xu, Lihui, Craven, Rolf J, Tumors, Human, Xu, Lihw, Craven, Roif J, Cance, William G, Dent, A, Weiner, Tim M, Kornberg, Lori, & Liu, Edison T. 1995. Overexpression of the Focal Adhesion Kinase (p125 FAK) in Invasive Human Tumors. *Cancer Res.*, **55**(13), 2752–2755.

Paszek, Matthew J, Zahir, Nastaran, Johnson, Kandice R, Lakins, Johnathon N, Rozenberg, Gabriela I, Gefen, Amit, Reinhart-King, Cynthia a, Margulies, Susan S, Dembo, Micah, Boettiger, David, Hammer, Daniel a, & Weaver, Valerie M. 2005. Tensional homeostasis and the malignant phenotype. *Cancer Cell*, **8**(3), 241–254.

Rape, Andrew, Guo, W.-h., & Wang, Y.-l. 2011. Microtubule depolymerization induces traction force increase through two distinct pathways. *J. Cell Sci.*, **124**(24), 4233–4240.

Ridley, Anne J, Schwartz, Martin A, Burridge, Keith, Firtel, Richard A, Ginsberg, Mark H, Borisy, Gary, Parsons, J Thomas, & Horwitz, Alan Rick. 2003. Cell migration: integrating signals from front to back. *Science*, **302**(5651), 1704–1709.

Stehbens, Samantha, & Wittmann, Torsten. 2012. Targeting and transport: How microtubules control focal adhesion dynamics. *J. Cell Biol.*, **198**(4), 481–489.

Stehbens, Samantha J, Paszek, Matthew, Pemble, Hayley, Ettinger, Andreas, Gierke, Sarah, & Wittmann, Torsten. 2014. CLASPs link focal-adhesion-associated microtubule capture to localized exocytosis and adhesion site turnover. *Nat. Cell Biol.*, **16**(6), 561–573.

Stricker, Jonathan, Aratyn-Schaus, Yvonne, Oakes, Patrick W, & Gardel, Margaret L. 2011. Spatiotemporal constraints on the force-dependent growth of focal adhesions. *Biophys. J.*, **100**(12), 2883–2893.

Wong, Stephanie, Guo, Wei-Hui, & Wang, Yu-Li. 2014. Fibroblasts probe substrate rigidity with filopodia extensions before occupying an area. *Proc. Natl. Acad. Sci.*, **111**(48), 17176–17181.

Zaman, Muhammad H, Trapani, Linda M, Sieminski, Alisha L, MacKellar, Drew, Gong, Haiyan, Kamm, Roger D, Wells, Alan, Lauffenburger, Douglas A, & Matsudaira, Paul. 2006. Migration of tumor cells in 3D matrices is governed by matrix stiffness along with cell-matrix adhesion and proteolysis. *Proc. Natl. Acad. Sci.*, **103**(29), 10889–10894.

Appendix A

Supplemental Data

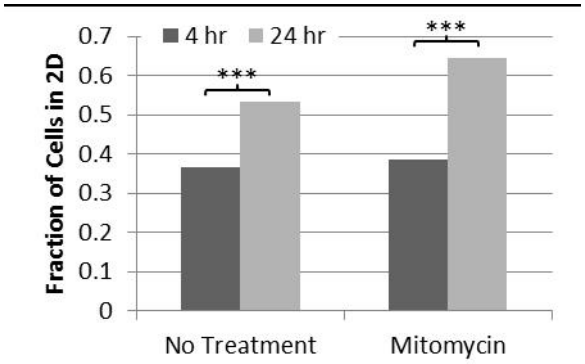

FIGURE A.1. Cell proliferation has no effect on dimension sensing. Both untreated NIH 3T3 cells (*left*) and those treated with 30 μM mitomycin for 2 hours (*right*) show significant accumulation in the 2D regions after 24 hours (Chi-square test, *** indicates $p<0.001$). N = 211, 303 untreated cells at 4 hours and 24 hours, respectively. N = 560, 538 cells treated with mitomycin at 4 hours and 24 hours.

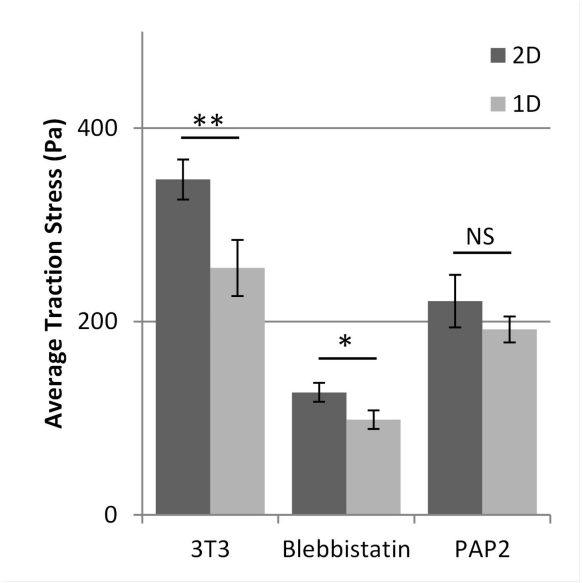

FIGURE A.2. Average traction stress of cells migrating in 1D lines and 2D rectangles. Average traction stress mirrors the trend of 95$^{\text{th}}$ percentile traction stress. These measurements are skewed by regions of the cell that do not generate traction forces. Average traction stress values are regularly reported by other groups, thus these values are useful for outside comparisons. N = 18,17 (NIH 3T3); 13,13 (blebbistatin); 18,19 (PAP2) on 2D and 1D respectively. Error bars represent standard error. * indicates p = 0.03; ** indicates p = 0.008.

		Speed (μm/hr)	**Persistence**	**2D Traction Stress (Pa)**
NIH 3T3	10 μm 1D Lines	26.9	0.89	
	50 μm Strips	35.3	0.77	765±63
	Unpatterned 2D	32.8	0.71	607±78
Blebbistatin	10 μm 1D Lines	37.0	0.96	
	50 μm Strips	31.1	0.81	253±49
	Unpatterned 2D	28.1	0.81	180±36
PAP2	10 μm 1D Lines	31.6	0.94	
	50 μm Strips	38.9	0.68	635±90
	Unpatterned 2D	34.3	0.64	570±59

TABLE A.1. Quantification of migration behavior. Speed, persistence and traction stress were measured for cells migrating on 10 μm wide lines, 50 μm wide strips (same width as 2D rectangles), and unpatterned surfaces. Persistence is given as the ratio of net distance to total distance traveled.

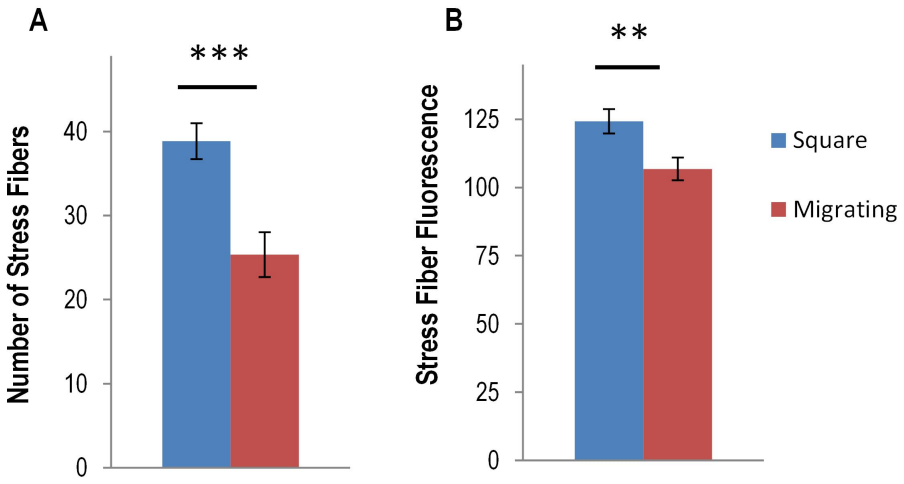

FIGURE A.3. Stationary cells have more numerous, thicker stress fibers than migrating cells. Stationary cells have significantly more stress fibers than migrating cells (A). Fluorescence intensity of stress fibers is greater in stationary cells than in migrating cells (B), indicating thicker actin fibers. N = 20 cells for both migrating and stationary conditions. ** indicates $p<0.01$, *** indicates $p<0.001$.

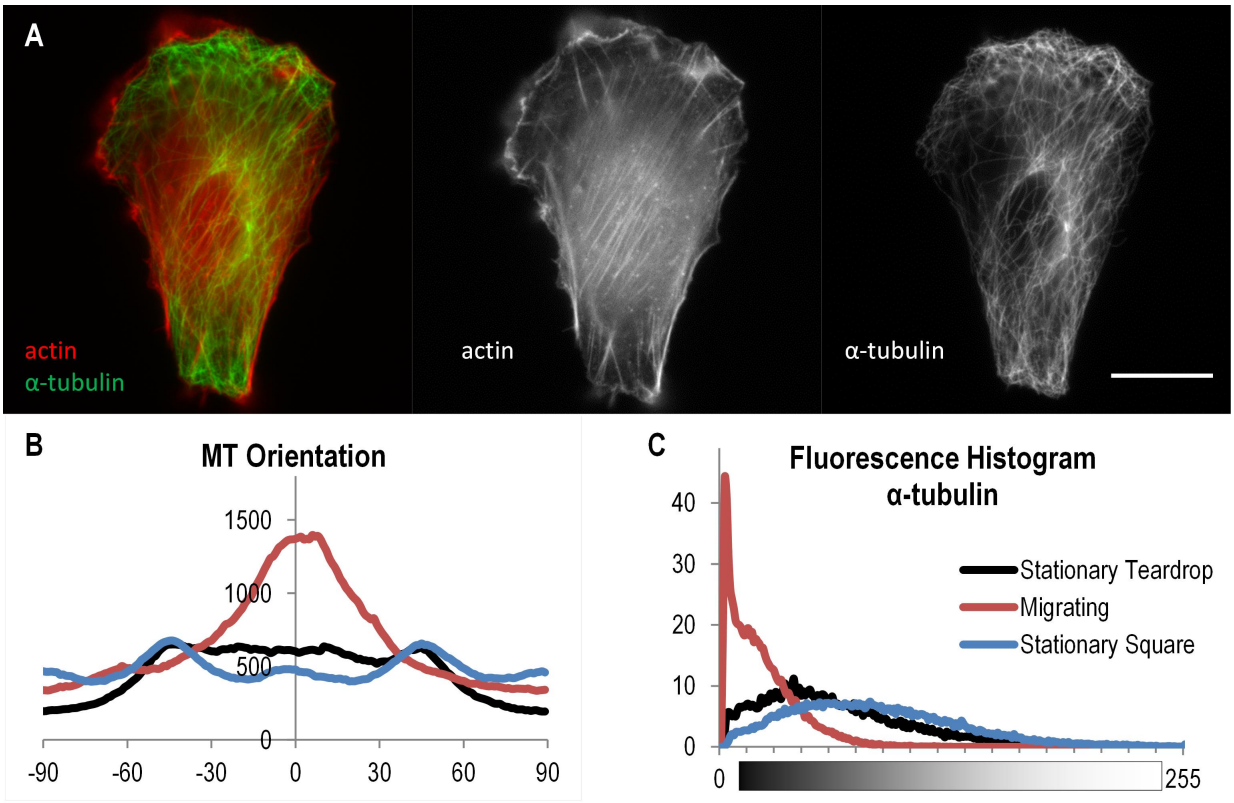

FIGURE A.4. Changes in the microtubule network are based on migration state, not cell shape. Immunofluorescence images of actin and microtubules in stationary cells on a teardrop-shaped island. Bar, 20 μm. (*A*). Orientation analysis of α-tubulin, with 0° set along the long axis of each cell, shows that microtubules are randomly oriented similar to stationary square cells (*B, black line*). Fluorescence histogram indicates that α-tubulin is readily found at the broad end of stationary teardrop cells (*C, black line*). N = 9 teardrop cells. Data for migrating (*red lines*) and stationary square (*blue lines*) cells are copied from Figure 4.2 to facilitate comparison.

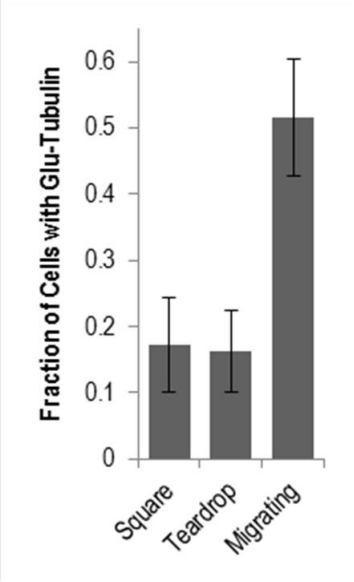

FIGURE A.5. Migrating cells are more likely to have stable microtubules than stationary cells. Graph shows the fraction of cells with positive staining for stable, detyrosinated (Glu) tubulin. N = 29, 37, 33 square, teardrop, and migrating cells respectively. (Data courtesy of Dr. Andy Rape).